

โคโพลิเมอร์ไรเซชันของเอทิลีนกับหนึ่งโอเลฟินด้วยตัวเร่งปฏิกิริยาไทเทเนียมและ  
เซอร์โคเนียมในระบบเอกพันธ์

นางสาวมิ่งขวัญ วรรณบวร

วิทยานิพนธ์นี้เป็นส่วนหนึ่งของการศึกษาตามหลักสูตรปริญญาวิศวกรรมศาสตรดุษฎีบัณฑิต

สาขาวิชาวิศวกรรมเคมี ภาควิชาวิศวกรรมเคมี

คณะวิศวกรรมศาสตร์ จุฬาลงกรณ์มหาวิทยาลัย

ปีการศึกษา 2556

ลิขสิทธิ์ของจุฬาลงกรณ์มหาวิทยาลัย

บทคัดย่อและแฟ้มข้อมูลฉบับเต็มของวิทยานิพนธ์ตั้งแต่ปีการศึกษา 2554 ที่ให้บริการในคลังปัญญาจุฬาฯ (CUIR)

เป็นแฟ้มข้อมูลของนิสิตเจ้าของวิทยานิพนธ์ที่ส่งผ่านทางบัณฑิตวิทยาลัย

The abstract and full text of theses from the academic year 2011 in Chulalongkorn University Intellectual Repository (CUIR)  
are the thesis authors' files submitted through the Graduate School.

COPOLYMERIZATION OF ETHYLENE/1-OLEFIN WITH TITANOCENE AND  
ZIRCONOCENE CATALYSTS IN HOMOGENEOUS SYSTEM

Miss Mingkwan Wannaborworn

A Dissertation Submitted in Partial Fulfillment of the Requirements  
for the Degree of Doctor of Engineering Program in Chemical Engineering

Department of Chemical Engineering

Faculty of Engineering

Chulalongkorn University

Academic Year 2013

Copyright of Chulalongkorn University

Thesis Title                    COPOLYMERIZATION OF ETHYLENE/1-OLEFIN WITH  
   TITANOCENE AND ZIRCONOCENE CATALYSTS IN  
   HOMOGENEOUS SYSTEM

By                                    Miss Mingkwan Wannaborworn

Field of Study                    Chemical Engineering

Thesis Advisor                    Associate Professor Bunjerd Jongsomjit, Ph.D.

---

Accepted by the Faculty of Engineering, Chulalongkorn University in Partial  
Fulfillment of the Requirements for the Doctoral Degree

..... Dean of the Faculty of Engineering  
(Professor Bundhit Eua-Arporn, Ph.D.)

THESIS COMMITTEE

..... Chairman  
(Associate Professor Muenduen Phisalaphong, Ph.D.)

..... Thesis Advisor  
(Associate Professor Bunjerd Jongsomjit, Ph.D.)

..... Examiner  
(Associate Professor ML. Supakanok Thongyai, Ph.D.)

..... Examiner  
(Assistant Professor Anongnat Somwangthanaroj, Ph.D.)

..... External Examiner  
(Ekrachan Chaichana, Ph.D.)

มิ่งขวัญ วรรณบวร : โคลิโพลิเมอร์ไรเซชันของเอทิลีนกับหนึ่งโอเลฟินด้วยตัวเร่งปฏิกิริยาไทเทเนียมและเซอร์โคเนียมในระบบเอกพันธ์ (COPOLYMERIZATION OF ETHYLENE/1-OLEFIN WITH TITANOCENE AND ZIRCONOCENE CATALYSTS IN HOMOGENEOUS SYSTEM) อ. ที่ปรึกษาวิทยานิพนธ์หลัก: รศ. ดร.บรรเจิด จงสมจิตร, 133 หน้า.

ในการผลิตพอลิเอทิลีน ตัวเร่งปฏิกิริยาที่นิยมใช้ได้แก่ ตัวเร่งปฏิกิริยาซีเกลอร์-นัตตาและตัวเร่งปฏิกิริยาเมทัลโลซีน แต่ทั้งนี้การใช้ตัวเร่งปฏิกิริยาเมทัลโลซีนควบคู่กับการใช้ตัวเร่งปฏิกิริยาร่วมเมทิลอะลูมิเนียมออกเซนจะให้ค่าความว่องไวที่สูงมาก ดังนั้นการศึกษาในปัจจุบันจึงมุ่งเน้นที่จะพัฒนาและปรับปรุงตัวเร่งปฏิกิริยาเมทัลโลซีน โดยงานวิจัยชิ้นนี้แบ่งการศึกษาออกเป็น 3 ส่วน ในส่วนแรกเป็นการศึกษาผลของหมู่แทนที่ออกตะเมทิลเตตระไฮโดโรโคเบนโซเบนฟลูออรีนลิแกนด์ ในระบบตัวเร่งปฏิกิริยากอนสเตรนจ์โอเมทรี ที่มีต่อการโคลิโพลิเมอร์ไรเซชันของเอทิลีนกับหนึ่งเฮกซีน ผลที่ได้พบว่าหมู่แทนที่ชนิดนี้สามารถเพิ่มความว่องไวในการเกิดปฏิกิริยาและสามารถผลิตพอลิเมอร์ที่มีน้ำหนักโมเลกุลสูงมีการกระจายตัวของน้ำหนักโมเลกุลที่แคบ เนื่องจากหมู่แทนที่ที่เติมลงไปช่วยเพิ่มความหนาแน่นอิเล็กทรอนิกส์ที่ว่องไว ทำให้อัตราการต่อสายโซ่พอลิเมอร์เพิ่มขึ้น จากการวิเคราะห์ด้วยเครื่องนิวเคลียร์แมกเนติก เรโซแนนซ์ ยังแสดงให้เห็นว่าตัวเร่งปฏิกิริยาที่สังเคราะห์ขึ้นมีความสามารถในการให้หนึ่งเฮกซีนเข้าร่วมในพอลิเมอร์ได้มาก จึงเป็นตัวเร่งปฏิกิริยาที่ให้ประสิทธิภาพสูงสำหรับการโคลิโพลิเมอร์ไรเซชันของเอทิลีนกับหนึ่งโอเลฟิน ดังนั้นจึงได้นำตัวเร่งปฏิกิริยาชนิดนี้มาศึกษาต่อในงานวิจัยส่วนที่สอง ซึ่งเป็นการพิจารณาผลของเทอร์โมโนเมอร์ในระบบเอทิลีน หนึ่งเฮกซีน และไดไซโคลเพนตะไดอิน เทอร์พอลิเมอร์ไรเซชัน โดยพบว่าตัวเร่งปฏิกิริยาชนิดนี้มีประสิทธิภาพในการสังเคราะห์เทอร์พอลิเมอร์ การใช้ไดไซโคลเพนตะไดอินเป็นวิธีหนึ่งที่สามารถผลิตพอลิโเลฟินให้มีหมู่ฟังก์ชันในโครงสร้างสามารถผลิตพอลิโเลฟินชนิดใหม่ที่มีคุณสมบัติดีขึ้น สำหรับงานวิจัยชิ้นที่สามซึ่งศึกษาผลของหนึ่งโอเลฟิน โคลิโพลิเมอร์ที่มีความยาวสายโซ่แตกต่างกัน ด้วยตัวเร่งปฏิกิริยาเซอร์โคเนียม ผลที่ได้พบว่าสามารถแบ่งการพิจารณาออกเป็น 2 ประเภทคือ โคลิโพลิเมอร์ที่มีความยาวสายโซ่สั้น และโคลิโพลิเมอร์ที่มีความยาวสายโซ่ยาว แต่ทั้งนี้ความยาวของสายโซ่โคลิโพลิเมอร์พบว่าส่งผลไม่มากนักต่ออุณหภูมิในการหลอมเหลวและการกระจายตัวของโคลิโพลิเมอร์

ภาควิชา วิศวกรรมเคมี.....ลายมือชื่อนิสิต.....

สาขาวิชา วิศวกรรมเคมี.....ลายมือชื่อ อ.ที่ปรึกษาวิทยานิพนธ์หลัก.....

ปีการศึกษา 2556

# # 5271820521 : MAJOR CHEMICAL ENGINEERING

KEYWORDS : METALLOCENE / ETHYLENE POLYMERIZATION /MONOMER REACTIVITY RATIO

MINGKWAN WANNABORWORN : COPOLYMERIZATION OF ETHYLENE/1-OLEFIN WITH TITANOCENE AND ZIRCONOCENE CATALYSTS IN HOMOGENEOUS SYSTEM. ADVISOR : ASSOC.PROF. BUNJERD JONGSOMJIT, Ph.D., 133 pp.

For polyethylene production, Ziegler-Natta and metallocene catalysts are commonly used for producing polyethylene. The use of metallocene catalyst activated with methylaluminumoxane exhibits very high activity in polymerization. Therefore, many studies have been considered to develop and improve the catalytic performance of metallocene catalyst. The study was divided into three parts. Regarding to the first part, the effect of octamethyltetrahydrodibenzo substituent on fluorenyl ligand of CGC catalyst for ethylene/1-hexene copolymerization was investigated. The results show that this substituent on fluorenyl ligand enhanced the activity. The obtained polymer possessed high molecular weight with narrow molecular weight distribution. This is because the substituent increases electron density on active species leading to an increase in the propagation rate. NMR analysis also shows that the octamethyltetrahydrodibenzofluorenyl-ligated complex had the higher 1-hexene incorporation. This complex was found to be an excellent catalyst for ethylene and 1-olefin copolymerization. Thus, the second part was chosen this complex as catalyst and applied it for ethylene and 1-hexene with dicyclopentadiene terpolymerization. It was found that this complex shows high efficient for synthesizing terpolymer. Dicyclopentadiene was found to be a promising alternative termonomer to produce polyolefin containing functional group and offered new polyolefin with specified functions. For the third study, the influence of comonomer chain length in zirconocene system was investigated. The observed results can be divided into two cases; short chain length comonomer and long chain length comonomer. However, comonomer chain length does not significantly affect on the melting temperature and comonomer distribution.

Department : Chemical Engineering Student's Signature.....

Field of Study : Chemical Engineering Advisor's Signature.....

Academic Year : 2013.....

## ACKNOWLEDGEMENTS

I would like to extend my gratitude to my advisor, Associate Professor Dr. Bunjerd Jongsomjit, for his continuous guidance and support in my graduate research for Ph.D. degree. His advices are always worthwhile and without him this work could not be possible. I sincerely appreciate his great help.

I would also like to thank Associate Professor Dr. Muenduen Phisalaphongtion as the chairman, Associate Professor Dr. ML. Supakanok Thongyai, and Assistant Professor Dr. Anongnat Somwangthanaroj and Dr. Ekrachan Chaichana as the members of the thesis committee for their valuable guidance and revision throughout my thesis.

My most sincere thank to the graduate school and department of chemical engineering at Chulalongkorn University for the financial support. And many thanks are given to the Thailand Research Fund (TRF), the Office of Higher Education Commission (CHE), The Royal Golden Jubilee Ph.D. for funding the research.

Special thanks belong to Prof. Takeshi Shiono, Prof. Zhengguo Cai and Dr. Yuushou Nakayama for their kind support, helpful experimental contributions and useful discussion. Thanks are also due to Haruki Yano, Yuki Kasai and my friend at Polymer Chemistry Group (Shiono Lab) for their help in any form during I did the research at Hiroshima University.

I got a lot of help in my research from my ZM group. They are Sasiradee Jantasee, Auksarapuk Puriwathana, Wanna Phiwkleang and Arunrat Kijjarean. They gave me not only help, support but also encourage me to do the research.

Finally, I would like to thank my family for the continuous support and encourage me during this research.

# CONTENTS

	<b>Page</b>
ABSTRACT (THAI).....	iv
ABSTRACT (ENGLISH).....	v
ACKNOWLEDGEMENTS.....	vi
CONTENTS .....	vii
LIST OF TABLES.....	x
LIST OF FIGURES .....	xi
LIST OF ABBREVIATIONS.....	xv
LIST OF SYMBOLS .....	xvi
CHAPTER I.....	1
CHAPTER II .....	5
<b>2.1 Metallocene catalysts.....</b>	<b>7</b>
<b>2.2 Constrained geometry catalysts (CGCs) .....</b>	<b>9</b>
2.2.1 Structure of CGC catalysts.....	9
2.2.2 Diversity of CGC catalysts .....	10
<b>2.3 Cocatalysts .....</b>	<b>13</b>
<b>2.4 Polymerization mechanism.....</b>	<b>15</b>
2.4.1 Mechanism of chain growth.....	15
2.4.2 Chain transfer reactions .....	16
<b>2.5 Ethylene Homopolymerization.....</b>	<b>16</b>
<b>2.6 Copolymerization of ethylene/<math>\alpha</math>-olefins.....</b>	<b>17</b>
<b>2.7 Ethylene terpolymerization .....</b>	<b>19</b>
<b>2.8 Performance improvement of polyolefin with metallocene catalysts .....</b>	<b>20</b>

	<b>Page</b>
<b>2.9 Polyolefin Industry-Outlook.....</b>	<b>22</b>
CHAPTER III .....	24
<b>3.1 Objectives of this research.....</b>	<b>24</b>
<b>3.2 Scopes of this research .....</b>	<b>25</b>
<b>3.3 Research methodology .....</b>	<b>26</b>
<b>3.4 Experimental .....</b>	<b>27</b>
3.4.1 Materials.....	27
3.4.2 Equipments.....	27
3.4.3 Characterization techniques .....	30
3.4.4 Synthesis of CGC catalysts .....	32
3.4.5 Ethylene Polymerization Procedures .....	37
<b>3.5 Research benefits.....</b>	<b>38</b>
CHAPTER IV .....	39
<b>4.1 Effect of substituent on fluorenyl ligand of CGC catalyst for ethylene/ 1-hexene copolymerization .....</b>	<b>39</b>
4.1.1 Synthesis of ligand precursors and Ti complexes .....	41
4.1.2 Copolymerization of ethylene and 1-hexene.....	46
4.1.3 Characterization of ethylene and 1-hexene copolymer.....	49
<b>4.2 Effect of termonomers on properties of poly(ethylene-<i>ter</i>-1-hexene-<i>ter</i>- dicyclopentadiene) by CGC catalyst.....</b>	<b>58</b>
4.2.1 Terpolymerization of ethylene/1-hexene/dicyclopentadiene .....	59
4.2.2 Properties of Poly(ethylene- <i>ter</i> -1-hexene- <i>ter</i> -dicyclopentadiene).....	64
<b>4.3 Effect of comonomer chain-length on ethylene and 1-olefins copolymerization using zirconocene/MMAO catalysts.....</b>	<b>67</b>



	<b>Page</b>
4.3.1 Homo- and co-polymerization activities.....	68
4.3.2 Characterization of resulting polymer.....	73
CHAPTER V .....	79
<b>5.1 CONCLUSIONS .....</b>	<b>79</b>
<b>5.2 RECOMMENDATIONS.....</b>	<b>81</b>
REFERENCES .....	83
APPENDICES .....	97
<b>APPENDIX A .....</b>	<b>98</b>
<b>APPENDIX B .....</b>	<b>115</b>
<b>APPENDIX C .....</b>	<b>125</b>
VITA.....	133

## LIST OF TABLES

	Page
<b>Table 2.1 Schematic activation and propagation reactions in polymerization ....</b>	<b>15</b>
<b>Table 4.1 Ethylene/1-hexene copolymerization with 1 and 2 activated by MMAO .....</b>	<b>47</b>
<b>Table 4.2 <sup>13</sup>C NMR analysis of ethylene/1-hexene copolymer .....</b>	<b>51</b>
<b>Table 4.3 Monomer reactivity ratios of ethylene/1-hexene copolymerization with 1 and 2.....</b>	<b>53</b>
<b>Table 4.4 Monomer reactivity ratios in ethylene/1-hexene copolymerization with several single-site catalysts .....</b>	<b>57</b>
<b>Table 4.5 Terpolymerization of ethylene/1-hexene/dicyclopentadiene with Me<sub>2</sub>Si(<math>\eta^3</math>-C<sub>29</sub>H<sub>36</sub>)(<math>\eta^1</math>-N<sup>t</sup>Bu)TiMe<sub>2</sub>/MMAO .....</b>	<b>60</b>
<b>Table 4.6 Copolymerization of ethylene with longer chained 1-olefins by using <i>rac</i>-Et[Ind]<sub>2</sub>ZrCl<sub>2</sub>/MAO, as catalytic system.....</b>	<b>69</b>
<b>Table 4.7 Chemical-shift assignment of ethylene/1-dodecene, ethylene/1- tetradecene and ethylene/1-octadecene copolymers [104].....</b>	<b>76</b>
<b>Table 4.8 Triad distribution and properties of the resulting ethylene/1-olefin copolymers .....</b>	<b>77</b>

## LIST OF FIGURES

	Page
Figure 2.1 Structure of metallocene and nomenclature .....	8
Figure 2.2 Examples of modifications of the cyclopentadienyl ring.....	8
Figure 2.3 Metallocene, CGC and Fe-catalyst.....	9
Figure 2.4 Constrained Geometry Catalyst.....	10
Figure 2.5 Sites of modification in ligands with constrained geometry [27].....	10
Figure 2.6 Idealized structure of MAO cocatalyst [44] .....	14
Figure 2.7 The activation of zirconocene catalyst by MAO cocatalyst [46] .....	14
Figure 2.8 Schematic representation of molar mass distribution (MWD) [44]....	22
Figure 2.9 Schematic representation of comonomer distribution [44] .....	22
Figure 3.1 Flow diagram of research methodology .....	26
Figure 3.2 Inert gas supply system .....	28
Figure 3.3 Schlenk line .....	29
Figure 3.4 Diagram of system in slurry phase polymerization .....	30
Figure 3.5 two constrained geometry titanium complexes.....	32
Figure 3.6 Synthesis of complex 1.....	33
Figure 3.7 Synthesis of octamethyloctahydrodibenzofluorene .....	35
Figure 3.8 Synthesis of complex 2.....	36
Figure 4.1 Ethylene/1-hexene copolymerization catalyzed with 1 and 2 .....	41
Figure 4.2 Synthesis of complex 1.....	41
Figure 4.3 $^1\text{H}$ NMR spectrum of synthesized $\text{Me}_2\text{CNHMe}_2\text{Si}(\text{C}_{13}\text{H}_9)$ ligand .....	42
Figure 4.4 $^1\text{H}$ NMR spectrum of $\text{Me}_2\text{Si}(\eta^3\text{-C}_{13}\text{H}_8)(\eta^1\text{-N}^t\text{Bu})\text{TiMe}_2$ complex.....	43
Figure 4.5 Synthesis of octamethyloctahydrodibenzofluorene .....	43
Figure 4.6 $^1\text{H}$ -NMR spectrum of octamethyloctahydrodibenzofluorene ring.....	44
Figure 4.7 Synthesis of complex 2.....	44
Figure 4.8 $^1\text{H}$ NMR spectrum of synthesized $\text{Me}_2\text{CNHMe}_2\text{Si}(\text{C}_{29}\text{H}_{37})$ ligand .....	45
Figure 4.9 $^1\text{H}$ NMR spectrum of $\text{Me}_2\text{Si}(\eta^3\text{-C}_{29}\text{H}_{36})(\eta^1\text{-N}^t\text{Bu})\text{TiMe}_2$ complex.....	46

Figure 4.10 Plots of a) Fineman-Ross method for the copolymers obtained with complex 1.; b) Kelen-Tüdös method for the copolymers obtained with complex 1 .....	54
Figure 4.11 Plots of c) Fineman-Ross method for the copolymers obtained with complex 2.; d) Kelen-Tüdös method for the copolymers obtained with complex 2 .....	55
Figure 4.12 Terpolymerization of ethylene/1-hexene/dicyclopentadiene.....	59
Figure 4.13 Rate-time profile of ethylene/dicyclopentadiene copolymerization ..	62
Figure 4.14 Rate-time profile of ethylene/1-hexene copolymerization.....	63
Figure 4.15 Terpolymerization of ethylene/1-hexene/dicyclopentadiene.....	63
Figure 4.16 <sup>13</sup> C NMR spectrum of poly(ethylene- <i>ter</i> -1-hexene- <i>ter</i> -dicyclopentadiene).....	65
Figure 4.17 Copolymerization of ethylene and 1-olefin with zirconocene/MMAO catalysts.....	68
Figure 4.18 Redrawn conceptual idea by Braunschweig and Breitling [27] .....	71
Figure 4.19 Rate-time profile of ethylene polymerization with various comonomer .....	72
Figure 4.2 SEM micrograph of LLDPE produced with metallocene catalyst; (a) homopolymer (b) ethylene/1-hexene copolymer (c) ethylene/1-octadecene copolymer.....	73
Figure 4.21 X-ray diffractograms of different samples. From bottom to top; (a) homopolymer (b) ethylene/1-C <sub>6</sub> (c) ethylene/1-C <sub>8</sub> (d) ethylene/1-C <sub>10</sub> (e) ethylene/1-C <sub>12</sub> (f) ethylene/1-C <sub>14</sub> and (g) ethylene/1-C <sub>18</sub> copolymers.....	74
Figure 4.22 Resonance of the main chain methylenes and the side chain of the ethylene/1-olefin copolymer .....	75
Figure A-1 <sup>1</sup> H NMR spectrum of octamethyloctahydrodibenzofluorene.....	99
Figure A-2 <sup>1</sup> H NMR spectrum of ClSiMe <sub>2</sub> (C <sub>29</sub> H <sub>37</sub> ) .....	100
Figure A-3 <sup>1</sup> H NMR spectrum of Me <sub>2</sub> CNHMe <sub>2</sub> Si(C <sub>29</sub> H <sub>37</sub> ) ligand .....	101
Figure A-4 <sup>1</sup> H NMR spectrum of Me <sub>2</sub> Si( $\eta^3$ -C <sub>29</sub> H <sub>36</sub> )( $\eta^1$ -N <sup>t</sup> Bu)TiMe <sub>2</sub> complex....	102

	Page
<b>Figure A-5</b> $^1\text{H}$ NMR spectra of (a) $\text{Me}_2\text{CNHMe}_2\text{Si}(\text{C}_{29}\text{H}_{37})$ ligand and (b) $\text{Me}_2\text{Si}(\eta^3\text{-C}_{29}\text{H}_{36})(\eta^1\text{-N}^t\text{Bu})\text{TiMe}_2$ complex.....	103
<b>Figure A-6</b> $^{13}\text{C}$ NMR spectrum of ethylene/1-hexene copolymer (0.15H) entry 1 .....	103
<b>Figure A-7</b> $^{13}\text{C}$ NMR spectrum of ethylene/1-hexene copolymer (0.45H) entry 2 .....	104
<b>Figure A-8</b> $^{13}\text{C}$ NMR spectrum of ethylene/1-hexene copolymer (0.75H) entry 3 .....	104
<b>Figure A-9</b> $^{13}\text{C}$ NMR spectrum of ethylene/1-hexene copolymer (1.5H) entry 4 ...	105
<b>Figure A-10</b> $^{13}\text{C}$ NMR spectrum of ethylene/1-hexene copolymer (0.15H) entry 5 .....	105
<b>Figure A-11</b> $^{13}\text{C}$ NMR spectrum of ethylene/1-hexene copolymer (0.45H) entry 6 .....	106
<b>Figure A-12</b> $^{13}\text{C}$ NMR spectrum of ethylene/1-hexene copolymer (0.75H) entry 7 .....	106
<b>Figure A-13</b> $^{13}\text{C}$ NMR spectrum of ethylene/1-hexene copolymer (1.50H) entry 8 .....	107
<b>Figure A-14</b> $^{13}\text{C}$ NMR spectrum of ethylene/1-hexene/DCP terpolymer entry 4 .....	107
<b>Figure A-15</b> $^{13}\text{C}$ NMR spectrum of ethylene/1-hexene/DCP terpolymer entry 5 .....	108
<b>Figure A-16</b> $^{13}\text{C}$ NMR spectrum of ethylene/1-hexene/DCP terpolymer entry 6 .....	108
<b>Figure A-17</b> $^{13}\text{C}$ NMR spectrum of ethylene/1-hexene/DCP terpolymer entry 7 .....	109
<b>Figure A-18</b> $^{13}\text{C}$ NMR spectrum of ethylene/1-hexene/DCP terpolymer entry 8 .....	109
<b>Figure A-19</b> $^{13}\text{C}$ NMR spectrum of ethylene/1-hexene/DCP terpolymer entry 9 .....	109

	Page
Figure A-20 <sup>13</sup> C NMR spectrum of ethylene/1-hexene/DCP terpolymer entry 10 .....	110
Figure A-21 <sup>13</sup> C NMR spectrum of ethylene/1-hexene/DCP terpolymer entry 11 .....	110
Figure A-22 <sup>13</sup> C NMR spectrum of polyethylene (part 3).....	111
Figure A-23 <sup>13</sup> C NMR spectrum of ethylene/1-hexene copolymer .....	111
Figure A-24 <sup>13</sup> C NMR spectrum of ethylene/1-octene copolymer .....	112
Figure A-25 <sup>13</sup> C NMR spectrum of ethylene/1-decene copolymer .....	112
Figure A-26 <sup>13</sup> C NMR spectrum of ethylene/1-dodecene copolymer .....	113
Figure A-27 <sup>13</sup> C NMR spectrum of ethylene/1-tetradecene copolymer .....	113
Figure A-29 <sup>13</sup> C NMR spectrum of ethylene/1-octadecene copolymer .....	114
Figure B-1 DSC curve of ethylene homopolymer entry 1 .....	116
Figure B-2 DSC curve of ethylene/1-hexene copolymer entry 2.....	116
Figure B-3 DSC curve of ethylene/dicyclopentadiene copolymer entry 3 .....	117
Figure B-4 DSC curve of ethylene/1-hexene/DCP terpolymer entry 4 .....	117
Figure B-5 DSC curve of ethylene/1-hexene/DCP terpolymer entry 5 .....	118
Figure B-6 DSC curve of ethylene/1-hexene/DCP terpolymer entry 6 .....	118
Figure B-7 DSC curve of ethylene/1-hexene/DCP terpolymer entry 7 .....	119
Figure B-8 DSC curve of ethylene/1-hexene/DCP terpolymer entry 8 .....	119
Figure B-9 DSC curve of ethylene/1-hexene/DCP terpolymer entry 9 .....	120
Figure B-10 DSC curve of ethylene/1-hexene/DCP terpolymer entry 10 .....	120
Figure B-11 DSC curve of ethylene/1-hexene/DCP terpolymer entry 11 .....	121
Figure B-12 DSC curve of ethylene/1-hexene copolymer (part 3).....	121
Figure B-13 DSC curve of ethylene/1-octene copolymer.....	122
Figure B-14 DSC curve of ethylene/1-decene copolymer .....	122
Figure B-15 DSC curve of ethylene/1-dodecene copolymer .....	123
Figure B-16 DSC curve of ethylene/1-tetradecene copolymer .....	123
Figure B-17 DSC curve of ethylene/1-octadecene copolymer .....	124

## LIST OF ABBREVIATIONS

### Abbreviations

CCD	comonomer-composition distribution
CGCs	constrained geometry catalysts
Cp	cyclopentadienyl
DCP	dicyclopentadiene
DFT	density functional theory
dMMAO	dried modified methylaluminoxane
DSC	differential scanning calorimetry
EPDM	(ethylene-ter-propylene-ter-diene)polymer
GPC	gel permeation chromatography
HDPE	high density polyethylene
LLDPE	linear low density polyethylene
MAO	methylaluminoxane
MMAO	modified methylaluminoxane
MMAO-BHT	modified methylaluminoxane-butylated hydroxy toluene
MWD	molecular-weight distribution
NMR	nuclear magnetic resonance
PE	polyethylene
PP	polypropylene
SEM	scanning electron microscopy
TMA	trimethylaluminum
XRD	X-ray diffraction spectroscopy

## LIST OF SYMBOLS

$\chi_c$	degree of crystallinity
$\rho$	persistence ratio
$C^*$	number of active center
F-R	Finemann-Ross
K-T	Kelen-Tüdös
$M_n$	number-average molecular weight
$M_w$	weight-average molecular weight
$M_w/M_n$	molecular-weight distribution
$N$	number of polymer chains
$r_E$	reactivity ratio of ethylene
$r_H$	reactivity ratio of 1-hexene
$T_m$	melting temperature
wt	weight



# CHAPTER I

## INTRODUCTION

Nowadays, polyolefin is one of the largest-volume commodities in plastics industry, especially polyethylene. This is because of its better physical and chemical properties such as low density, high tensile strength and excellent chemical resistance as well as being cost-effective. Therefore, polyethylene has been widely used to produce many products such as plastics bags, packaging films and containers [1]. The global demand for polyethylene is forecast to increase and strongly advances through 2016. In general, polyethylene is commercially produced by using the metal catalyst such as metallocene catalysts [2-4] and Ziegler-Natta catalysts [5]. However, metallocene catalysts exhibit high efficiency to polymerize polyolefin and produce polymer with narrow molecular-weight (MWD) and comonomer composition distribution (CCD) than the conventional Ziegler-Natta catalysts [6-10]. Therefore, most of research in the field of olefin polymerization has focused on the metallocene catalysts as the active catalyst for polyolefin.

In the recent years, team researchers of DOW Chemical Co., discovered the new metal complexes which provide many advantages over the conventional metallocene ones not only exhibit high catalytic activity, but also show high thermal stability and high comonomer incorporation [11-12]. The new metal catalysts are called “constrained geometry catalysts” or CGCs. These catalysts can be categorized as one of the metallocene groups. The common structure of catalysts is typically based on cyclopentadienyl (Cp) derivatives and amido fragments or N-based ligand. According to the greater efficiency to polymerize polyolefin, therefore, many efforts have been made to improve the catalytic performance of CGC catalysts. As is well-known, the steric and electronic properties of the ligand of these catalysts play an important role on the catalytic activity and properties of polymer. Thus, an improvement in these catalysts, especially through changing the steric and electronic properties of their ligands should be considered.

In fact, in the class of polyethylene, linear low density polyethylene or LLDPE is important in plastic industry for packaging films and containers. These polymers are mainly synthesized via the copolymerization of ethylene with  $\alpha$ -olefins such as 1-butene, 1-hexene and 1-octene. As known in Ziegler-Natta and metallocene catalysts, the characteristics in terms of catalytic activity and polymer properties are dependent on  $\alpha$ -olefin comonomer. This behavior is called “comonomer effect” [13-14]. If the introduction of  $\alpha$ -olefins increases the catalytic activity, this behavior will be called positive comonomer effect, whereas the decrease in catalytic activity will be called negative effect.

The explanations to define these effects are not only physical reasons, but also chemical reasons. For the physical reason, it deals with an enhancement of monomer diffusion to active site and the generating of new active sites during copolymerization in case of heterogeneous system. The chemical reason is possibly described by an activation of dormant sites by comonomer. Although most of researches have only focused on how the catalytic activity and the properties of polymer would be affected when varying the concentration of comonomer in ethylene and  $\alpha$ -olefin copolymerization, the study on comonomer chain-length is one of important factors influencing on behavior of copolymerization. Thus, the relationship between copolymerization ability and comonomer chain-length should be investigated.

Instead of LLDPE, copolymerization of ethylene with  $\alpha$ -olefin are commercial important for elastomer production. These materials have been commercially used in rubber and latex industries. The well known elastomer is (ethylene-*ter*-propylene-*ter*-diene) polymer or EPDM. According to their unique properties such as good weather and chemical resistance, good electrical insulating properties as well as excellent low temperature flexibility, the various efforts have been made to find the factor affecting polymerization ability. Many researches apply various kinds of monomers for ethylene terpolymerization, including (ethylene-*ter*-1-octene-*ter*-styrene) polymer [15], (ethylene-*ter*-norbornene-*ter*-1-octene) polymer [16] and (ethylene-*ter*-propylene-*ter*-1-octadecene) polymer [17]. In the beginning of terpolymer process,

vanadium catalysts were applied due to their high efficiency for polymerization. However, the drawback of catalysts such as toxicity, aging and discoloration in polymer makes these systems do not suitable for terpolymer production. Therefore, the efficient way to remove or reduce residual catalysts is very considered [18]. A plausible solution is to the use of metallocene catalysts. These catalysts not only allow avoiding from vanadium residue, but also providing excellent catalytic abilities.

In this study, metallocene catalyst and constrained geometry catalysts were selected as catalyst for ethylene homo-, co- and terpolymerization. The major aspect of this research is to obtain a better understanding on homogeneous single-site catalyst. The objective and outline are divided into three parts as mentioned below.

In the first part, we considered how modification on the fluorenyl ring would affect on the catalytic ability of Ti complex based on constrained geometry catalysts. Two constrained geometry catalysts, *ansa*-Dimethylsilylene(fluorenyl)(*t*-butylamido)-dimethyl-titanium complex,  $\text{Me}_2\text{Si}(\eta^3\text{-C}_{13}\text{H}_8)(\eta^1\text{-N}^t\text{Bu})\text{TiMe}_2$  (**complex 1**), and its tetraalkylsubstituted-fluorenyl derivative,  $\text{Me}_2\text{Si}(\eta^3\text{-C}_{29}\text{H}_{36})(\eta^1\text{-N}^t\text{Bu})\text{TiMe}_2$  (**complex 2**), were synthesized and used as catalyst for ethylene/1-hexene copolymerization activated by modified methylalminoxiane cocatalyst (MMAO).

Second aim is to obtain a better understand on ethylene terpolymerization behavior. We have chosen  $\text{Me}_2\text{Si}(\eta^3\text{-C}_{29}\text{H}_{36})(\eta^1\text{-N}^t\text{Bu})\text{TiMe}_2$  as catalyst precursor and conducted terpolymerization of ethylene-ter-1-hexene-ter-dicyclopentadiene activated with MMAO cocatalyst.

In the final aspect, the purpose is to find out the influence of comonomer chain-length on the characteristics in terms of catalytic activity, polymer properties and morphology. In this part, *rac*-Et(Ind)<sub>2</sub>ZrCl<sub>2</sub> was selected as a catalyst and applied for copolymerization of ethylene with various 1-olefins in combination with MMAO cocatalyst.

The present study is mainly divided into five parts. Chapter 1 is to introduce the overall concept of homogeneous single site catalysts and the objective of this

work. After that the literature review, is dealing with background theory and previous research related to metallocene and constrained geometry catalysts and ethylene polymerization. It provides the basic of knowledge of this work. Regarding to the experimental chapter, the laboratory procedure for the preparation of catalyst, ethylene polymerization and the characterization method are described. In the fourth section, the result and discussion found from this research are present. The last part is the conclusions and recommendation.

## CHAPTER II

### LITERATURE REVIEWS

Nowadays, polyolefin is one of the largest businesses with a lot of worldwide production. Polyolefin is commonly produced using metal catalyst in order to achieve the high conversion for changing the reactant into the reaction products. The commercially catalyst that are widely used in olefin polymerization are Ziegler-Natta catalysts, metallocene catalysts, Philip catalysts, and other metal complexes. After the discovery by Karl Ziegler, in 1953, linear high-density polyethylene (HDPE) was firstly produced in the manufacture of olefin polymerization. He found the way to produce HDPE at low pressure by using the mixture of transition metal salts (known as the catalyst) and metal alkyls (known as the cocatalyst). And in the next year, the study with corresponding catalysts, Giulio Natta revealed that these catalysts have ability to provide isotactic and syndiotactic polypropylene. The discovery of Ziegler-Natta catalysts has considerable initiated research in the field of olefin polymerization catalysts. And after the novel prize in Chemistry in 1963 was awarded jointly to Karl Ziegler and Giulio Natta, the name of these catalysts, Ziegler-Natta catalysts, were called to be their landmark discoveries for polyolefin catalysts [19-20].

Ziegler-Natta catalysts are organometallic catalysts which can be active by reacting metal transition compound with metal alkyl group. Although there are many transition metals used as metal compound such as vanadium (V), chromium (Cr). As the active metal transition for the manufacture of polyolefin is titanium (Ti) compound. These catalysts give high efficiency to polymerize polyolefins when reacting with metal alkyl of a base metal from groups I to III such as  $\text{AlEt}_3$ ,  $\text{Al}^i\text{Bu}_3$ ,  $\text{AlEt}_2\text{Cl}$  and  $\text{AlEt}_2\text{OR}$ . Ziegler-Natta catalysts are multi-sites catalysts. It means that each active site is different, thus leading to polyolefin with broad molecular-weight (MWD) and comonomer-composition distribution (CCD) [21].

In 1957, the study of Breslow and Newberg encouraged the research in the field of olefin polymerization catalysts once again. They replaced chloride ligand of the Ziegler-Natta catalysts by bis(cyclopentadienyl)titanium derivatives and activated them with an activator like alkylaluminum compound for ethylene polymerization. However, these catalysts still exhibited low catalytic activity, gave polymer with low molecular weight and also showed less reactive for propylene polymerization [22]. Until the discovery of methyl aluminoxane as cocatalyst by Kaminsky and coworkers, an enhancement of catalytic activity was observed. An addition of water to trialkyl aluminum during polymerization resulted in significantly enhanced catalytic activity. Kaminsky described that the occurred reaction between water and trialkyl aluminum generates alkyl aluminoxane compound, which is considered as an activator or cocatalyst, thus, improving catalytic activity. Therefore, a breakthrough in metallocene catalysts with aluminoxane makes more attractive not only in academic area but also in the polymer industry [23-24].

Metallocene catalysts are organometallic compound in which dicyclopentadienyl ring (Cp) are bounded to metal transition atom. Metallocene catalysts are single-site systems. Each active site is similar, thus leading to produce polymer with narrow molecular-weight distribution ( $MWD \approx 2$ ) and comonomer-composition distribution polymer (CCD). These catalysts provide many advantages compared to the conventional Ziegler-Natta catalysts such as high catalytic activity, uniform comonomer incorporation and tailor-made microstructure (polymer properties can be controlled through changing the catalyst structure). Therefore, much of research has been focused in metallocene single-site catalysts [19,25].

The advantages of metallocene catalysts can be described in the following:

(1) Metallocene catalysts show catalytic activity approximately 100 times higher than the conventional Ziegler-Natta catalysts.

(2) Propylene produced from metallocene catalyst has stereospecific. The obtained polypropylene can be isotactic, syndiotactic and hemitactic. These variations open the door to new innovative polyolefin production.

(3) Metallocene catalysts are single-site systems. Thus, uniform type of active species present in this system. The obtained polymers are narrow molecular-weight distribution ( $M_w/M_n \approx 2$ ) and comonomer-composition distribution (CCD). The better physical and mechanical properties such as tear resistance, tensile strength and impact properties can be obtained when polymerize with metallocene catalysts.

From these advantages, many attempts have been done to modify and apply metallocene catalysts for the synthesis of the desired polymers.

## 2.1 Metallocene catalysts

- **Structure of metallocene catalyst**

Metallocene catalysts are organometallic compound. These catalysts have metal transition atom, especially group IV-B such as zirconocene (Zr), titanium (Ti) and hafnium (Hf) which are bounded to two organic molecules such as cyclopentadienyl ring (Cp) and cyclopentadienyl derivatives. The coordination between metal atom and cyclopentadienyl rings can be in a parallel form or bent form as seen in **Figure 2.1**.

Besides cyclopentadienyl ring is used as an organic molecule in metallocene structure, the modification on cyclopentadienyl ring by substituting hydrogen atom through methyl-, pentamethyl-, trimethylsilyl- or phenyl group can be used. The modification of cyclopentadienyl ring by hydrogen substitution through anellated rings are indenyl ring (Ind) and fluorenyl ring (Flu). In addition, C-H group on cyclopentadienyl ring can also be modified by replacing with an isoelectric nitrogen or phosphorus atom like pyrrolyl ring and phosphoryl ring (**Figure 2.2**).

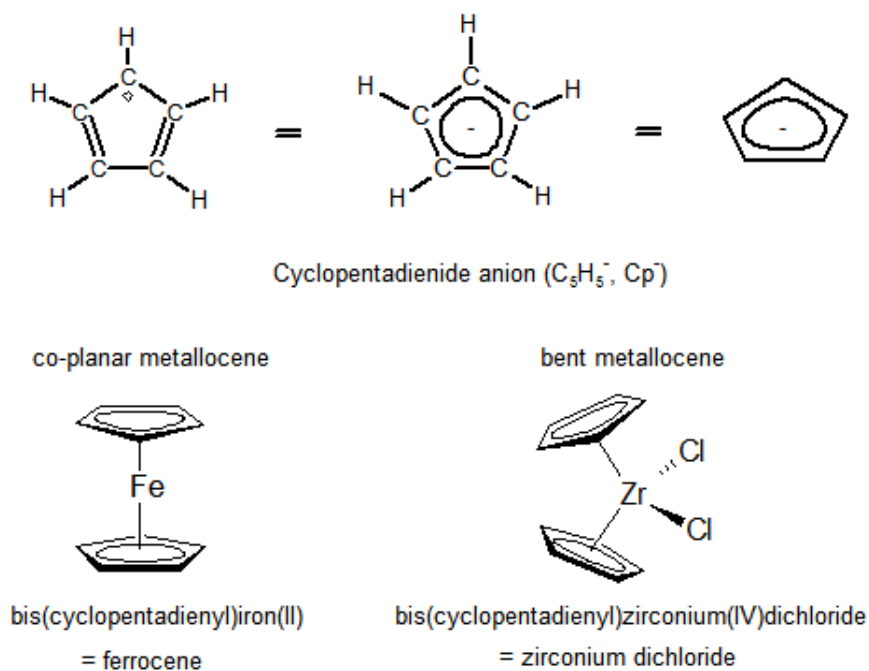


**Figure 2.1 Structure of metallocene and nomenclature**

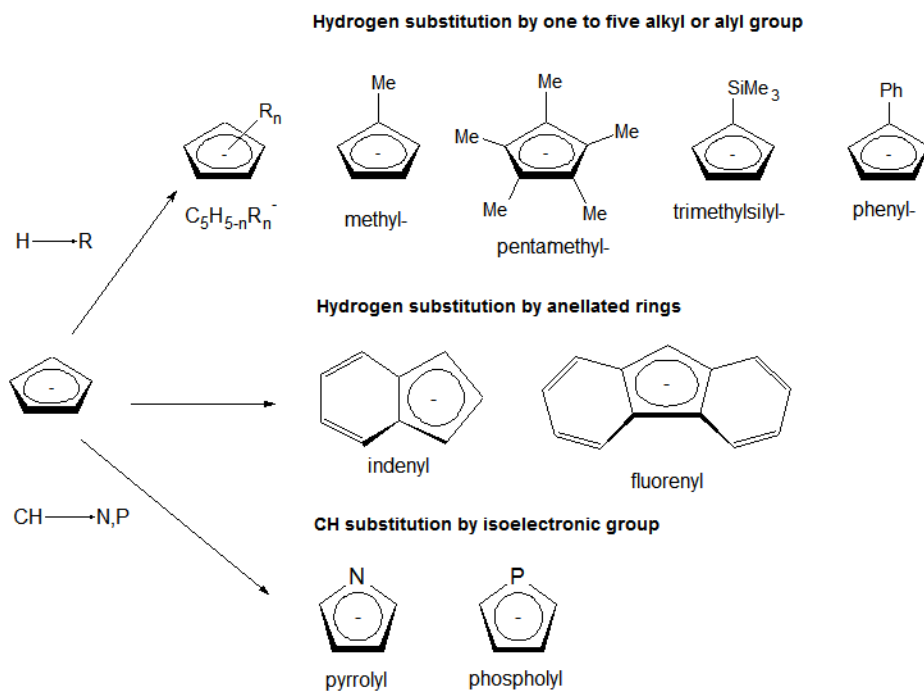


**Figure 2.2 Examples of modifications of the cyclopentadienyl ring**



## 2.2 Constrained geometry catalysts (CGCs)

After the first single-site catalyst namely metallocene catalyst was discovered, many studies have been attempted in order to develop and improve the catalytic performance of these catalysts. In 1990s, researchers from Dow chemical successfully synthesized the new metal complex. They reported that these catalysts significantly showed high catalytic activity, high thermal stability and increased comonomer incorporation in polymer chain compared to the conventional metallocene catalysts. In primary studies, the metal atom is an early or late transition metals, such as scandium (Sc), ferrous (Fe) and nickel (Ni) [26]. These catalysts have half-sandwich Cp ring coordinated to metal atom group III or IV and coordinated to amino fragment or amino based ligand (**Figure 2.3**).

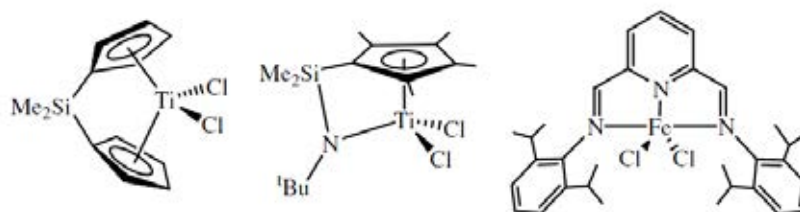


**Figure 2.3 Metallocene, CGC and Fe-catalyst**

And in the same year, Bercrow and Shapiro replaced one of cyclopentadienyl compound by *tert*-butylamido groups in metallocene catalysts. They found that these catalysts showed high performance for olefin polymerization. These catalysts are named “constrained geometry catalysts or CGCs”

### 2.2.1 Structure of CGC catalysts

Constrained geometry catalysts or CGC catalysts can be categorized as one of the metallocene group. The common structure of CGC catalysts can be seen in **Figure 2.4**. In general, these complexes typically have two ligand components; the first one is cyclopentadienyl derivatives and the second one is amino fragment or amino based ligand. Cyclopentadienyl (Cp) ring is attached amino donor ligand via covalent bond. Because of their advantages over the conventional metallocene catalyst, therefore, the

investigative efforts to develop the performance of these catalysts are very considered. The nature of catalyst can be classified by the environmental around metal atom as seen in the following.

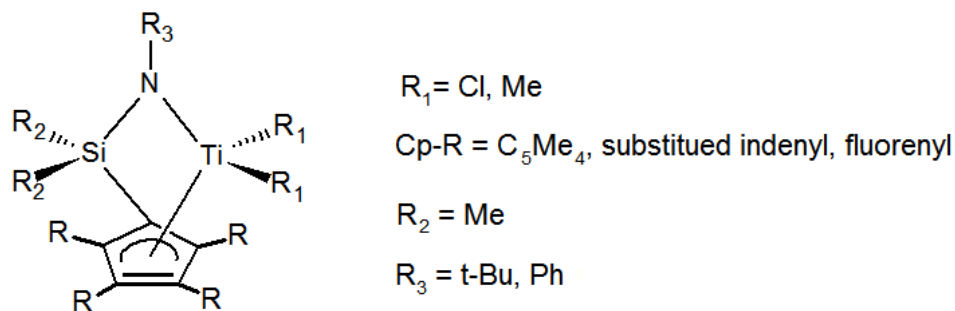


**Figure 2.4 Constrained Geometry Catalyst**

### 2.2.2 Diversity of CGC catalysts

Constrained geometry catalysts can be modified by varying the surrounding around metal atom. These catalysts can be modified by the different modification on the amido group, the cyclopentadienyl derivatives, the *ansa*-bridge or a combination thereof. The sites of modification in ligands are shown in **Figure 2.5**.

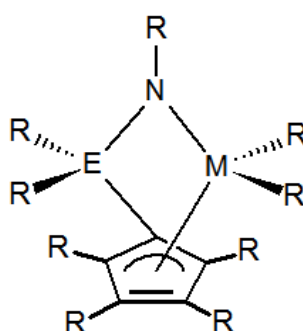


**Figure 2.5 Sites of modification in ligands with constrained geometry [27]**

- **Modification on the cyclopentadienyl ring**

Several studies have been investigated on modification on the cyclopentadienyl ring, for instance

Stevens revealed the modification on cyclopentadienyl ring by introducing the substituent such as indenyl,  $C_5H_4$  and  $C_5Me_4$ . When increasing electron density at metal atom, the higher catalytic activity was observed. An electron density at metal atom is in the order of  $C_5Me_4 > C_5H_4 >$  indenyl. In addition, the comonomer incorporation and molecular weight were also depended on the electron density at active site [28].

Cai et al. [29] investigated the effect of substituent on fluorenyl ligand by introducing *tert*-butyl group at 2,7- or 3,6-position. They synthesized [*t*-BuNSiMe<sub>2</sub>Flu)]TiMe<sub>2</sub>, [*t*-BuNSiMe<sub>2</sub>(2,7-*t*-Bu<sub>2</sub>Flu)]TiMe<sub>2</sub> and [*t*-BuNSiMe<sub>2</sub>(3,6-*t*-Bu<sub>2</sub>Flu)]TiMe<sub>2</sub> and applied them for propylene polymerization. The results show that the introduction of *tert*-butyl substituents on the fluorenyl ligand enhanced the catalytic activity and produced propylene with the syndiotactic-specificity.

McKnight et al. [30] described the effect of cyclopentadienyl ring on the productivity and molecular weight. It was found that Me<sub>4</sub>C<sub>5</sub>-based catalysts are able to produce polymer with high molecular weight and have productivities higher than the indenyl ligands. It may be due to an increase of electron density of Me<sub>4</sub>C<sub>5</sub> ligand, thus leading to an improvement on propagation rate. The catalytic activity increased.

*ansa*-dimethylsilylene(fluorenyl)(amido)dimethyltitanium, Me<sub>2</sub>Si(η<sup>3</sup>-C<sub>13</sub>H<sub>8</sub>)(η<sup>1</sup>-N<sup>*t*</sup>Bu)TiMe<sub>2</sub>, combined with a suitable cocatalyst conducted not only a syndiotactic-specific living polymerization of propylene and α-olefin [31], but also homo- and copolymerization of norbornene with ethylene or α-olefin [32].

In addition, many researchers have also used other fused ring compounds for olefin polymerization, such as sterically expanded fluorenyl CGC [33].

The study of Li et al. [34] was done to report the effect of the substituents on the cyclopentadienyl (Cp) ring of these catalysts Cp'(OAr)TiCl<sub>2</sub> [Cp'=Me<sub>5</sub>C<sub>5</sub> (**1**), Me<sub>4</sub>PhC<sub>5</sub> (**2**), and 1,2-Ph<sub>2</sub>-4-MeC<sub>5</sub>H<sub>2</sub> (**3**) on the catalytic ability of Ti complexes. The order of catalytic activity is as follow: **1**>**2**>**3**. These results are related to the electronic effect of the substituent group on the cyclopentadienyl ligand. The

introduction of electron-donating group on the Cp ring increases the catalytic activity, whereas the catalytic activity would be decreased if the substituent is replaced by electron-withdrawing group

- **Variation of donor fragment**

For the modification on donor fragment, many cases have been done to describe the influence of donor fragment in order to improve the catalytic performance of CGC catalysts. They have used C<sub>6</sub>H<sub>5</sub> ring [35], smaller bulkier alkyl group (cyclododecyl or adamantyl) [36] or chiral substituents [37] for olefin polymerization. However, among a number of the substituent on donor ligand, *tert*-butyl substituent was found to be an excellent donor ligand that has been discovered to date.

Several studies have indicated that the variation of the amido fragment play an important role in catalytic activity and properties of obtained polymer. Examples of the variation of donor ligand of CGC catalysts are reported as below.

Li et al. [38] investigated the influence of alkyl group on the catalytic activity and the incorporation of comonomer by changing the substituent group on amido donor ligand. They report that the catalytic activity of [C<sub>5</sub>Me<sub>4</sub>-4-R<sub>1</sub>-6-R-C<sub>6</sub>H<sub>2</sub>O]TiCl<sub>2</sub> R=*t*-Bu (**1,2**), Me (**3**), Ph (**4**) and R<sub>1</sub>= *t*-Bu (**1**), H (**2,3,4**) complexes is in the order **1** > **2** > **3** > **4**. If the substituent on R<sub>1</sub> is an electron-donating group, the catalytic activity increased whereas if the substituent is hydrogen atom, the catalytic activity was low. This is due to an increasing of electron density around metal atom when introducing electron-donating group. However, if replaced R<sub>1</sub> with hydrogen atom and replaced R with methyl group, the obtained catalytic activity were lower than **2**. And when the methyl group at R position is replaced by phenyl group, the lowest catalytic activity was observed.

Lü et al. [39] used three Ti complexes; 2-(tetramethylcyclopentadienyl)-4,6-di-*tert*-butylphenoxytitanium dichloride (**1**), 2-(tetramethylcyclopentadienyl)-6-*tert*-butylphenoxytitanium dichloride (**2**), and 2-(tetramethylcyclopentadienyl)-6-

phenylphenoxytitanium dichloride (**3**) as catalyst and applied them for propylene polymerization. The result shows that the catalytic activity was found to be **1** > **2** > **3**. This behavior is related to the electronic nature of the substituent on the phenolate ligand and the electronic property of the substituent at both *para* and *ortho* positions of phenolate ligand plays a significant role.

- **Variation of the metal center**

After discovered constrained geometry catalysts, the metal transition like zirconium (Zr), titanium (Ti) and hafnium (Hf) have been applied as metal center for homo- and copolymerization of  $\alpha$ -olefins. Based on cyclopentadienyl Group 4 complex, zirconium was found to be the most active metal center among the other metal complexes [40].

## 2.3 Cocatalysts

Since the discovery of metallocene catalysts, there have been many attempts to improve the catalytic activity through changing the catalyst structure and condition for polymerization. As the reacting metallocene catalyst with an activator like aluminoxane cocatalyst was found to be an effective way to enhance catalytic activity.

The structure of aluminoxane compound is a “black box chemical” Aluminoxane cocatalysts are understood as molecular species which consist of aluminium atom bridged to oxygen atom. In practice, aluminoxanes can be obtained from hydrolysis reaction. It is synthesized by reacting trimethylaluminum (TMA) with crystal water of  $\text{CuSO}_4 \cdot 5\text{H}_2\text{O}$  or  $\text{MgCl}_2 \cdot 6\text{H}_2\text{O}$  [41-43]. Although there are many types of aluminoxane cocatalysts to activate metallocene catalysts such as ethyl-, iso- or tert-, butyl-aluminoxane, only methylaluminoxane (MAO) cocatalyst exhibits higher catalytic activity. The most favorable model for MAO species is to assume as a cage built from six-membered rings consisting of MeAlO building blocks (**Figure 2.6**).

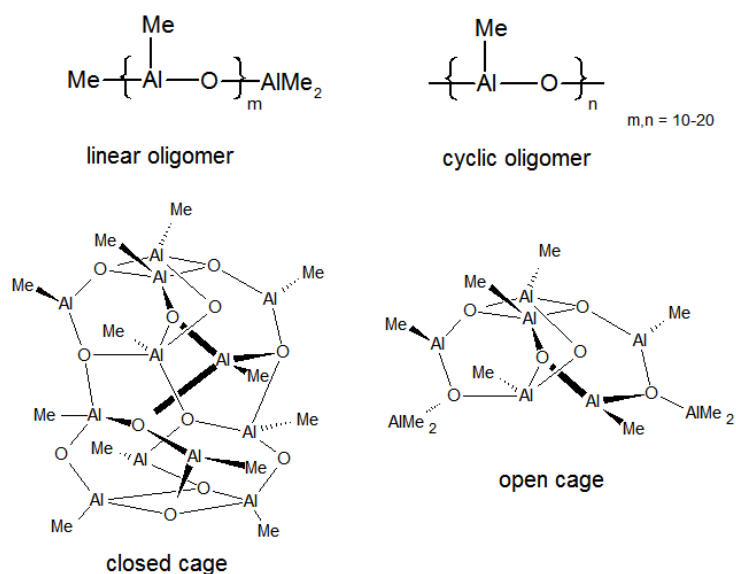


**Figure 2.6** Idealized structure of MAO cocatalyst [44]

The functions of MAO cocatalyst in metallocene catalyst system can be described as below

- MAO methylates the metallocene dihalide ( $\text{Cp}_2\text{ZrCl}_2$ ) to give  $\text{Cp}_2\text{ZrMeCl}$  and  $\text{Cp}_2\text{ZrMe}_2$  species
- MAO abstracts chloride or methide anion with the formation of a  $[\text{Cp}_2\text{ZrMe}]^+$  cation and a weakly coordinating  $[\text{Cl-MAO}]^-$  or  $[\text{Me-MAO}]^-$  anion [45]
- MAO is a scavenger for deactivating impurities in the monomer or solvent.

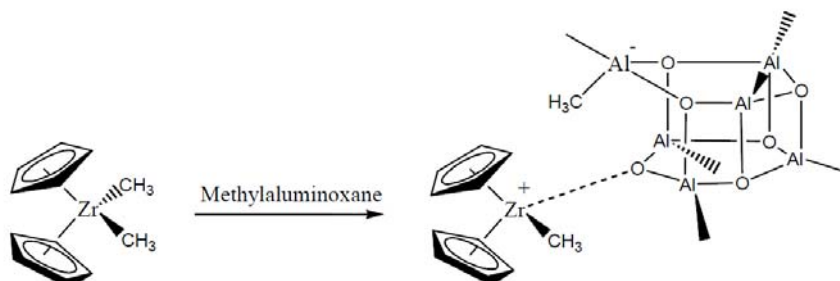


**Figure 2.7** The activation of zirconocene catalyst by MAO cocatalyst [46]

Modified methylaluminoxane (MMAO): MAO is readily soluble in aromatic solvents such as benzene and toluene but it has limited solubility in aliphatic hydrocarbons. To overcome this limitation, methyl group in MAO was replaced with isobutyl groups. This new product is called “modified methylaluminoxane or MMAO”. MMAO can be synthesized by hydrolyzing the mixture of  $\text{AlMe}_3$  and  $\text{Al}^i\text{-Bu}_3$ . Comparing the efficiency between MAO and MMAO, it demonstrated that their efficiency is similar, but its solubility of MMAO in aliphatic hydrocarbons makes it more attractive in polyolefin field.

## 2.4 Polymerization mechanism

The better understanding on mechanisms and kinetics involved in polymerization reaction help us predicting the structure of the obtained polymer. It can describe rates of propagation and chain termination from the molecular weight, molecular weight distribution and comonomer composition results. Therefore, it is important to know how mechanism and kinetic do in polymerization reaction.

### 2.4.1 Mechanism of chain growth

**Table 2.1** presents the catalyst activation and propagation mechanism in metallocene-catalyzed polymerization. Firstly, neutral metallocene catalyst ( $\text{L}_2\text{MCl}_2$ ) is activated by Lewis acid (i.e. methylaluminoxane) to form a cationic metal center [47-48]. After that, 1-olefin monomer is coordinated and inserted via a metal transition center [48-49].

**Table 2.1 Schematic activation and propagation reactions in polymerization**

Reaction	Reaction path
Activation	$\text{L}_2\text{MCl}_2 + \text{MAO} \rightarrow \text{L}_2\text{M}^+-\text{CH}_3 + [\text{MAO}-\text{Cl}_2]^-$
Propagation	$\text{L}_2\text{M}^+-\text{CH}_2\text{CH}_2\text{R} + \text{CH}_2=\text{CH}_2 \rightarrow \text{L}_2\text{M}^+-\text{CH}_2\text{CH}_2\text{CH}_2\text{CH}_2\text{R}$

L= ligand, MAO= methylaluminoxane; M= Ti, Zr, or Hf [50]

For homogeneous metallocene catalyst systems, the termination of the growing polymer chain is mostly caused by chain transfer reactions, including transfer to monomer, to metal alkyls and to the transfer agent, as well as also caused by thermal cleavage of the active center involving  $\beta$ -H elimination. The chain transfer reactions are described as below.

#### **2.4.2 Chain transfer reactions**

The most common chain transfer mechanisms involved in metallocene catalyzed ethylene polymerization are described as follows [46]

For the  $\beta$ -hydrogen elimination, metal active center abstracts hydrogen atom bonded  $\beta$ -C of the growing polymer chain, thus leading to the formation of M-H bond (M=transition metal) and polymer with an unsaturated end. While the chain transfer by monomer,  $\beta$ -Hydrogen elimination and olefin monomer insertion at the active center take place simultaneously without forming the M-H bond. In case of chain transfer to aluminum, growing polymer chain exchanges methyl group of MAO at the attached position. M-CH<sub>3</sub> bond is formed and polymer chain is terminated with Al. However, all of the mechanisms as described above are dependent on the nature of the metallocene, aluminoxane cocatalyst, and the polymerization conditions.

### **2.5 Ethylene Homopolymerization**

Ethylene homopolymerization is usually done in order to understand the basic of the influence of catalyst structure, the catalyst concentration, effect of polymerization temperature and effect of type and concentration of cocatalyst. Ethylene homopolymerization reaction can be simplified described as following:

Firstly, MAO cocatalyst alkylates catalyst precursor to form active site. It is well known that the active species of metallocene catalyst is an ion pair of a metallocenium cation and anion derived from cocatalyst. The active site is stabilized with an excess of MAO. After that,  $\alpha$ -olefin monomer diffuses to active center, and competitive interacts between monomer and active center. It causes the chain



initiation and chain propagation at active site. Lastly, it is terminated to form precipitated solid polymer.

**Table 2.2 Schematic chain transfer reactions in polymerization [51]**

Chain transfer reaction	Reaction components	End-groups
Chain transfer to monomer	$M^+-CH_2CH_2R + CH_2=CH_2$	$\rightarrow M^+-CH_2CH_3 + CH_2=CHR$
$\beta$ -H elimination	$M^+-CH_2CH_2R$	$\rightarrow M^+-H + CH_2=CHR$
Chain transfer to aluminum	$M^+-CH_2CH_2R + AlR'_3$	$\rightarrow M^+-R' + R'_2AlCH_2CH_2R$
Chain transfer to hydrogen	$M^+-CH_2CH_2R + H_2$	$\rightarrow M^+-H + CH_3CH_2R$

M= Ti, Zr or Hf

## 2.6 Copolymerization of ethylene/ $\alpha$ -olefins

According to strong demand of linear low density polyethylene (LLDPE), copolymerization of ethylene and  $\alpha$ -olefin is an important reaction for polyolefin production. Although Ziegler-Natta catalysts have been commonly used in the LLDPE production due to their low cost, some plastics industries for film and container also continuously produce LLDPE with metallocene catalysts. This is because LLDPE obtained from metallocene catalysts have many outstanding properties compared to the conventional Ziegler-Natta ones. For example, LLDPE produced with single-site metallocene catalysts exhibit an improvement of toughness, puncture, tensile and impact properties. At the same strength, metallocene can produce LLDPE film thinner than Ziegler-Natta catalysts [52]. Therefore, these catalysts are of interest for many reasons. LLDPE is the copolymer of ethylene and  $\alpha$ -

olefins such as 1-butene, 1-hexene and 1-octene. The used  $\alpha$ -olefin affects on the properties of LLDPE. Therefore, the better understanding on basic of comonomer effect would increase the development of polyolefin process [53].

An improvement of polymerization rate in ethylene polymerization by adding comonomer is called “comonomer effect”. This effect can be found not only in Ziegler-Natta catalysts but also in metallocene catalysts in zirconium and titanium metal atom. This interesting phenomenon can be described in chemical and physical functions [54-56].

For chemical function, an addition of comonomer increases the number of active center ( $C^*$ ). Taniike et al. [57] revealed that comonomer can activate potential active site which is not easily to activate by ethylene monomer, thus leading to an increase in polymerization rate. For physical function, the introduction of comonomer decreases the crystallinity of the obtained polymer, resulting in a less-crystalline copolymer. Therefore, monomer is easier to diffuse and react with active site, and thus leads to the better catalytic activity. Moreover, it is also found that comonomer can accelerates the fragmentation of catalyst during polymerization and causes the new active sites in heterogeneous system.

Due to its higher electrophilicity of metal center, Karol et al. [58] reported that  $\alpha$ -olefin can act as ligands, coordinate to the active center, and cause the greater separation between cationic metal centers. Thus, an enhancement on the catalytic activity was observed.

The study of Hong et al. [59] reported that when increasing comonomer content, the catalytic activity was increased. And the order of catalytic activity was 1-decene > 1-octene > 1-hexene. The enhancement of catalytic activity is related to an improvement of monomer diffusion in the lower crystalline copolymer.

Jin-San Yoon et al. [60] described the copolymerization results of ethylene and 1-hexene catalyzed with  $(2\text{-MeInd})_2\text{ZrCl}_2$  catalyst. It depicted that the catalytic activity was increased with an increase in 1-hexene concentration in feed. This

behavior is attributed to the fact that the presence of comonomer resulted in lower polymer crystallinity, leading to more polymer swelling in medium. It would allow easier monomer to enter to active site.

However, the opposite trend has been reported. Z. Yu et al. [61] studied the effect of termonomers on terpolymerization. They found that an increase in 1,4-hexadiene content decreased catalytic activity. This is attributed to the forming chelates with active center of catalyst. A similar tendency was observed in (ethylene-*ter*-1-octene-*ter*-styrene) terpolymerization. This behavior is called “negative comonomer effect”.

## 2.7 Ethylene terpolymerization

Nowadays, polyolefins play a fundamental role in life because they exhibit many useful properties. They have been used to produce many products such as plastics film, shopping bags and house appliances. In addition, in the recent years, it was found that the new polymer namely “elastomers” is one of the most-in demand groups of materials. The world demand for elastomers is forecasted to increase over 6 percent per year through 2013. Therefore, an improvement in these materials is crucial and will keep on playing an important role in the future. The well-known elastomer is (ethylene-*ter*-propylene-*ter*-diene) polymer or EPDM. The beginning of commercial production to produce this terpolymer used Ziegler-Natta catalysts for solution polymerization process. Vanadium compound such as  $VCl_4$  and  $VOCl_3$  was applied in this process. However, due to the remaining vanadium in the polymer over 10 ppms, it causes the toxicity, aging and discoloration in polymer [18]. Therefore, it is needed to overcome these drawbacks.

After metallocene catalysts was found to be an attractive catalysts for olefin polymerization. Many researches both in academic and industrial institutions have focused on developing these catalysts. By applying metallocene catalysts in terpolymerization production, the obtained products are free from the toxic vanadium

compound and have uniform molecular weight distribution. Therefore, it is interesting to apply metallocene catalysts to produce new polymer material.

Instead of EPDM, several monomers have been applied for producing terpolymer materials such as (ethylene-*ter*-propylene-*ter*-butadiene) polymer [15], (ethylene-*ter*-norbornene-*ter*-1-octene) polymer [16], and (ethylene-*ter*-propylene-*ter*-1-octadecene) polymer [17]. Moreover, one of the most interesting aspects in this field is the introduction of polar functional group in polyolefin. The introduction of functional group into polymer not only makes the new material, but also improves the properties of polymer such as compatibility, adhesion and dyeability. However, the deactivation of these catalysts caused by the coordination of functional groups to the metal center is the limitation for applying these catalysts [62]. Therefore, the possible way for synthesizing polymer containing functional group is to the use of a precursor monomer possessing double bond in molecule. The functionalized polyolefin is obtained by converting double bond into polar functional group. Most of reacting groups that have been applied for synthesizing functionalized polyolefin is vinyl, vinylidene, epoxide and alcohol. Dicyclopentadiene (DCP) is one of the attractive precursor monomer used for synthesizing functionalized polyolefin due to its industrially available at low price and its many desirable properties such as good transparency [63]. Dicyclopentadiene is a molecule that contains both norbornene unit and cyclopentene unit. If one of double bond in dicyclopentadiene selectively participates in ethylene and  $\alpha$ -olefin terpolymerization, the remaining double bond in dicyclopentadiene may possibly generated the cross-linking leading to the synthesizing elastomer material as well as the functionalized material that can be obtained via converting reacting group into desirable polar material [64-65].

## **2.8 Performance improvement of polyolefin with metallocene catalysts**

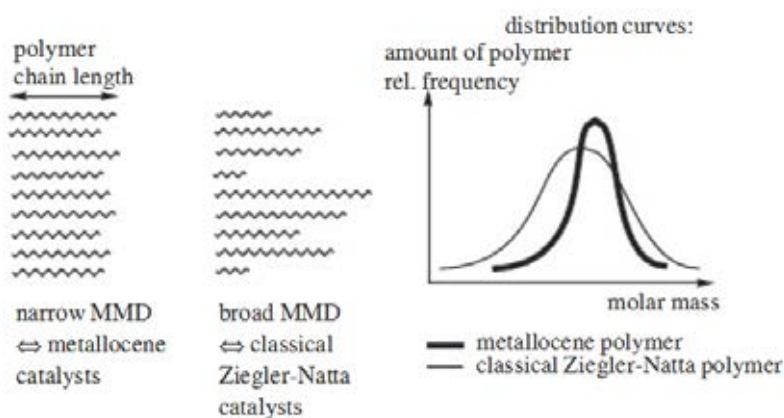
Due to the tailor-made property of metallocene catalysts, the properties of polymer can be controlled by tuning the catalyst structure. Metallocene catalysts

exhibit an improvement in chemical and mechanical properties. Some of properties that are modified include better clarity, reduced haze and increased toughness and chemical resistance [66]. Additional improvement in polyolefin performance with metallocene catalysts are described as below;

(i) These catalysts eliminate very low and very high molar mass polymer fractions presented in the conventional Ziegler-Natta catalysts [44] (**Figure 2.8**). The properties of polyethylene with narrow molecular weight distribution ( $MWD \approx 2$ ) such as toughness, puncture, tensile, tear, and impact performance are enhanced. It is found that for LLDPE film, at the same strength, LLDPE film produced by metallocene catalysts afford thinner than obtained from Ziegler-Natta catalysts. For polypropylene, a narrow molecular weight distribution polypropylene improves processability in fiber extrusion processes. Polypropylene with narrow molecular weight distribution is harder, more crystalline, and more transparent. In addition, it can be recycled more often without losing toughness [66].

(ii) Metallocene catalysts produce polymer with uniform amount of comonomer and comonomer distribution. These catalysts offer better optical properties, such as, better clarity and less haze. And they also improve sealing performance and lower seal initiation temperature versus conventional polyolefins (**Figure 2.9**).

(iii) Ziegler-Natta catalysts produce isotactic polypropylene with some fraction of atactic thus leads to some of properties such as the stiffness, heat distortion temperature, and cleanliness properties are declined. While polymer obtained from metallocene catalysts is absence of atactic polypropylene. The stiffness property is improved and can be applied them at the high temperature.



**Figure 2.8 Schematic representation of molar mass distribution (MWD) [44]**

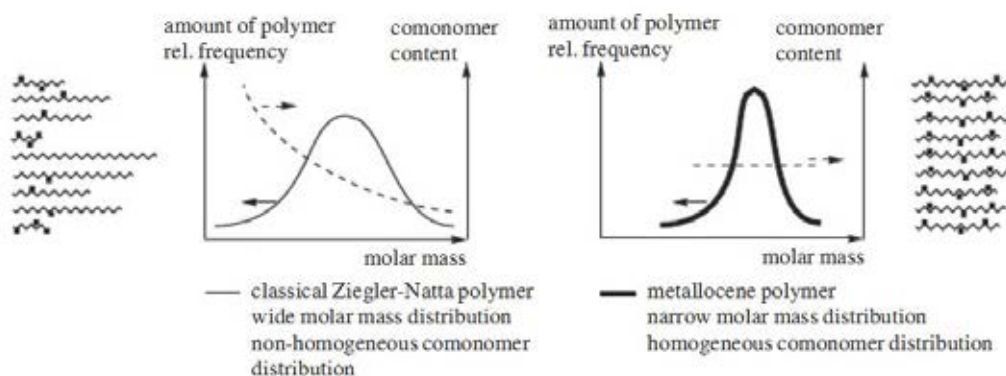


**Figure 2.9 Schematic representation of comonomer distribution [44]**

## 2.9 Polyolefin Industry-Outlook

In plastics industry, polyolefin is one of the largest businesses with a lot of worldwide production, especially polyethylene. This is because they exhibit many useful properties such as low density, high strength and resistance to chemical attack, as well as being cost effective. Therefore, it has been used to produce many products such as shopping bags, plastics films and house appliances. The global polyethylene consumption is forecasted to increase in the next three years and the consumption is also continued.

In fact in the class of polyethylene, linear low-density polyethylene (LLDPE) is important for the plastic industry for film and container. The LLDPE demand by region continuously increases from the year 2005 and up to now [67]. Although in 2002, the market share of LLDPE produced from metallocene catalysts shows only 2-3%, the demand of linear low-density polyethylene produced from metallocene (mLLDPE) is forecast to strong advances nearly to 7-10% in 2006. North America is the leader consuming region with approximately 42% of the global consumption. The reasons for the still low market share are economics and process ability. Metallocene-catalyzed polymers are more expensive due to the high cost of aluminoxane cocatalyst.

In order to overcome this drawback, many methods have been made to reduce the amount of MAO in polymerization. The effective way is to immobilize aluminoxane cocatalyst on support materials. This method is called “Heterogenization of single-center catalysts”.

# CHAPTER III

## EXPERIMENTAL

### 3.1 Objectives of this research

The first objective is to evaluate the influence of catalyst structure on catalytic activities, polymer properties and monomer reactivity ratios. It is generally accepted that monomer reactivity ratios are an important parameter for determining copolymerization behavior. They allow predicting and estimating comonomer composition and microstructure of polymers. The copolymerization of ethylene and 1-hexene with two constrained geometry titanium complexes are investigated.

In the second aim, the influence of termonomers on terpolymerization system is investigated. As known, these characteristics were mainly dependent on “comonomer effect” which is found in Ziegler-Natta and metallocene catalysts with the presence of comonomer. Therefore, it is possible to change catalytic activity and properties of polymer by varying termonomer concentration.

The third aim of this research is to obtain an understanding of comonomer chain length on copolymerization systems. We selected comonomers with varied chain length from 1-hexene (1-C6) up to 1-octadecene (1-C18) in order to define the influence of comonomer chain length on copolymerization activity and polymer properties. It is well known that polymer properties such as melting temperature and degree of crystallinity are found to be significantly affected by comonomer concentration. These results depend on not only concentration in feed, but also on the comonomer chain length. Although comonomer short chain length is widely used in LLDPE commercial production, comonomer with long chain length which has not been studied so far may become more potential in future commodity applications.



### 3.2 Scopes of this research

- Preparation of *ansa*-Dimethylsilylene(fluorenyl)(*t*-butylamido)-dimethyl titanium dimethyltitanium complex,  $\text{Me}_2\text{Si}(\eta^3\text{-C}_{13}\text{H}_8)(\eta^1\text{-N}^t\text{Bu})\text{TiMe}_2$  (**complex 1**), and its tetraalkylsubstituted-fluorenyl derivative,  $\text{Me}_2\text{Si}(\eta^3\text{-C}_{29}\text{H}_{36})(\eta^1\text{-N}^t\text{Bu})\text{TiMe}_2$  (**complex 2**)
  - Characterization of ligands and complexes by  $^1\text{H}$  NMR
  - Study and characterization for the effect of CGC catalyst structure on catalytic activity and polymer properties during ethylene/1-hexene copolymerization by GPC and  $^{13}\text{C}$  NMR analysis (as referred in Part 1).
    - Study the influence of termonomers on terpolymerization behavior and thermal properties during ethylene/1-hexene/dicyclopentadiene terpolymerization by DSC and  $^{13}\text{C}$  NMR measurements (as referred in Part 2).
    - Study the effect of comonomer chain length to ethylene with various 1-olefins copolymerization in terms of catalytic activity, morphology and polymer properties. These characteristics were determined by SEM, XRD, DSC and  $^{13}\text{C}$  NMR measurements (as referred in Part 3).

### 3.3 Research methodology

The flow diagram research methodology is shown in **Figure 3.1**.

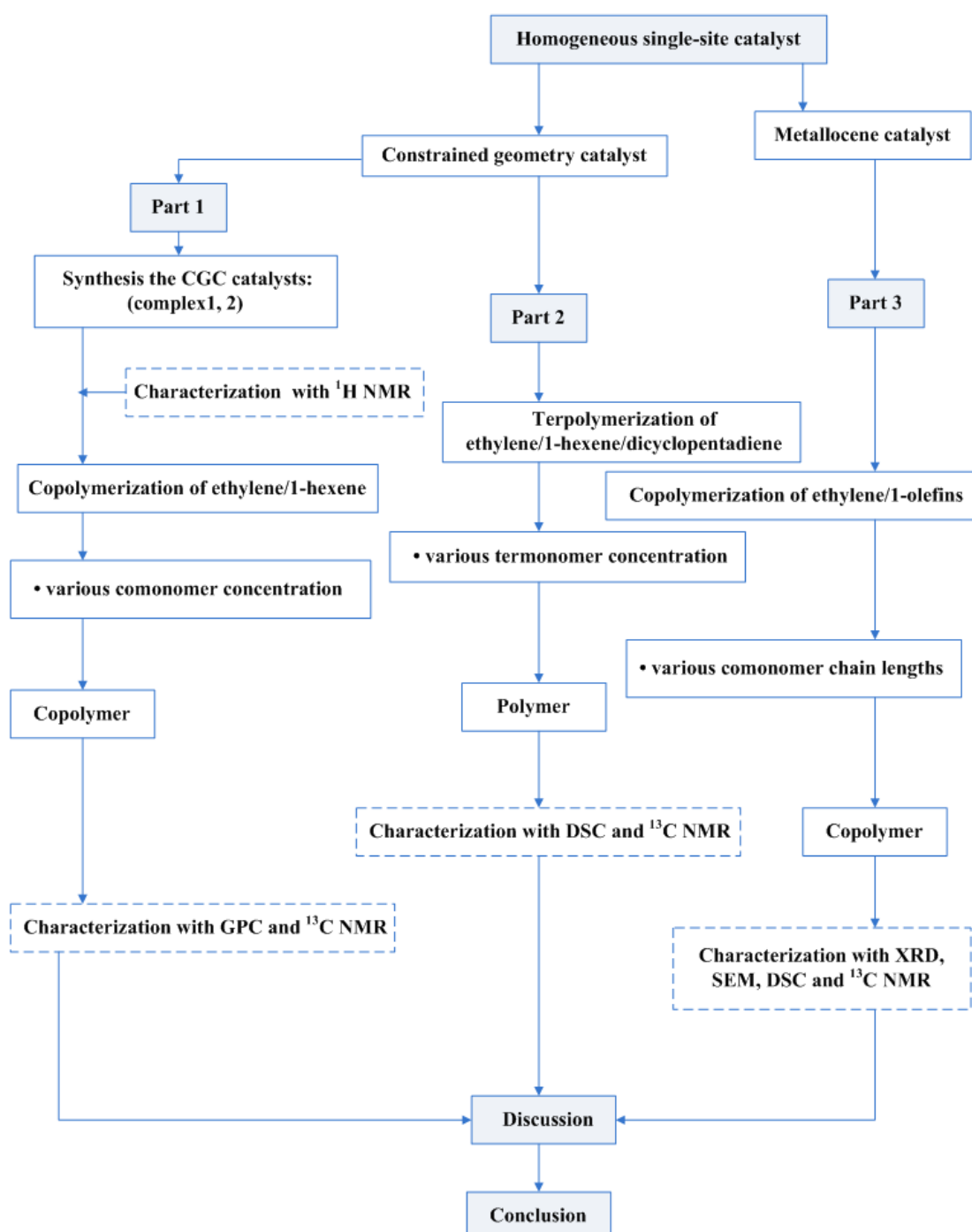


**Figure 3.1** Flow diagram of research methodology

## 3.4 Experimental

### 3.4.1 Materials

All reactions were performed under argon atmosphere. Catalysts were handled in a glove box under an inert atmosphere with maximum O<sub>2</sub> and H<sub>2</sub>O levels of 0.1 ppm and 0.1 ppm, respectively. *racemic* Ethylene bis(indenyl)zirconium dichloride (*rac*-Et(Ind)<sub>2</sub>ZrCl<sub>2</sub>) was purchased from Sigma Aldrich. A 20 wt% of the modified methylaluminoxane (MMAO) in toluene was donated from PTT Public Co., Ltd., Thailand, while MMAO (1.86M in toluene) was donated from Tosoh Akso, Japan. Toluene and n-hexane (SR Lab) was distilled over sodium/benzophenone under argon atmosphere before use. 1-olefins (99+%) was purchased from Aldrich Chemical Company, Inc. and purified by distilling over CaH<sub>2</sub> before use. TiCl<sub>4</sub> (99+ %) was purchased from Wako. Tetrahydrofuran (THF) (anhydrous grade) and Dichloromethane (CH<sub>2</sub>Cl<sub>2</sub>) (Anhydrous grade) were purchased from Aldrich Chemical Company, Inc. and used without further purification, while 1.63 M of *n*-butyllithium (*n*-BuLi) in hexane and 1.6 M *n*-methyllithium (*n*-MeLi) in hexane were purchased from Aldrich Chemical Company, Inc. Diethyl ether (Et<sub>2</sub>O) (Anhydrous grade) was purchased from Aldrich Chemical Company, Inc. and purified by distilling over sodium/benzophenone under argon atmosphere before used. Fluorene (99 %) and *tert*-butylamine (99 %) were purchased from Aldrich Chemical Company, Inc. Ethylene (99.96%) was purchased from Thai Industrial Gas Co., Ltd. Ultra high purity argon gas (99.999%) was purchased from Linde Co., Ltd., and purified by passing over columns of BASF Catalyst R3-11G, sodium hydroxide (NaOH), phosphorus pentoxide (P<sub>2</sub>O<sub>5</sub>) and molecular sieve 3A before introduction into schlenk line.

### 3.4.2 Equipments

Because of the organometallic compound is sensitive to air and moisture. Thus, all manipulations were performed under an argon atmosphere, using standard Schlenk techniques. And additional components were described below.

- **Cooling system**

The cooling system is in the solvent distillation in order to condense the freshly evaporated solvent.

- **Inert gas supply**

The inert gas (argon) was purified by passing over columns of BASF catalyst R3-11G supported oxygen scavenger and molecular sieves 3 Å. The BASF catalyst will be regenerated by treatment with hydrogen at 300 °C overnight before flowing of the argon gas through all of the columns mentioned above.

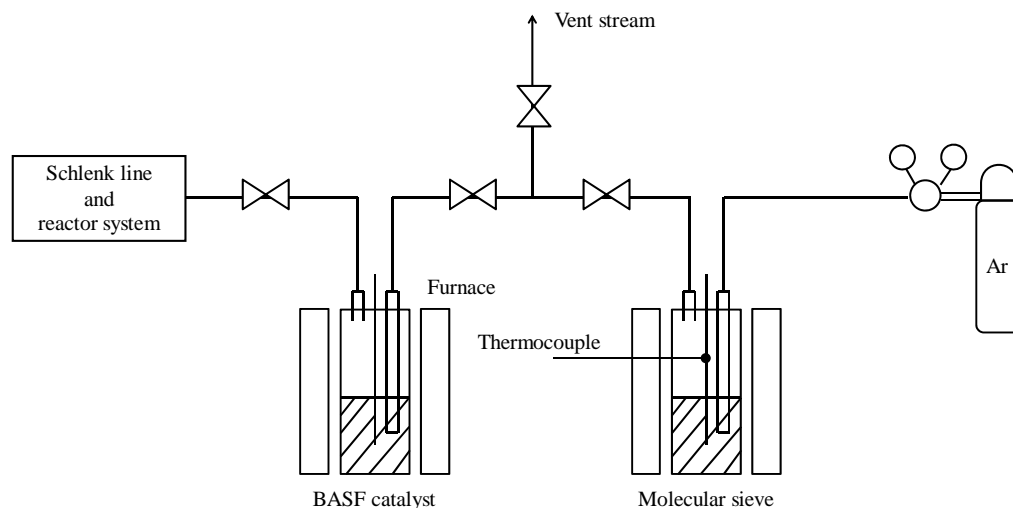


**Figure 3.2 Inert gas supply system**

- **Magnetic stirrer and heater**

The magnetic stirrer and heater model RTC basis from IKA Labortechnik was used.

- **Reactor**

A 100 ml of glass flask was connected with three-ways valve used as the copolymerization reactor for atmospheric pressure system and a 100 ml stainless steel autoclave was used as the copolymerization reactor for high pressure systems.

- **Schlenk line**

Schlenk line consists of vacuum and argon lines. The vacuum line will be equipped with the solvent trap and vacuum pump, respectively.

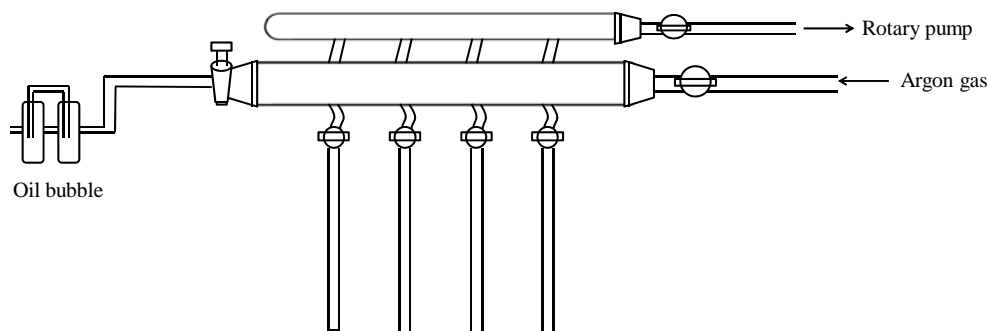


**Figure 3.3 Schlenk line**

- **Schlenk tube**

Schlenk tube is a tube with a ground glass joint and side arm, which is three-way glass valve. Schlenk tubes having size of 50, 100 and 200 ml. will be used for catalyst preparation and storage materials which are sensitive to oxygen and moisture.

- **Vacuum pump**

The vacuum pump model 195 from Labconco Corporation was used. A pressure of  $10^{-1}$  to  $10^{-3}$  mmHg will be adequate for the vacuum supply to the vacuum line in the Schlenk line.

- **Polymerization line**

Polymerization line is composed of ethylene storage tank, pressure regulator for ethylene consumption, mass flow meter, 100 ml semibatch stainless steel autoclave reactor equipped with magnetic stirrer, thermometer, water bath, hot plate and other fittings. This system is schematically represented in **Figure 3.4**.

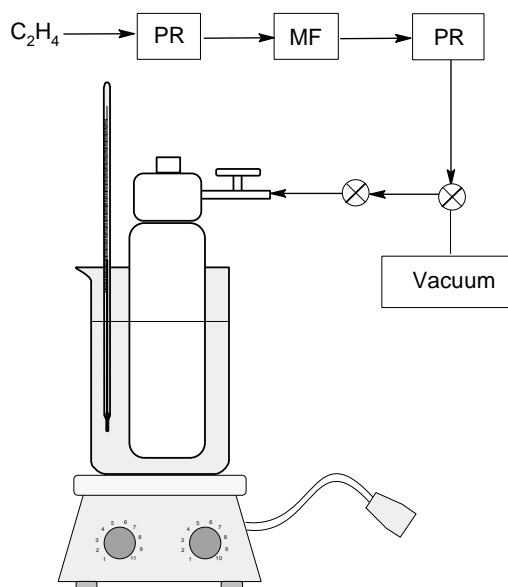


**Figure 3.4 Diagram of system in slurry phase polymerization**

### 3.4.3 Characterization techniques

- **X-ray diffraction analysis (XRD)**

The X-ray diffraction (XRD) patterns of the obtained polymers were performed by an X-ray diffractometer SIEMENS D5000 connected to a personal computer with Diffract AT version 3.3 program for fully control of the XRD analyzer at Center of Excellences on Catalysis and Catalytic Reaction Engineering, Chulalongkorn university. Samples were carried out by using  $CuK_{\alpha}$  radiation with Ni filter and the operating conditions for measurement is shown below.

$2\theta$  range of detection :  $20 - 80^{\circ}$

Resolution :  $0.04^{\circ}$

Number of scan : 10

The functions of based line subtraction and smoothing were used in order to get the well formed XRD spectra..

- **Nuclear magnetic resonance spectroscopy (NMR) part 1, 2**

Polymers were determined by  $^{13}\text{C}$  NMR (125.65 MHz) spectroscopy at 130°C on a JEOL GX 500 NMR spectrometer operated at in the pulse Fourier-Transform mode. The pulse angle was 45° and about 10,000 scans were accumulated in pulse repetition of 5.0 s. Polymer samples were prepared by dissolved in 1,1,2,2-tetrachloroethane- $d_2$  and the central peak of the solvent (74.47 ppm) was used as an internal reference.

- **Nuclear magnetic resonance spectroscopy (NMR) part 3**

The  $^{13}\text{C}$  NMR spectra were determined at 110 °C using BRUKER Bruker 400 MHz NMR Spectrometer (Germany). Polymer samples were dissolved in 1,2,4-trichlorobenzene with deuterated chloroform- $d_3$  as lock solvent. The central peak of the solvent was appeared at 77.0 ppm used as an internal reference.

- **Scanning electron microscope (SEM)**

Polymer morphology was studied on a Hitachi VP-SEM S-3400N Scanning Electron Microscope (Germany) at Centre of Research and Technology Development Chulalongkorn University, (MMCT-CU). The coating of sample surface was required

- **Differential scanning calorimetry (DSC)**

The melting temperature of ethylene homopolymers and ethylene with 1-olefin copolymers were determined with a Perkin-Elmer diamond DSC (Germany) from MEKTEC, at the Center of Excellence on Catalysis and Catalytic Reaction Engineering, Chulalongkorn University. Samples (1.5-2.5 mg) were heated to 150°C at the heating rate of 20 °C min<sup>-1</sup> and cooled down at the same speed to 50°C. This was repeated and the second heating scan was used for data analysis, because the first scan will be influenced by the mechanical and thermal history of samples.

- **Gel Permeation Chromatography (GPC)**

Gel Permeation Chromatography (GPC) was used for the determination of molecular weight and molecular weight distribution of the obtained polymer. The polymers were dissolved in *o*-dichlorobenzene at 135°C on a Waters 150CV. The

parameters for universal calibration were  $K=7.36 \times 10^{-5}$ ,  $\alpha = 0.75$  for polystyrene standard.

### 3.4.4 Synthesis of CGC catalysts

*ansa*-Dimethylsilylene(fluorenyl)(*t*-butylamido)-dimethyl-titanium dimethyltitanium complex,  $\text{Me}_2\text{Si}(\eta^3\text{-C}_{13}\text{H}_8)(\eta^1\text{-N}^t\text{Bu})\text{TiMe}_2$  (**complex 1**), and its tetraalkylsubstituted-fluorenyl derivative,  $\text{Me}_2\text{Si}(\eta^3\text{-C}_{29}\text{H}_{36})(\eta^1\text{-N}^t\text{Bu})\text{TiMe}_2$  (**complex 2**) were synthesized using procedure published in literatures [68-70]. The chemical structure of **1** and **2** is shown in **Figure 3.5**. The route for synthesized **1** and **2** are described below.

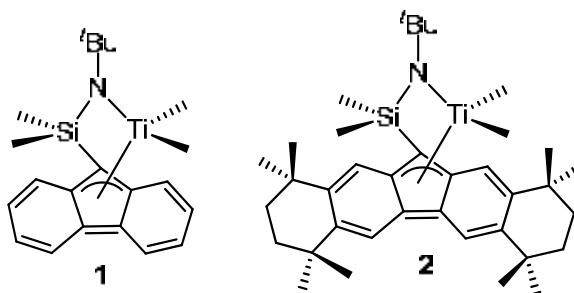


**Figure 3.5** two constrained geometry titanium complexes

- **Synthesis of  $\text{Me}_2\text{Si}(\eta^3\text{-C}_{13}\text{H}_8)(\eta^1\text{-N}^t\text{Bu})\text{TiMe}_2$  (complex 1)**

The synthesis of  $\text{Me}_2\text{Si}(\eta^3\text{-C}_{13}\text{H}_8)(\eta^1\text{-N}^t\text{Bu})\text{TiMe}_2$  (**1**) was carried out followed procedure published in the literature [68-69] and will be briefly described below. (**Figure 3.6**)



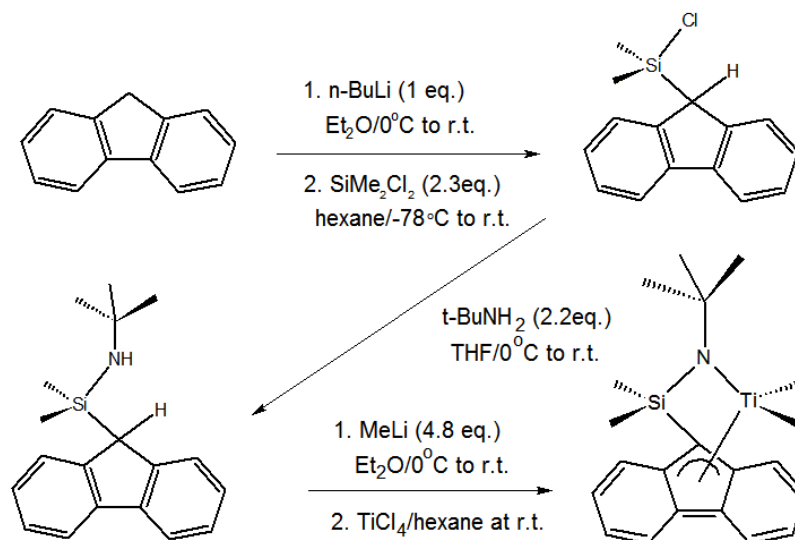


**Figure 3.6 Synthesis of complex 1**

**$\text{ClSiMe}_2(\text{C}_{13}\text{H}_9)$**

$n\text{-BuLi}$  solution (18.49 ml, 30 mmol, 1.63 M in hexane) was dropwise added to a solution of fluorene (5.01 g, 30 mmol) in diethyl ether (70 ml) at  $0^\circ\text{C}$ , and the mixture was stirred for 3 h. at room temperature. Next, the diethyl ether was removed from the  $\text{Li}[\text{Flu}]$  salt and diethyl ether (50 ml) transferred in. After stirring the orange-slurry overnight, it was transferred into the solution of  $(\text{CH}_3)_2\text{SiCl}_2$  flask at  $-78^\circ\text{C}$  over 15 min., resulting in pale-orange slurry. The resultant suspension was stirred overnight at room temperature, and the solvent and the remained dichlorodimethylsilane were removed in vacuum. After the addition of hexane (130 mL), lithium chloride was precipitated and the solution was decanted, followed by removal of the solvent, 6.978 g (27.02 mmol) of 9-(chlorodimethylsilyl) fluorene was obtained as off-white solid.

**$\text{Me}_2\text{CNHMe}_2\text{Si}(\text{C}_{13}\text{H}_9)$**

To a solution of 9-(chlorodimethylsilyl)fluorene in THF (45 mL) was added  $t$ -butylamine (6.25 mL, 59.44 mmol) at  $0^\circ\text{C}$ . Stirring for 5 h. at room temperature gave a yellow-orange suspension. Lithium chloride was precipitated and the solution was

decanted. Removal of the solvent gave *t*-BuNHSiMe<sub>2</sub>Flu as yellow oil (6.696 g, 22.66 mmol, 75% yield).

### **Me<sub>2</sub>Si(η<sup>3</sup>-C<sub>13</sub>H<sub>8</sub>)(η<sup>1</sup>-N<sup>t</sup>Bu)TiMe<sub>2</sub> (1)**

To a solution of Me<sub>2</sub>Si(η<sup>3</sup>-C<sub>13</sub>H<sub>8</sub>)(η<sup>1</sup>-N<sup>t</sup>Bu)TiMe<sub>2</sub> (1.44 g, 4.88 mmol) in Et<sub>2</sub>O (60 mL) was slowly added excess MeLi (20.6 mL, 23.42 mmol 1.14 M in Et<sub>2</sub>O) at 0°C and the mixture was stirred for 5 h. A new flask, TiCl<sub>4</sub> (0.54 mL, 4.88 mmol) diluted with 30 mL of hexane and was added a solution of the dilithium salt in Et<sub>2</sub>O at room temperature. The resulting dark green suspension was stirred overnight at room temperature. After the solvent was removed, the residue was extracted with hexane (100 mL). To the hexane solution was added MeMgBr (4.1 mL of a 3.0 M solution in Et<sub>2</sub>O), and the resulting mixture was stirred for 1 h at room temperature. After the solvent was removed, the residue was extracted with hexane (80 mL). The hexane solution was concentrated and cooled overnight at -30°C to give orange-red crystals (0.48 g, 1.30 mmol, 27%).

- **Synthesis of Me<sub>2</sub>Si(η<sup>3</sup>-C<sub>29</sub>H<sub>36</sub>)(η<sup>1</sup>-N<sup>t</sup>Bu)TiMe<sub>2</sub> (complex 2)**

A sterically expanded complex 2 was synthesized according to the literature [70] and will be described below.

### **Octamethyloctahydrodibenzofluorene**

The octamethyloctahydrodibenzofluorene (C<sub>29</sub>H<sub>38</sub>) was prepared according to the literature (**Figure 3.7**) [33]. A flask was charged with fluorine (10g, 60 mmol) and 2,5-dichloro-2,5dimethylhexane (22 g, 120 mmol), which were dissolved in 450 ml of nitromethane. The flask was equipped with a dropping funnel, which was charged with AlCl<sub>3</sub> solution was added over 10 min, and the purple reaction mixture was stirred for 24 h. before it was slowly poured into 500 ml of ice water. The precipitates were collected by filtration and wash with 400 ml of refluxing ethanol for 2 h. The solid was collected by filtration, and further washed with 300 ml of refluxing hexane for 2 h. The solid was collected by filtration and dried in vacuum, giving the final product as a white-needle solid.

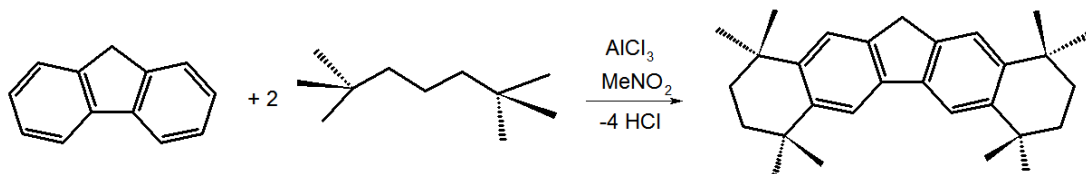
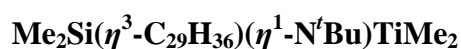
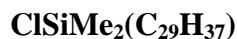


**Figure 3.7 Synthesis of octamethyloctahydrodibenzofluorene**



The synthesis route for  $\text{Me}_2\text{Si}(\eta^3\text{-C}_{29}\text{H}_{36})(\eta^1\text{-N}^t\text{Bu})\text{TiMe}_2$  catalyst were describe below (**Figure 3.8**)

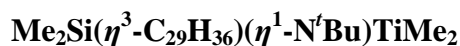


A 300 mL round bottom flask was charged with 3.0 g (7.76 mmol) of octamethyloctahydrodibenzofluorene and diethyl ether (200 mL) was transferred in. Next, *n*-BuLi (5.24 ml, 1.63 M in hexanes) was syringed in over 10 min. and the orange-red slurry was stirred for 4 h. Meanwhile, hexane (40 ml) was transfer into 300 ml round bottom flask, followed by an excess of  $(\text{CH}_3)_2\text{SiCl}_2$  (5.8 mL, 46 mmol). Next, the diethyl ether was removed from the lithium salt  $\text{Li}[\text{OctFlu}]$  prepared earlier and diethyl ether transferred in. After stirring the orange-red slurry overnight, it was transferred into the mixture of  $(\text{CH}_3)_2\text{SiCl}_2$  flask at  $-78^\circ\text{C}$  over 15 min., resulting in pale-orange slurry. After stirring overnight, the hexane and excess  $(\text{CH}_3)_2\text{SiCl}_2$  were removed under vacuum and hexane (130 mL) was transferred in. The LiCl and hexane was removed under vacuum. The product was collected as an off-white solid: 7.429 g (95.51% yields).



THF (50 ml) was added to a  $\text{ClSiMe}_2\text{OctFlu}$  flask, and transferred a solution of *t*-BuNH<sub>2</sub> (8.3 ml, 13 mmol) in diethyl ether to a solution of  $\text{ClSiMe}_2\text{OctFlu}$  at  $0^\circ\text{C}$  and stirred for 5 h. The round bottom flask was allowed to warm slowly to room temperature resulting in the formation of an off-white suspension. Next the

precipitation of ammonium salt and THF were removed. The off-white solid product was collected yielding 3.628 g (90.42%).



$\text{Me}_2\text{Si}(\eta^3\text{-C}_{29}\text{H}_{36})(\eta^1\text{-N}^t\text{Bu})\text{TiMe}_2$  (3.00 g, 6.26 mmol) was charged into a 300 ml round bottom flask, then diethyl ether (120 mL) was transferred in. Next, *n*-BuLi solution (4.8 mL, 7.6 mmol, 1.60 M in hexane) was syringed in. The orange slurry was stirred at 0°C for 4 h. and then a solution of MeLi (15.28 ml, 17.42 mmol) was transferred into. Meanwhile,  $\text{TiCl}_4$  (0.76 ml, 6.968 mmol) was added in 300 ml round bottom flask and hexane (35 mL) transferred in. After slowly warming to room temperature and stirring the slurry for 30 min, the solution was transferred into the  $\text{TiCl}_4$  solution flask, resulting dark-green solution. After stirring the suspension overnight, the mixture was evaporated in vacuum and the residue was extract with hexane 100 ml. Then the hexane solution was concentrated and cooled at -30°C to give catalyst as red crystals.

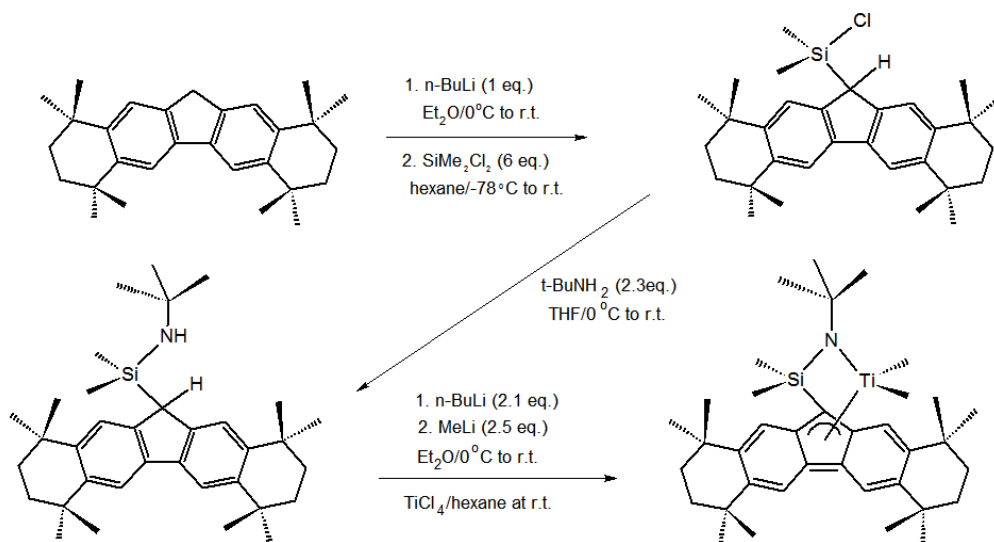


**Figure 3.8** Synthesis of complex 2

### 3.4.5 Ethylene Polymerization Procedures

Referring to the research methodology in **Figure 3.1**, the copolymerization procedure can be classified under each part of the investigation.

- **Ethylene/1-hexene copolymerization Procedure for part 1**

Polymerization was performed in a 100 mL glass reactor equipped with a magnetic stirrer. Under a nitrogen gas flow, the reactor was charged with desired amount of toluene and MMAO cocatalyst. Ethylene gas was charged at an atmospheric pressure after the reactor was evacuated. The reactor was kept in an ice bath until reaching required reaction temperature. After 1-hexene as comonomer was added in reactor, a 1 mL of complex solution (20  $\mu$ mol) in toluene was added to start polymerization. After polymerization finished, acidic methanol was added in. Lastly, it was filtrated, adequately washed with methanol, and dried under vacuum at 373K for 6 h. Experimentally, the polymerization was performed at least three times for each run and only the average yield and activity are reported.

- **Ethylene/1-hexene/dicyclopentadiene terpolymerization**

Terpolymerization was performed in 100 ml stainless steel reactor equipped with a magnetic stirrer. Firstly, the reactor was charged with toluene, desired amount of MMAO cocatalyst and 1 ml of complex solution in toluene. Then, the reactor was kept in liquid nitrogen to stop reaction and was charged with 1-hexene and dicyclopentadiene, respectively. The reactor was feed with ethylene (6 psi) to start polymerization reaction. The reaction was terminated by adding acidic methanol and the obtained polymers were filtrated and dried under vacuum at 323K. The polymerization of each batch was performed at least three times, and only the average yield was reported.

- **Ethylene/ $\alpha$ -olefins copolymerization for Part 3**

Copolymerizations were carried out in a 100 mL semi-batch stainless steel autoclave reactor equipped with a magnetic stirrer. Firstly, in the glove box, the desired amounts of toluene, MMAO and *rac*-Et[Ind]<sub>2</sub>ZrCl<sub>2</sub> catalyst were introduced

into the reactor. After that, the reactor was frozen in liquid nitrogen to stop any reactions and the proper amount of comonomer was injected into the reactor. Then, the reactor was evacuated to remove argon and heated up to polymerization temperature. The polymerization was started by feeding ethylene gas. At the end of polymerization, it was terminated by an addition of acidic methanol. Lastly, the resultant polymer was precipitated, and washed with acidic methanol, then filtered and dried. Experimentally, the polymerization was performed at least three times for each run and only the average yield and activity are reported.

### **3.5 Research benefits**

- Improve the structure feature and electron-donating property of CGC catalyst through the substituent Cp ring in order to make better activity and polymerization ability
- Produce new polyolefin and offer an alternative approach to synthesize polyolefin containing functional group
- Obtain a better understanding on how comonomer chain length would affect on catalytic activity and polymer properties.
- Use this information as reference for academia and industry
- Produce international articles based on this research

## CHAPTER IV

### RESULTS AND DISCUSSION

#### 4.1 Effect of substituent on fluorenyl ligand of CGC catalyst for ethylene/1-hexene copolymerization

Nowadays, in plastics industry, polyolefin is one of the largest businesses with a lot of worldwide production, especially polyethylene. This is because of its useful properties, thus it has been used to produce many products. In fact in the class of polyethylene, linear low-density polyethylene or LLDPE is very important commercial product in plastics industry for film and container. The LLDPE demand by region continuously increases from the year 2005 and up to now. Due to its light weight and good flow property as well as excellent chemical and weather resistance, it has been widely used such as packages, films, and cable coatings. LLDPE is commonly produced by using Ziegler-Natta and metallocene catalysts.

Although Ziegler-Natta catalysts are widely used in LLDPE production, not a few papers have reported that so-called single site catalysts such as metallocene catalysts exhibit good catalytic activity to produce copolymers with narrow molecular-weight and comonomer-composition distributions, leading to better physical properties of LLDPE compared to those produced by Ziegler-Natta catalysts [5-8]. Therefore, many efforts have been made for developing new single catalysts for the synthesis of LLDPE.

Constrained geometry catalysts (CGCs) which possess an *ansa*-cyclopentadienylamido ligand provide many advantages over the conventional metallocene catalysts, including a high comonomer incorporation and high thermal stability. Therefore, many attempts have been made to improve the catalytic performance of CGC by changing the steric and electronic properties of the ligand [9, 11-12].

It was found that *ansa*-dimethylsilylene(fluorenyl)(amido)dimethyltitanium,  $\text{Me}_2\text{Si}(\eta^3\text{-C}_{13}\text{H}_8)(\eta^1\text{-N}^t\text{Bu})\text{TiMe}_2$  (**1**), combined with a suitable cocatalyst conducted not only a syndiotactic-specific living polymerization of propylene and  $\alpha$ -olefin [31], but also homo- and copolymerization of norbornene with ethylene or  $\alpha$ -olefin [32]. The effects of substituent on the fluorenyl ligand was also investigated and found that the introduction of *tert*-butyl groups at 2,7- or 3,6-position improved the activity and the syndiotactic-specificity without disturbing the living nature of the catalyst [29].

Miller et al. synthesized  $\text{Me}_2\text{Si}(\eta^1\text{-C}_{29}\text{H}_{36})(\eta^1\text{-N}^t\text{Bu})\text{ZrCl}_2\cdot\text{OEt}_2$  and reported that the catalytic activity of the complex activated by methylaluminoxane (MAO) for ethylene/1-octene copolymerization was 106 times higher than that for ethylene homopolymerization [33]. They also found that the complex produced highly syndiotactic polypropylene and poly(4-methyl-1-pentene) with high activity. We succeeded in the synthesis of the corresponding Ti derivative,  $\text{Me}_2\text{Si}(\eta^1\text{-C}_{29}\text{H}_{36})(\eta^1\text{-N}^t\text{Bu})\text{TiMe}_2\cdot\text{thf}$ , where tetrahydrofuran was coordinated in place of diethyl ether. We applied it for ethylene/norbornene copolymerization using modified MAO (MMAO) as a cocatalyst and found that the catalytic system showed the excellent ability for the copolymerization [71]. We also synthesized a donor-free Ti derivative,  $\text{Me}_2\text{Si}(\eta^3\text{-C}_{29}\text{H}_{36})(\eta^1\text{-N}^t\text{Bu})\text{TiMe}_2$  (**2**), which was found to show higher activity than the corresponding di-*tert*-butylfluorenyl Ti complexes for homo- and copolymerization of propylene with norbornene [70].

Therefore, in this study, how the modification of fluorenyl ligand on catalytic ability of Ti complexes are considered. Two constrained geometry titanium complexes,  $\text{Me}_2\text{Si}(\eta^3\text{-C}_{13}\text{H}_8)(\eta^1\text{-N}^t\text{Bu})\text{TiMe}_2$  (**1**) and  $\text{Me}_2\text{Si}(\eta^3\text{-C}_{29}\text{H}_{36})(\eta^1\text{-N}^t\text{Bu})\text{TiMe}_2$  (**2**) were synthesized and used as catalyst for ethylene and 1-hexene copolymerization activated by modified methylaluminoxane (MMAO) (**Figure 4.1**).



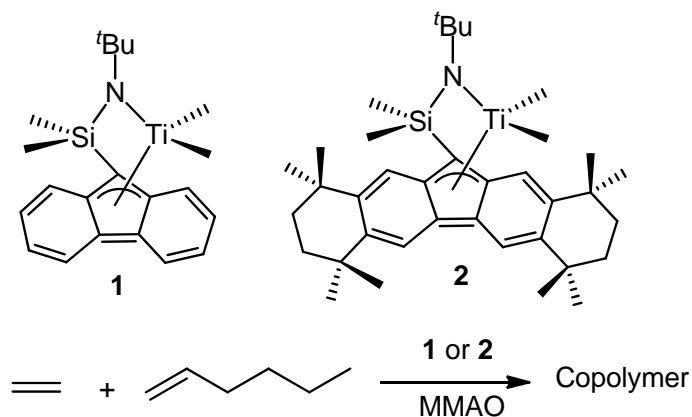


**Figure 4.1** Ethylene/1-hexene copolymerization catalyzed with **1** and **2**

#### 4.1.1 Synthesis of ligand precursors and Ti complexes

For *ansa*-Dimethylsilylene(fluorenyl)(*t*-butylamido) dimethyltitanium complex,  $\text{Me}_2\text{Si}(\eta^3\text{-C}_{13}\text{H}_8)(\eta^1\text{-N}^t\text{Bu})\text{TiMe}_2$  (**1**), it was synthesized via one-pot method which was described in the literatures [66-67] as follows in **Figure 4.2**.

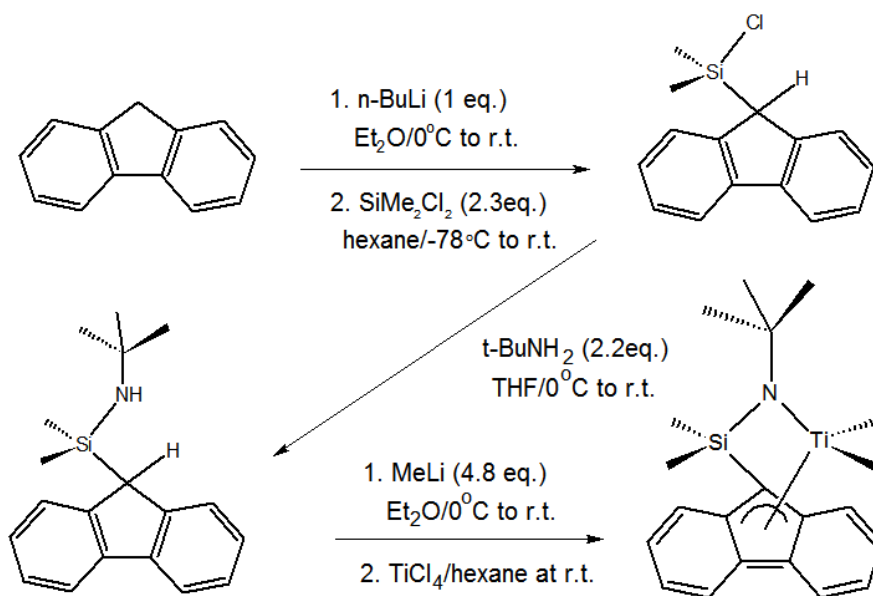


**Figure 4.2** Synthesis of complex **1**

After (chlorodimethylsilyl)fluorene is treated with *tert*-butylamine in THF, the pale yellow oil ligand about 75 % yield is afforded. In order to confirm its structure, the obtained sample was characterized by NMR techniques. The  $^1\text{H}$ -NMR spectrum of this product is shown in **Figure 4.3**. And then, the corresponding ligand was reacted with  $\text{TiCl}_4$  at room temperature to synthesized **1**. The orange-red crystals about 27% yielded from the above reaction. From  $^1\text{H}$ -NMR spectrum as shown in **Figure 4.4**, the signal at chemical shift of  $\delta= 3.76$  ppm which is assigned to proton of  $\text{C}_{13}\text{H}_9$  does not appear. It means that *ansa*-Dimethylsilylene(fluorenyl)(*t*-butylamido)dimethyltitanium complex,  $\text{Me}_2\text{Si}(\eta^3\text{-C}_{13}\text{H}_8)(\eta^1\text{-N}^t\text{Bu})\text{TiMe}_2$  (**1**) is succeeded in synthesizing corresponds to the reference.

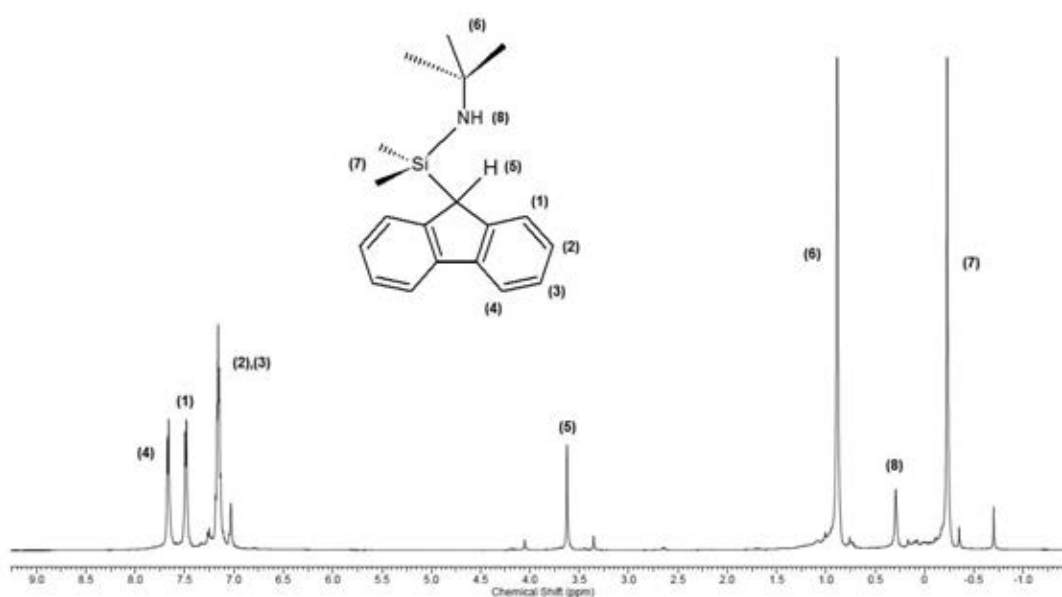


**Figure 4.3**  $^1\text{H}$  NMR spectrum of synthesized  $\text{Me}_2\text{CNHMe}_2\text{Si}(\text{C}_{13}\text{H}_9)$  ligand

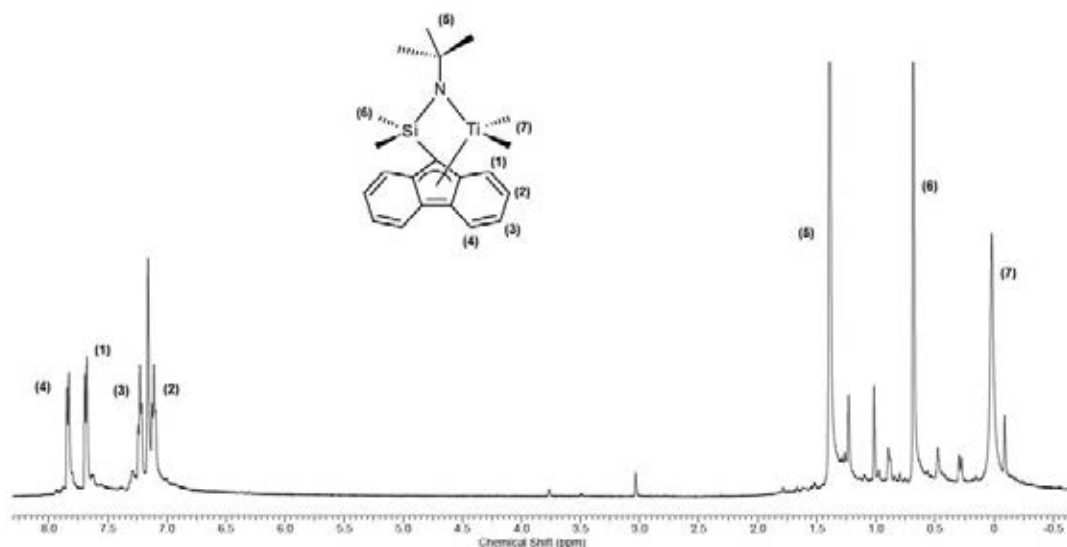


**Figure 4.4**  $^1\text{H}$  NMR spectrum of  $\text{Me}_2\text{Si}(\eta^3\text{-C}_{13}\text{H}_8)(\eta^1\text{-N}^t\text{Bu})\text{TiMe}_2$  complex

For the synthesis of  $\text{Me}_2\text{Si}(\eta^3\text{-C}_{29}\text{H}_{36})(\eta^1\text{-N}^t\text{Bu})\text{TiMe}_2$  (**2**), the octamethyloctahydrodibenzofluorene ( $\text{C}_{13}\text{H}_{38}$ ) was firstly synthesized according to the procedure [33]. As a result, the white needle-like crystals 52% in yields are found from this reaction (**Figure 4.5**). The  $^1\text{H}$ -NMR spectrum of the complex is shown in **Figure 4.6**.

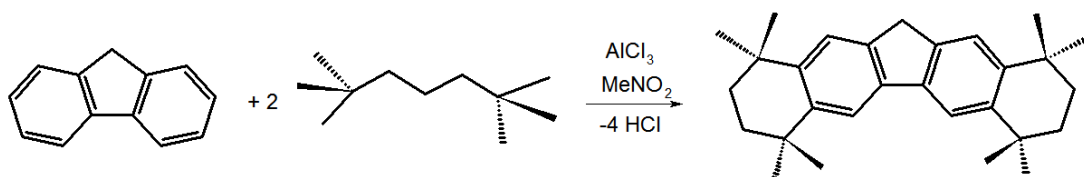


**Figure 4.5** Synthesis of octamethyloctahydrodibenzofluorene

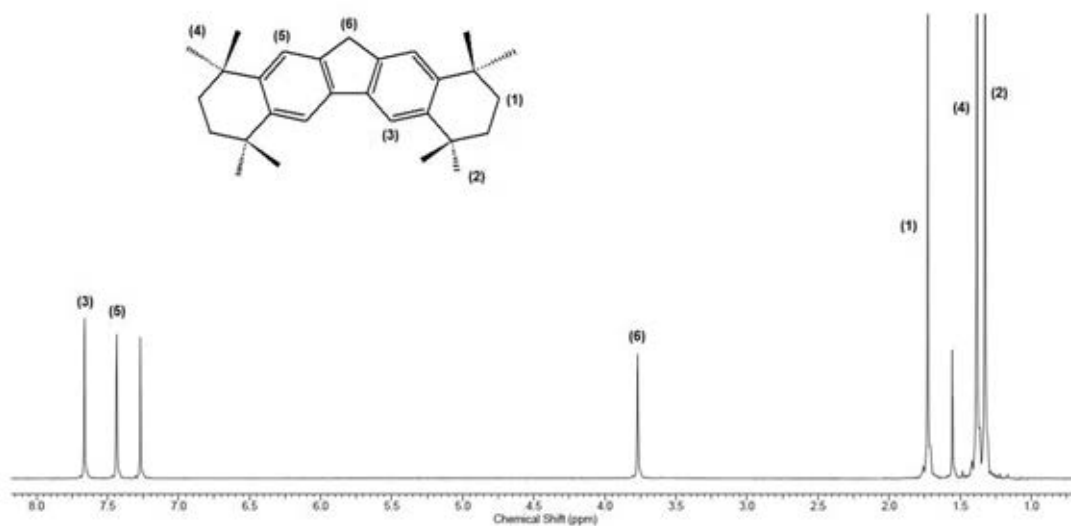


**Figure 4.6**  $^1\text{H-NMR}$  spectrum of octamethyloctahydrodibenzofluorene ring

Complex **2** was synthesized via one-pot method as the same procedure for the preparation of **1**, excepting octamethyloctahydrodibenzofluorene was applied instead of fluorene. The synthetic procedure for  $\text{Me}_2\text{Si}(\eta^3\text{-C}_{29}\text{H}_{36})(\eta^1\text{-N}^t\text{Bu})\text{TiMe}_2$  complex is shown in **Figure 4.7**.

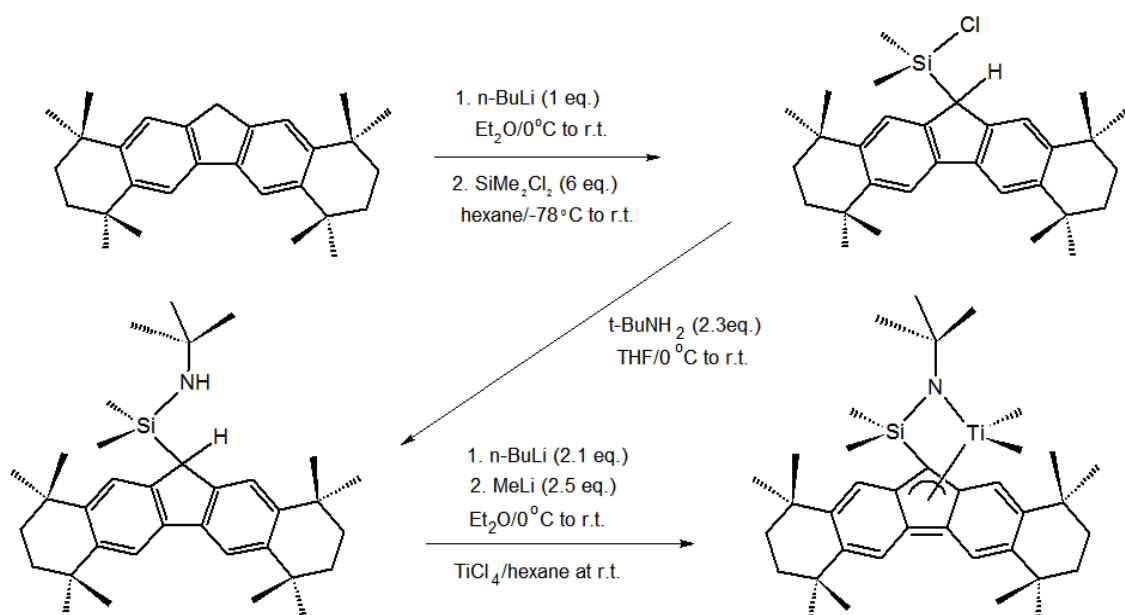


**Figure 4.7** Synthesis of complex **2**

According to the above reactions, the  $\text{Me}_2\text{CNHMe}_2\text{Si}(\text{C}_{29}\text{H}_{37})$  ligand yielding 90% as white solid was obtained by the reaction of  $t\text{-BuNH}_2$  with  $\text{ClSi}(\text{CH}_3)_2(\text{C}_{29}\text{H}_{37})$ . The results characterized by elemental analysis indicated that this sample has C 82.42%, N 3.18%, H 11.80%, which are in good agreement with the calculated results (C 81.88%, N 2.72%, H 10.38%). In addition, based on  $^1\text{H}$  NMR spectrum (**Figure 4.8**), it was confirm that the resultant ligand exhibited similar pattern in accordance with the previous research.

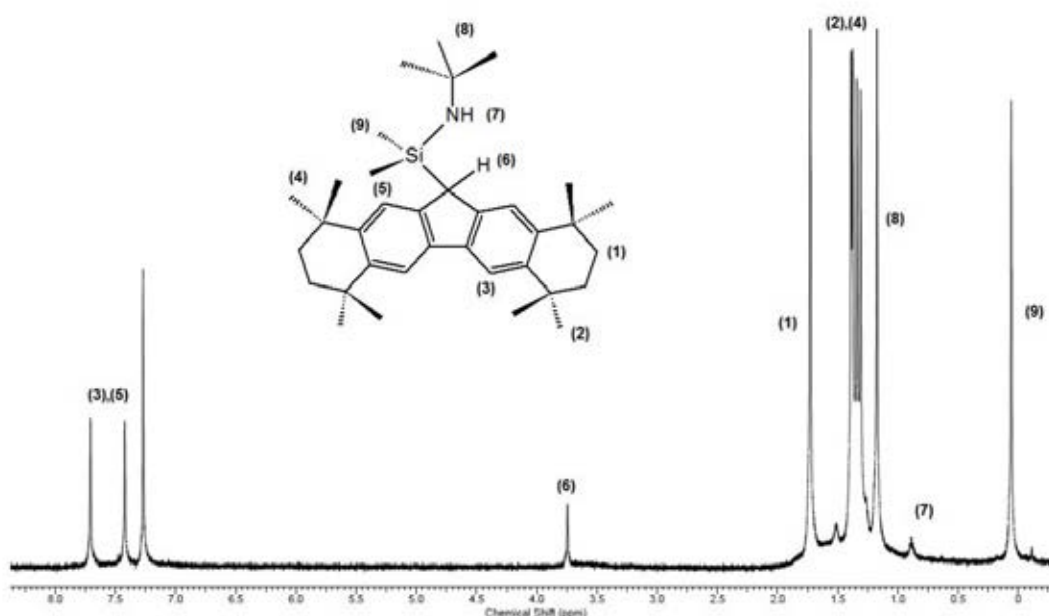


**Figure 4.8**  $^1\text{H}$  NMR spectrum of synthesized  $\text{Me}_2\text{CNHMe}_2\text{Si}(\text{C}_{29}\text{H}_{37})$  ligand

When reacting the resultant ligand with  $\text{TiCl}_4$ , it was found that only 22% yield of red crystal was gained from this procedure. The obtained results from elemental analysis measurement indicates that this synthesized titanium complex has C 71.02%, N 3.16% and H 9.0% which is in agreement with the calculated results (C 75.09 %, N 2.37 % and H 9.71%). In addition, from the  $^1\text{H}$  NMR spectrum of the obtained complex as shown in **Figure 4.9** which is consistent with the report of Shiono et al. [70], it can be concluded that  $\text{Me}_2\text{Si}(\eta^3\text{-C}_{29}\text{H}_{36})(\eta^1\text{-N}^t\text{Bu})\text{TiMe}_2$  (**2**) was successfully synthesized.

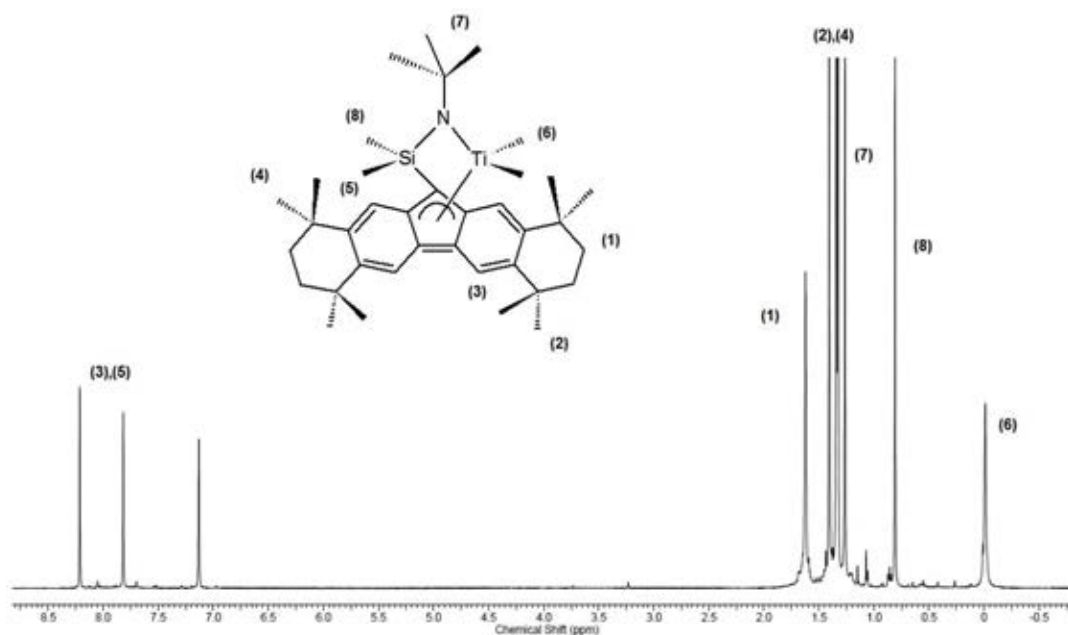


**Figure 4.9**  $^1\text{H}$  NMR spectrum of  $\text{Me}_2\text{Si}(\eta^3\text{-C}_{29}\text{H}_{36})(\eta^1\text{-N}^t\text{Bu})\text{TiMe}_2$  complex

#### 4.1.2 Copolymerization of ethylene and 1-hexene

Two constrained geometry catalysts, *ansa*-Dimethylsilylene(fluorenyl)(*t*-butylamido) dimethyltitanium complex,  $\text{Me}_2\text{Si}(\eta^3\text{-C}_{13}\text{H}_8)(\eta^1\text{-N}^t\text{Bu})\text{TiMe}_2$  (**1**), and its tetraalkylsubstituted-fluorenyl derivative,  $\text{Me}_2\text{Si}(\eta^3\text{-C}_{29}\text{H}_{36})(\eta^1\text{-N}^t\text{Bu})\text{TiMe}_2$  (**2**) were used as catalysts for ethylene and 1-hexene copolymerization with MMAO cocatalyst. The results are summarized in **Table 4.1**.

The copolymerization of **1** was performed with 0.15 M of 1-hexene at 298 K, however, it exhibited the high catalytic activity ( $22 \text{ kg-polymer molTi}^{-1}\cdot\text{h}^{-1}$ ) (data not shown in Table). Therefore, all systems were conducted at 273K to provide the low comonomer conversion.

**Table 4.1 Ethylene/1-hexene copolymerization with 1 and 2 activated by MMAO**

Entry	Complex	1-Hexene Feed (M)	Time (min)	Yield (g)	Activity <sup>c)</sup>	$M_n^d$ ( $\times 10^{-4}$ )	$M_w/M_n^d$	$N/Ti^e$ (mol/mol)	1-Hexene in copolymer (mol%) <sup>f)</sup>
1 <sup>a)</sup>	<b>1</b>	0.15	25	0.0227	5	2.5	1.54	0.09	16
2 <sup>a)</sup>	<b>1</b>	0.45	25	0.1290	30	2.2	1.49	0.59	33
3 <sup>a)</sup>	<b>1</b>	0.75	25	0.1335	32	2.1	1.40	0.64	47
4 <sup>a)</sup>	<b>1</b>	1.50	25	0.0510	12	1.1	1.36	0.46	58
5 <sup>b)</sup>	<b>2</b>	0.15	5	0.0299	359	5.1	2.38	0.59	17
6 <sup>b)</sup>	<b>2</b>	0.45	5	0.1093	1312	15.2	1.83	0.72	36
7 <sup>b)</sup>	<b>2</b>	0.75	5	0.1758	2110	19.1	2.09	0.92	52
8 <sup>b)</sup>	<b>2</b>	1.50	5	0.1738	2086	18.4	2.08	0.94	66

<sup>a)</sup>Polymerization conditions: Ti = 10  $\mu$ mol, MMAO as cocatalyst Al/Ti = 400, solvent = toluene, total volume = 30 ml, temperature = 273K.;

<sup>b)</sup>Polymerization conditions: Ti = 1  $\mu$ mol, MMAO as cocatalyst Al/Ti = 400, solvent = toluene, total volume = 30 ml, temperature = 273K.;

<sup>c)</sup>Activity in kg-polymer $\cdot$ mol-Ti<sup>-1</sup> $\cdot$ h<sup>-1</sup>.

<sup>d)</sup>Measured by GPC using polystyrene standards.

<sup>e)</sup>Number of polymer chains per Ti calculated from the polymer yield, the  $M_n$  value and the amount of Ti used.

<sup>f)</sup>1-Hexene in copolymer calcu.

In order to keep the comonomer conversion below 10%, the copolymerization was performed at 273K with 10 $\mu$ mol of **1** for 25 min, whereas 1 $\mu$ mol of **2** for 5 min, respectively.

The result from **Table 4.1** indicates that the catalytic activity of **2** was approximately 60 times higher than that of **1** irrespective of comonomer composition in feed. The enhancement of catalytic activity is related to the electronic effects of the substituent group on the fluorenyl ligand. It is well known for metallocene catalysts that the active species of metallocene catalysts is an ion-pair of a metallocenium cation and an anion derived from cocatalyst. The introduction of electron-donating group on the Cp ring improved the catalytic activity [72]. The increase in the activity by reducing the positive charge on the metallocenium cation can be explained by the enhancement of the ion-pair separation to form coordinatively unsaturated active cationic species. On the contrary, if the substituent is replaced by electron-withdrawing groups, the catalytic activity was decreased which is due to the formation of contact ion-pair [72-73]

Although, the steric hindrance of the ligand should also affect the separation of ion pair, this is not the case in the present catalyst. Cai et al. [29] previously reported that the introduction of *tert*-butyl groups at 2,7- and 3,6-position of the fluorenyl ligand of **1** increased the activity of propene polymerization to the same extent, although the syndiotacticity of the produced PP were depended on the position of *tert*-butyl groups.

Therefore, the high catalytic activity of **2** compared to **1** can be explained by the increase in the electron density at the active Ti species to enhance the propagation rate for the ethylene/1-hexene copolymerization. Miller and coworkers [74] revealed that the octamethyloctahydrodibenzofluorenyl ligand which is a part of the ligand of **2**, exhibited remarkably high electron density compared to fluorenyl one by several experiments such as deprotonation, which was confirmed by DFT calculation.



In addition, **Table 4.1** also showed that the catalytic activity of **1** for the copolymerization increased with an increase of 1-hexene concentration in feed and showed the maximum at 0.75 M of 1-hexene. The enhancement of catalytic activity is ascribed to the increase of 1-hexene concentration under a constant ethylene concentration. The decrease in catalytic activity is probably due to the increase in the 1-hexene inserted active species which is more sterically hindered, and thus less reactive than the ethylene-inserted one [75]. Similar tendency was observed in the copolymerization with **2**. However, the decrease in catalytic activity of **2** was not significant compared with **1** which is probably due to higher reactivity of **2** for 1-hexene.

#### 4.1.3 Characterization of ethylene and 1-hexene copolymer

The number-average molecular weight ( $M_n$ ) and molecular weight distribution (MWD) of the obtained copolymer were measured by GPC analysis. The results as shown in **Table 4.1** indicate that **2** produced copolymer with higher molecular weight than **1**. In case of **2**, the  $M_n$  value was increased with an increase in 1-hexene concentration in feed and showed the maximum at 0.75 M of 1-hexene keeping the MWD values approximately 2. This indicates the frequent chain transfer reactions with uniform active species. In case of **1**, the  $M_n$  value was monotonously decreased with an increase in 1-hexene concentration followed by narrowing MWD from 1.54 to 1.36.

Living polymerization has been reported when trialkylaluminum-free MMAO was used as cocatalyst [76]. In the present polymerization system, chain transfer by  $i\text{Bu}_3\text{Al}$  in MMAO is likely, taking into account the high cocatalyst concentrations present. The used catalyst amounts in each polymerization were 10 and 1  $\mu\text{mol}$  for **1** and **2**, respectively, keeping an Al/Ti ratio of 400. Thus, the concentration of  $i\text{Bu}_3\text{Al}$  in the **1** system was 10 times higher than in the **2** system.

The number of polymer chains ( $N$ ) calculated from the polymer yield and the  $M_n$  value calibrated as polystyrene for each polymerization are presented in **Table 4.2**. In spite of the lower concentration of  $i\text{Bu}_3\text{Al}$  and the shorter polymerization time (25

min with **1** and 5 min with **2**), the  $N$  values with **2** are higher than those with **1**, indicating that the introduction of octamethyltetrahydrodibenzo substituent on fluorenyl ligand of **2** enhanced the chain transfer rate. Even the frequent chain transfer was presented in **2**, the higher molecular weights of the copolymer produced by **2** were observed. It means that the rate enhancement effect of the octamethyltetrahydrodibenzo substituent on the propagation rate is more significant than that on the chain transfer rate.

The obtained copolymers were characterized by  $^{13}\text{C}$  NMR. The triad distributions of the comonomers were determined from the spectra according to literature [77]. The results are presented in **Table 4.2**, which shows that the comonomer triad distribution obtained by **1** and **2** are very similar. When increasing 1-hexene concentration, the EEE triad decreased whereas the triad of HHH increased. The 1-hexene incorporations in the copolymers determined from the triad contents are shown in **Table 4.2**. The 1-hexene incorporation was increased as the 1-hexene concentration increases in both systems. However, **2** incorporated more 1-hexene than **1**, indicating that the introduction of the octamethyltetrahydrodibenzo group should enhance the insertion of 1-hexene more than that of ethylene.

**Table 4.2**  $^{13}\text{C}$  NMR analysis of ethylene/1-hexene copolymer

Complex	1-Hexene Feed (M)	Triad distribution						Dyad distribution			$\rho^a$
		EEE	EEH	HEH	EHE	EHH	HHH	EE	HE	HH	
<b>1</b>	0.15	0.567	0.242	0.035	0.13	0.024	0.002	0.688	0.298	0.014	0.92
<b>1</b>	0.45	0.246	0.317	0.108	0.211	0.098	0.02	0.405	0.527	0.069	0.84
<b>1</b>	0.75	0.108	0.249	0.182	0.142	0.194	0.125	0.233	0.546	0.222	0.92
<b>1</b>	1.50	0.032	0.178	0.214	0.078	0.242	0.256	0.121	0.502	0.377	0.93
<b>2</b>	0.15	0.534	0.266	0.028	0.122	0.045	0.005	0.667	0.306	0.028	0.97
<b>2</b>	0.45	0.218	0.312	0.112	0.147	0.167	0.044	0.374	0.499	0.128	0.94
<b>2</b>	0.75	0.101	0.236	0.148	0.142	0.245	0.128	0.219	0.531	0.251	0.94
<b>2</b>	1.50	0.036	0.152	0.156	0.101	0.296	0.259	0.112	0.481	0.407	0.95

<sup>a</sup>Persistence ratio:  $[\text{EH}]/(2[\text{E}][\text{H}])$ .

The monomer reactivity ratios of **1** and **2** were determined in order to evaluate their copolymerization ability. The ethylene concentration was kept constant by introducing an atmospheric pressure of ethylene during the copolymerization. In all the copolymerizations, the conversions of 1-hexene were confirmed below 10%. The reactivity ratios in each copolymerization were determined assuming the first-order Markovian process and the monomer feed ratio and the dyad contents in the copolymer according to Equations (1) and (2)

$$r_E = 2[EE] / [EH]F \quad (1)$$

$$r_H = 2F[HH] / [EH] \quad (2)$$

where [EE], [EH] and [HH] are the dyad contents, F is the molar ratio of ethylene and 1-hexene in feed

The reactivity ratios ( $r_E$ ,  $r_H$ ) determined by  $^{13}\text{C}$  NMR are shown in **Table 4.3**. In both catalytic systems,  $r_E$  values were larger than 1 whereas  $r_H$  values were lower than 1. The results indicated the preference of ethylene insertion over 1-hexene insertion. The average monomer reactivity ratios ( $r_E$ ,  $r_H$ ) obtained from  $^{13}\text{C}$  NMR of **1** were  $3.0 \pm 0.15$  and  $0.19 \pm 0.06$  respectively, while the average  $r_E$  and  $r_H$  values of **2** were  $2.9 \pm 0.15$  and  $0.27 \pm 0.02$ . Complex **2** possesses better copolymerization ability than complex **1**, which should be due to the  $\eta^1$ -tendency of the octamethyltetrahydrodibenzofluorenyl ligand [78-79]. The products of reactivity ratios  $r_E \cdot r_H$  obtained from **1** and **2** were 0.57 and 0.78, respectively, indicating random tendency of the copolymers obtained with these catalysts. The persistence ratios shown in **Table 4.2** also support the random distribution of the comonomers.

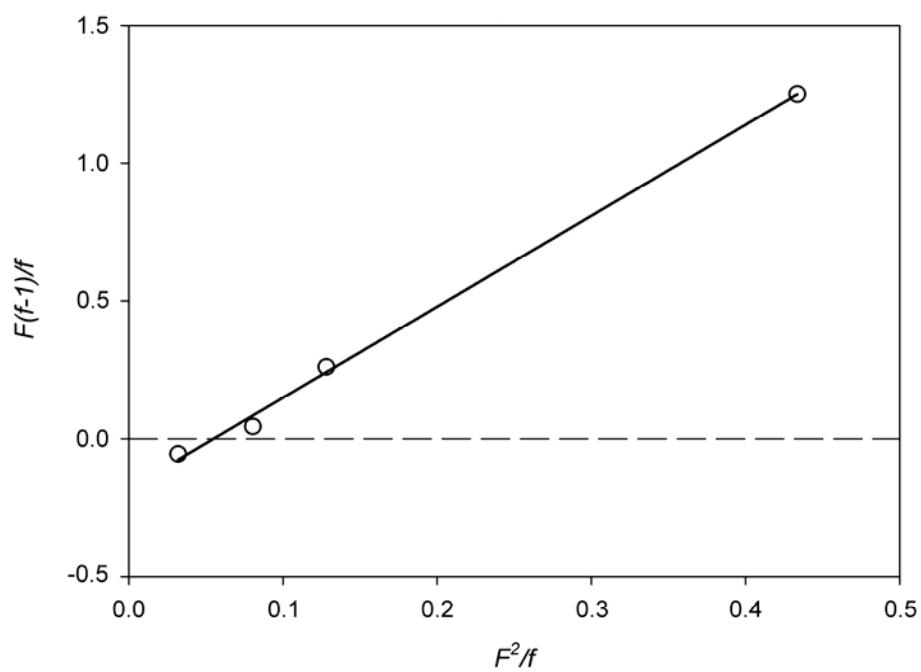
To confirm the monomer reactivity ratios determined by  $^{13}\text{C}$  NMR, the ratios were also determined by Finemann-Ross (F-R) [80] and Kelen-Tüdös (K-T) methods [81].

**Table 4.3 Monomer reactivity ratios of ethylene/1-hexene copolymerization with  
1 and 2**

<b>Complex</b>	<b>1-Hexene Feed (M)</b>	$r_E$	$r_H$
<b>1</b>	0.15	3.0	0.14
<b>1</b>	0.45	3.0	0.13
<b>1</b>	0.75	2.8	0.25
<b>1</b>	1.50	3.1	0.23
<b>1</b>	average	3.0	0.19
<b>1</b>	F-R <sup>a)</sup>	3.3	0.18
<b>1</b>	K-T <sup>b)</sup>	3.2	0.17
<b>2</b>	0.15	2.9	0.28
<b>2</b>	0.45	2.9	0.26
<b>2</b>	0.75	2.7	0.29
<b>2</b>	1.50	3.0	0.26
<b>2</b>	average	2.9	0.27
<b>2</b>	F-R <sup>a)</sup>	3.1	0.28
<b>2</b>	K-T <sup>b)</sup>	3.1	0.28

<sup>a)</sup> Finemann-Ross method. <sup>b)</sup> Kelen-Tüdös method.

(a)



(b)

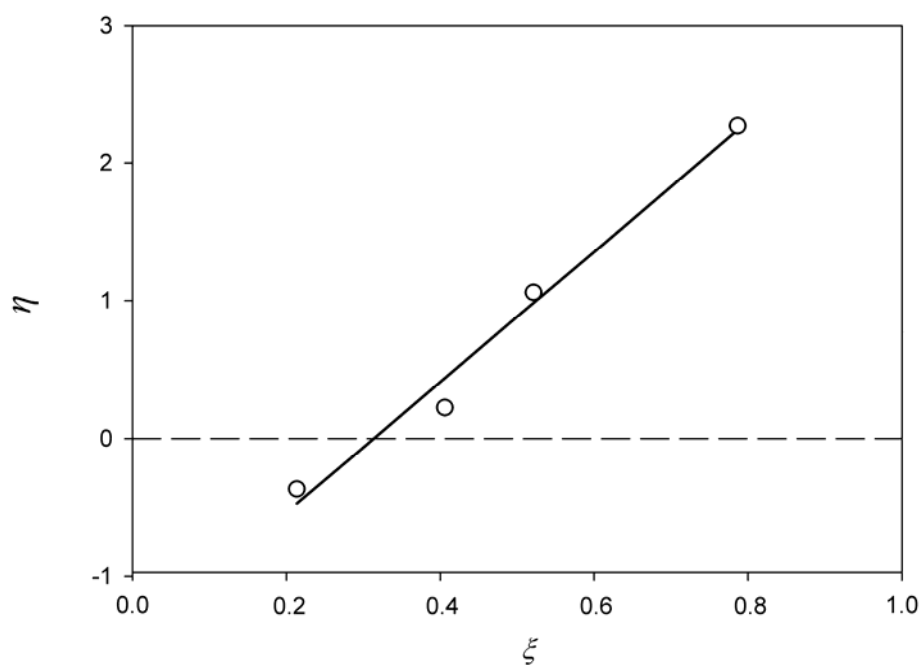


**Figure 4.10** Plots of a) Fineman-Ross method for the copolymers obtained with complex 1.; b) Kelen-Tüdös method for the copolymers obtained with complex 1

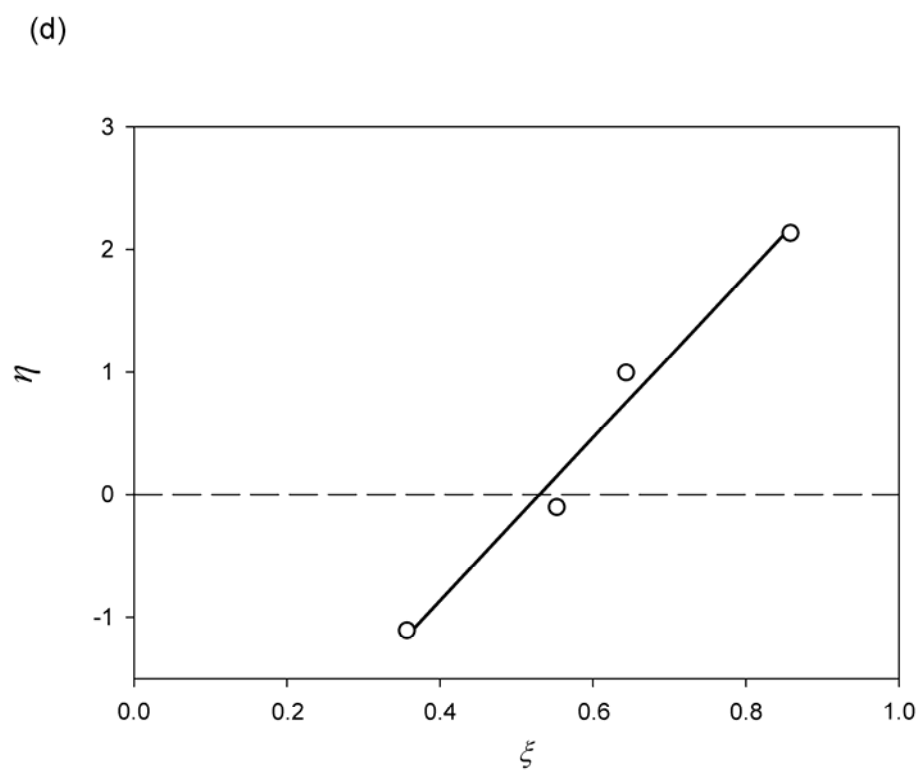
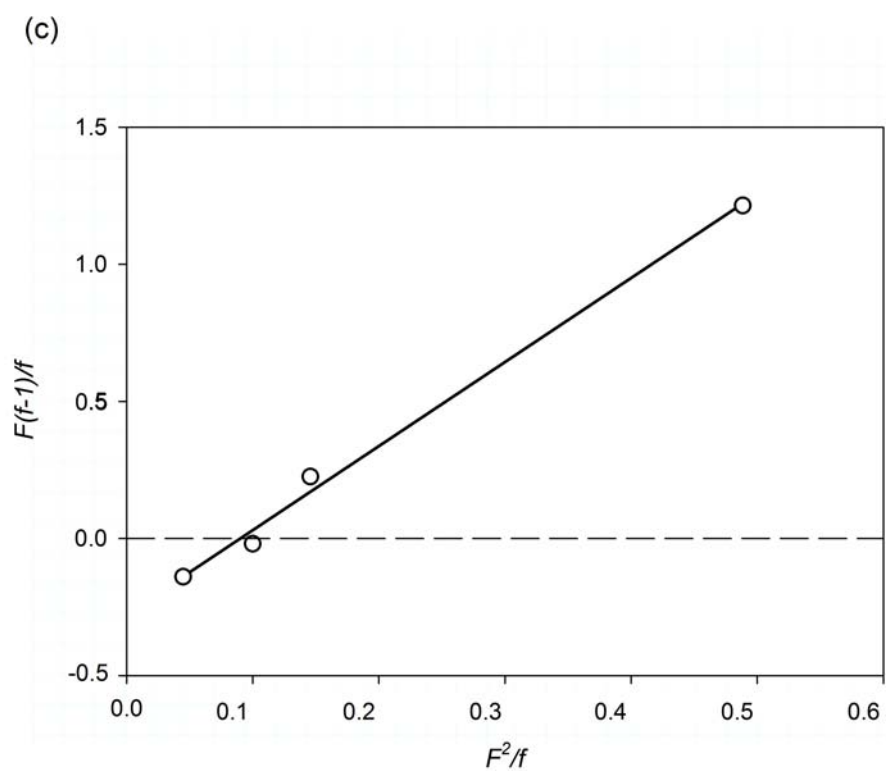


**Figure 4.11** Plots of c) Fineman-Ross method for the copolymers obtained with complex 2.; d) Kelen-Tüdös method for the copolymers obtained with complex 2

From the F-R and K-T plots as shown in **Figure 4.10** and **Figure 4.11**, it was found that each plot give good straight lines. The  $r_E$  and  $r_H$  values obtained from these plots are approximately 3.3 and 0.18, respectively for **1**, and 3.1 and 0.28, respectively for **2** as shown in **Table 4.3**. It indicates that the monomer reactivity ratios determined by the different methods are in good agreement each other.

**Table 4.4** shows the monomer reactivity ratios in ethylene/1-hexene copolymerization with representative single-site catalysts reported so far. The  $r_E$  and  $r_H$  values of **1** and **2** are comparable to those of a typical constrained geometry catalyst [82] and half-titanocene catalysts [83-84], which are superior to those of metallocene catalysts [85-88]. We have reported that complex **2** can promoted random copolymerization of 1-alkene and norbornene with high activity [89]. Thus, **2** is expected to be applied for the synthesis of a variety of olefin copolymers.



**Table 4.4 Monomer reactivity ratios in ethylene/1-hexene copolymerization with several single-site catalysts**

Catalyst <sup>c)</sup>	Temp. (°C)	$r_E^a)$	$r_H^b)$	$r_E \cdot r_H$	ref.
<b>1</b>	0	3.0	0.19	0.57	this work
<b>2</b>	0	2.9	0.27	0.78	this work
[Me <sub>2</sub> Si(C <sub>5</sub> Me <sub>4</sub> )(N <sup>t</sup> Bu)]TiCl <sub>2</sub>	40	3.42	0.29	0.99	82
(C <sub>5</sub> Me <sub>5</sub> )TiCl <sub>2</sub> (O-2,6- <sup>i</sup> Pr <sub>2</sub> C <sub>6</sub> H <sub>3</sub> )	40	2.7	0.11	0.29	83
( <sup>t</sup> BuC <sub>5</sub> H <sub>4</sub> )TiCl <sub>2</sub> (O-2,6- <sup>i</sup> Pr <sub>2</sub> C <sub>6</sub> H <sub>3</sub> )	40	2.46	0.18	0.45	83
(1,3- <sup>t</sup> BuC <sub>5</sub> H <sub>3</sub> )TiCl <sub>2</sub> (O-2,6- <sup>i</sup> Pr <sub>2</sub> C <sub>6</sub> H <sub>3</sub> )	40	3.23	0.14	0.45	83
CpTiCl <sub>2</sub> (N=C <sup>t</sup> Bu <sub>2</sub> )	25	4.5	0.08	0.35	84
Cp <sub>2</sub> ZrCl <sub>2</sub>	60	62.3	0.003	0.19	85
(Ind) <sub>2</sub> ZrCl <sub>2</sub>	60	88	0.005	0.44	85
Et(Ind) <sub>2</sub> ZrCl <sub>2</sub>	60	31	0.013	0.40	85
Et(IndH <sub>4</sub> ) <sub>2</sub> ZrCl <sub>2</sub>	40	12.1	0.028	0.34	86
Me <sub>2</sub> C(Cp)(Flu)ZrCl <sub>2</sub>	40	5.7	0.05	0.29	86
Et(2-Ind)(1-Ind)ZrCl <sub>2</sub>	20	18	0.021	0.38	87
Et(2-Ind)(2-Ph-1-Ind)ZrCl <sub>2</sub>	20	11	0.17	1.9	87
Me <sub>2</sub> Si(2-Ind)(2-Ph-1-Ind)ZrCl <sub>2</sub>	20	8.9	0.1	0.89	87
[PhN=C(Ph)CHC(CF <sub>3</sub> )O] <sub>2</sub> TiCl <sub>2</sub>	25	73.33	0.49	35.93	88

<sup>a)</sup> Reactivity ratio of ethylene. <sup>b)</sup> Reactivity ratio of 1-hexene. <sup>c)</sup> Activated by MAO or MMAO.

## **4.2 Effect of termonomers on properties of poly(ethylene-*ter*-1-hexene-*ter*-dicyclopentadiene) by CGC catalyst**

Polyolefins are important commercial products which are now widely used in many applications such as packaging films, fibers, pipes and container applications. Because of their unique physical and mechanical properties, polyolefins play a fundamental role in life [1]. Polyolefins are commonly produced by using Ziegler-Natta catalysts, metallocene catalysts and some metal complexes. Recently, the synthesis of polyolefins containing double bond has been considered. Since, the double bond of polyolefins can be converted into the functional group such as epoxide, alcohol and ester through the chemical reaction or can be used for crosslinking.

The effective approach to synthesis of polyolefins containing double bond group is the use of precursor monomers possessing double bond in molecule [62]. The monomer which contains double bond in molecule such as 1,4-hexadiene [90], 5-vinyl-2-norbornene [91], vinylcyclohexene [92] and styrene [64] were chosen because of its different reactivities of double bond in molecule. Dicyclopentadiene (DCP) is one of the attractive precursor monomers for synthesis of functionalized polyolefins because it has specified properties such as good transparency and high thermal resistance and it is industrially available at low price [63]. Dicyclopentadiene is a molecule containing both norbornene unit and cyclopentene unit in structure. If one of the double bonds in DCP selectively participates in ethylene and  $\alpha$ -olefin terpolymerization, the remaining double bond in DCP can be possibly modified by the introduction of functional group and converted into the functionality. Thus, a polymer which contains double bond in molecule can be used for crosslinking and produce a new polymer with specified functions [63-64]. In the beginning, these materials were synthesized by Ziegler-Natta catalysts. Due to their poor activity and low  $\alpha$ -olefin incorporation, this is the limitation of these catalysts for synthesizing functionalized polymer. After metallocene catalysts were found to be attractive catalysts for olefin polymerization, many researchers have been focused on the development of these catalysts for the synthesis of desired polymers.

Constrained geometry catalysts or CGCs, which are one of the metallocene groups are promising catalysts for the synthesis of new polyolefins because of their many advantages over conventional metallocene catalysts such as high comonomer incorporation and high thermal stability. Therefore, CGCs were chosen as the catalysts for the introduction of double bond into polyolefin.

Therefore, in this study, we focused on using constrained geometry catalysts (CGC) activated with MMAO to investigate the influence of termonomers on ethylene/1-hexene/dicyclopentadiene terpolymerization. (**Figure 4.12**).

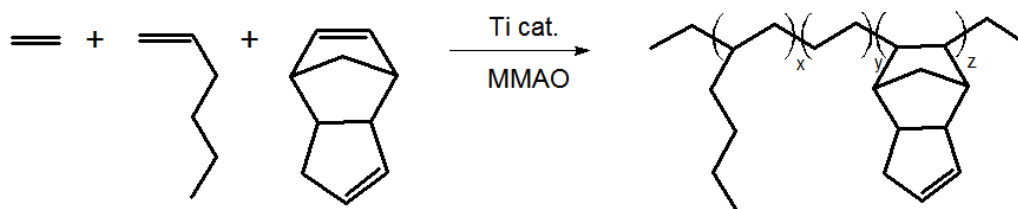


**Figure 4.12** Terpolymerization of ethylene/1-hexene/dicyclopentadiene

#### 4.2.1 Terpolymerization of ethylene/1-hexene/dicyclopentadiene

Terpolymerization of ethylene and 1-hexene with dicyclopentadiene was carried out using  $\text{Me}_2\text{Si}(\eta^3\text{-C}_{29}\text{H}_{36})(\eta^1\text{-N}^t\text{Bu})\text{TiMe}_2$  in the presence of MMAO cocatalyst. The octamethyltetrahydrodibenzofluorenyl-ligated complex **2** synthesized in **Part 4.1** was chosen as a catalyst for this study, because **2** not only enhanced the ethylene and 1-hexene copolymerization activity and promoted highly efficient comonomer incorporation (as indicated in **Part 4.1** and in entry 2), but also showed highly efficient in ethylene and dicyclopentadiene copolymerization (as indicated in [71] and in entry).

In order to control the comonomer conversion below 10%, terpolymerization was conducted at 323K with 2  $\mu\text{mol}$ . The results are summarized in **Table 4.5**.

**Table 4.5 Terpolymerization of ethylene/1-hexene/dicyclopentadiene with  $\text{Me}_2\text{Si}(\eta^3\text{-C}_{29}\text{H}_{36})(\eta^1\text{-N}^t\text{Bu})\text{TiMe}_2/\text{MMAO}$**

Entry <sup>a)</sup>	1-Hexene Feed (M)	DCP Feed (M)	Yield (g)	Activity <sup>b)</sup>	1-Hexene in terpolymer (mol%) <sup>c)</sup>	DCP in terpolymer (mol%) <sup>c)</sup>	T <sub>m</sub> (°C) <sup>d)</sup>
1	-	-	0.1759	5,277	-	-	137
2	1.5	-	1.504	45,115	44	-	116
3	-	0.0045	0.2307	6,921	-	6	109
4	0.15	0.0045	0.4432	13,296	32	4	n.o.
5	0.45	0.0045	0.6052	18,156	47	4	n.o.
6	0.75	0.0045	1.4567	43,701	52	5	n.o.
7	1.5	0.0045	0.5874	17,622	58	5	n.o.
8	1.5	0.0045	0.5874	17,622	58	5	n.o.
9	1.5	0.045	0.7058	21,174	56	8	n.o.
10	1.5	0.075	1.6110	46,878	59	13	n.o.
11	1.5	0.15	0.4402	13,206	60	14	n.o.

<sup>a)</sup>Polymerization conditions: Ti=2μmol, MMAO as cocatalyst Al/Ti=400, solvent=toluene, total volume=30ml, temperature=323K.

<sup>b)</sup>Activity in kg-polymer molTi<sup>-1</sup>·h<sup>-1</sup>.

<sup>c)</sup>1-hexene and DCP in copolymer calculated from the <sup>13</sup>C NMR spectrum of copolymer.

<sup>d)</sup>Determined by differential scanning calorimetry (DSC).

n.o. refers to not observe

Comparing ethylene homopolymerization to copolymerization, it was found that the presence of comonomer in copolymerization showed higher catalytic activity than the homogeneous one (entries 2-3 vs entry 1). This phenomenon is called “comonomer effect”. This can be positive or negative results depending on the effect on catalytic activity. The introduction of comonomer that increased the catalytic

activity is referred to the positive comonomer effect. On the contrary, if the catalytic activity decreases when adding comonomer, it will be referred to the negative effect. In this study, the positive effect is obtained which is attributed to an enhancement of monomer diffusion. The introduction of comonomer would decrease the crystallinity of polymer and make an easier for monomer to diffusion to active site. Thus, an increase in catalytic activity was observed [57,59,93].

As seen in **Table 4.5**, the influence of 1-hexene and DCP termonomers in terpolymerization can be divided into two cases. At ethylene and dicyclopentadiene constant (entry 4-7), it was found that the activity was increased with an increase in 1-hexene concentration and showed the maximum at 0.75M of 1-hexene. The catalytic activity decreased because of the increase in inserted 1-hexene on the active sites, which is more hindered, and thus leads to lower catalytic activity. A similar trend was observed in terpolymerization at ethylene and 1-hexene constant. Surprisingly, in this case, the observed terpolymerization activity was higher than that observed copolymerization activity (entry 3). An enhancement in catalytic activity is probably related to “the comonomer effect”. An increase in 1-hexene concentration would increase the diffusion of monomers through less-crystalline polymer to active sites resulting in an increase in monomer concentration at active sites. The higher catalytic activity can be obtained. From these results, it can be suggested that the catalytic activity was strongly affected by the addition of termonomers.

At constant ethylene and 1-hexene concentration in feed (entries 8-11), the catalytic activity increase with an increase in dicyclopentadiene concentration and showed the maximum at 0.075M of dicyclopentadiene. A decrease in catalytic activity is probably due to the increase in dicyclopentadiene inserted on the active sites. It seems that the steric bulk of dicyclopentadiene, which is more sterically-hindered, makes it difficult for ethylene and 1-hexene to insert to active sites. A similar tendency was observed in ethylene and styrene with 1-octene terpolymerization [15] and ethylene/propylene/1,4-hexadiene terpolymerization [61]. The previous results revealed that one of dicyclopentadiene double bond may chelate to active center of catalyst, and thus this possibly caused lower catalytic activity.

However, the observed activity was apparently lower when compared with copolymerization activity (entry 2).

- **Kinetic studies**

**Figures 4.13** and **4.14** show rate-time profiles for the copolymerization of ethylene and 1-hexene as well as for ethylene and dicyclopentadiene copolymerization with the different comonomer concentrations. It was found that all ethylene copolymerization, rate-time profiles increased rapidly in the beginning until reaching the maximum polymerization rate, it began to decrease which may be due to the catalyst deactivation. The ethylene consumption rate in copolymerization was found to depend on the comonomer concentration. The average rate of ethylene polymerization was increased according to the comonomer concentration. For the rate-time profile of ethylene and 1-hexene with dicyclopentadiene terpolymerization, the maximum polymerization rate is between the maximum rate of homopolymerization and copolymerization of ethylene and dicyclopentadiene.

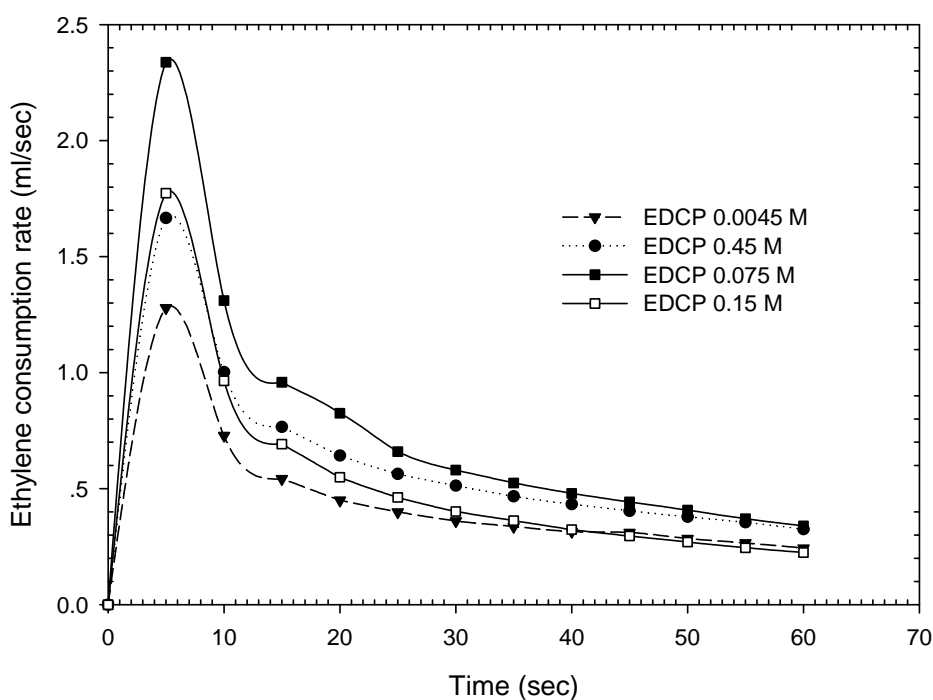


**Figure 4.13** Rate-time profile of ethylene/dicyclopentadiene copolymerization

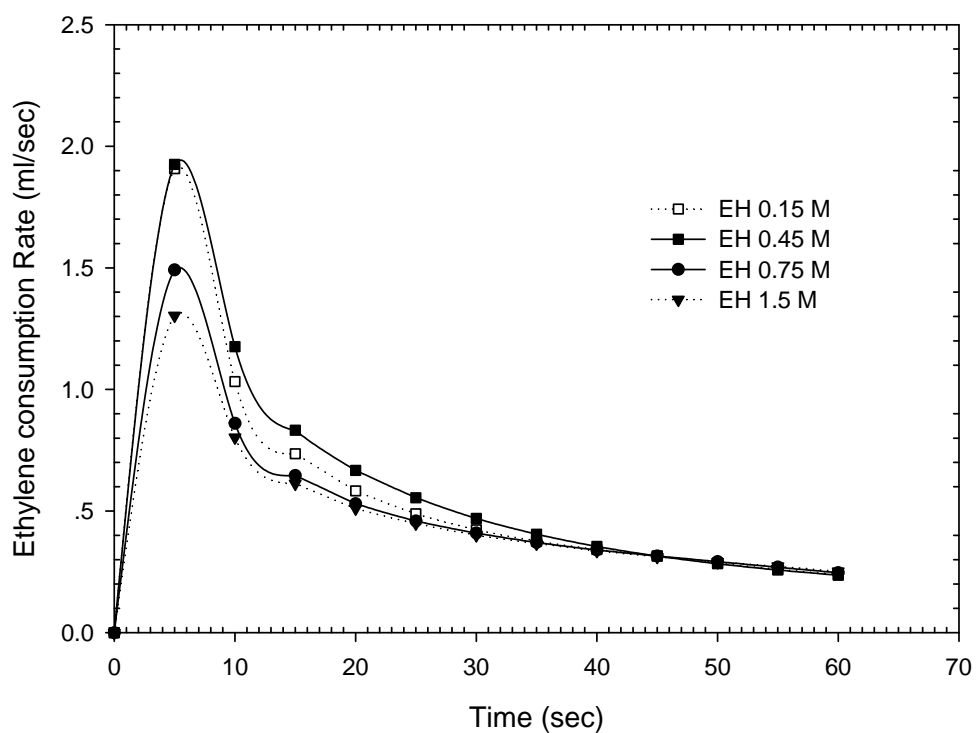


**Figure 4.14** Rate-time profile of ethylene/1-hexene copolymerization

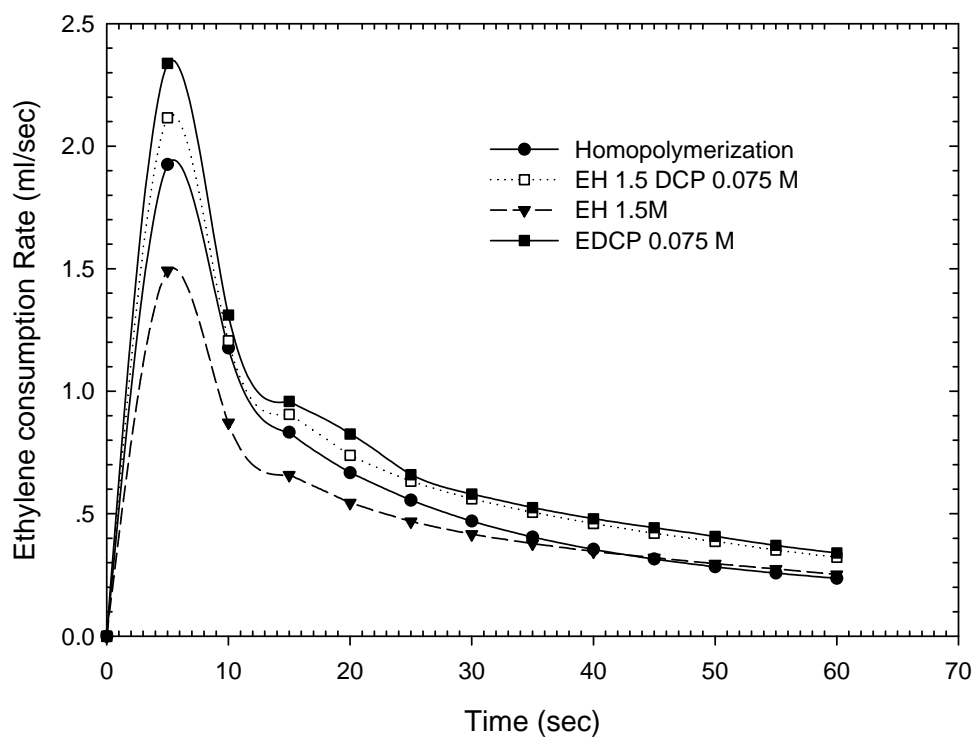


**Figure 4.15** Terpolymerization of ethylene/1-hexene/dicyclopentadiene

#### 4.2.2 Properties of Poly(ethylene-*ter*-1-hexene-*ter*-dicyclopentadiene)

Poly(ethylene-*ter*-1-hexene-*ter*-dicyclopentadiene) was analyzed by  $^{13}\text{C}$  NMR spectroscopy to determine microstructure and termonomer incorporation. A typical  $^{13}\text{C}$  NMR spectrum for poly(ethylene-*ter*-1-hexene-*ter*-dicyclopentadiene) is shown in **Figure 4.16**. According to previous reports [63,94-95], the chemical peak observed at 30.2 ppm is assigned to ethylene unit, whereas the chemical peaks of the 1-hexene unit are at 14.2, 23.5, 29.8, 34.4, 34.9 and 38.5 ppm. The chemical peaks at 130.6 and 132.8 ppm indicated the characteristic chemical shift of dicyclopentadiene.

As known, dicyclopentadiene is a molecule that contains both norbornene and cyclopentene unit. The results from **Figure 4.16** indicate that ethylene and 1-hexene with dicyclopentadiene terpolymerization is polymerized through the enchainment of norbornene unit due to the presence of chemical peaks of one double bond at 130.6 and 132.8 ppm. This is consistent with the previous report, which described that the double bond of norbornene unit is more reactive than cyclopentene. Therefore, it can be suggested that the present catalyst is active for norbornene than cyclopentene. According to the remaining double bond in polymers, it is highly possible that functionalized polymer can be synthesized from the obtained polymer via chemical reaction.



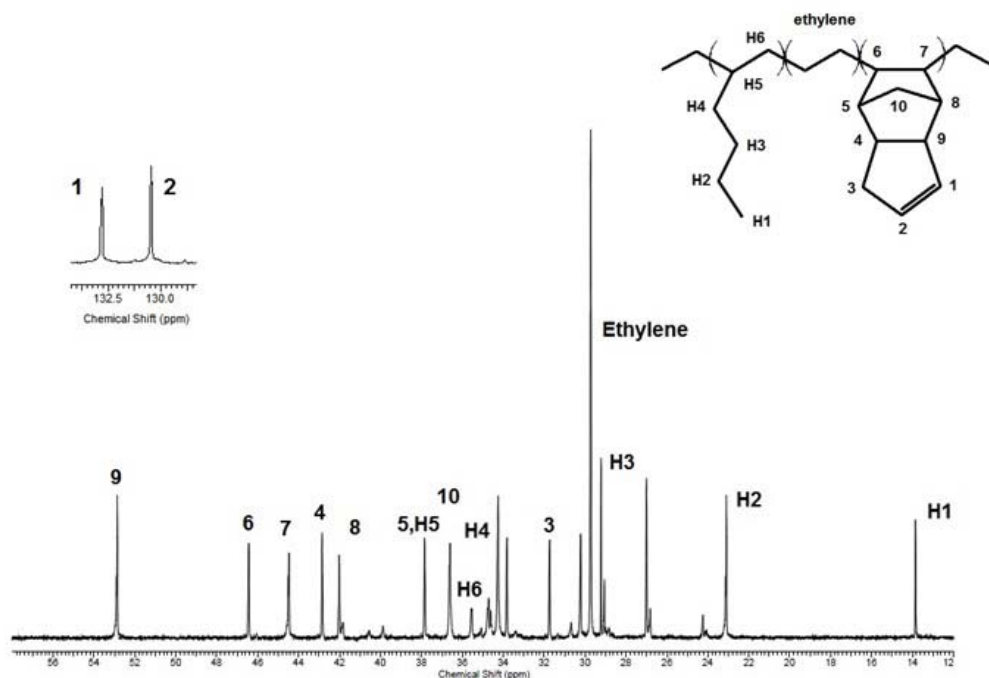


**Figure 4.16**  $^{13}\text{C}$  NMR spectrum of poly(ethylene-*ter*-1-hexene-*ter*-dicyclopentadiene)

In addition, **Table 4.5** also indicates that the 1-hexene incorporation was increased with an increase in 1-hexene concentration in feed (entry 4-7), and dicyclopentadiene content in terpolymers also increased with an increase in dicyclopentadiene (entry 8-11). A similar trend was observed in the ethylene and 1-hexene with styrene terpolymerization using aryloxo-modified half-titanocene catalysts [64]. Based on these results, it was found that dicyclopentadiene slightly increased when increasing 1-hexene concentration (entry 4-7) and 1-hexene incorporation also slightly increased according to dicyclopentadiene (entry 8-11). A similar tendency was observed in ethylene/1-hexene/dicyclopentadiene with bis( $\beta$ -enamino-ketonato)titanium catalysts [88]. Comparing entry 2, 3 and 7, the results showed that 1-hexene incorporation was significantly affected by dicyclopentadiene concentration, whereas 1-hexene concentration seems hardly affected on dicyclopentadiene incorporation. The similar trend was observed in ethylene and styrene with 1-octene terpolymerization using  $[\text{Me}_2\text{Si}(\text{C}_5\text{Me}_4)(\text{N}^t\text{Bu})]\text{TiCl}_2$  catalyst

combined with MAO cocatalyst [15] . As a result, the 1-hexene incorporation was achieved maximum at 60% (entry 11), while the dicyclopentadiene content in polymer showed the maximum at 14% (entry 11). This CGC catalyst afforded polymer with higher termonomer incorporation than bis( $\beta$ -enaminoketonato)titanium catalyst which was found to be 43 mol% of 1-hexene content , and 1.6 mol% of dicyclopentadiene [96].

For thermal study, the resulting polymer was measured by differential scanning calorimeter (DSC) in the temperature range of 50-170 °C. The results from second scan are reported in **Table 4.5**. The PE sample (entry 1) has melting temperature of 137 °C, while the introduction of comonomer decreased the crystallinity of polymer, and thus lowered the melting temperature of the polymer. The melting temperature was  $\approx$  116 °C for ethylene and 1-hexene copolymer (entry 2) and  $\approx$  109 °C for ethylene and dicyclopentadiene copolymer (entry 3) and. For ethylene and 1-hexene with dicyclopentadiene samples (entry 4-11), it cannot be observed the melting curve from DSC thermogram even with low 1-hexene and dicyclopentadiene contents. These results suggest that the resultant polymers were amorphous materials and the properties of polymer can be modified by varying the ratio of termonomer components.

Through these studies, we believe that terpolymerization of ethylene and 1-hexene with dicyclopentadiene with constrained geometry catalyst would be considered as a promising alternative approach of the synthesis of new polyolefins and preparing polyolefin containing functional group. The attention would be paid to precise synthesis of unsaturated polymers by ethylene terpolymerization with dienes by introducing the functional group through the chemical reactions. Ethylene and 1-hexene with dicyclopentadiene terpolymerization would be a new promising possibility to develop polymer industry. .

### 4.3 Effect of comonomer chain-length on ethylene and 1-olefins copolymerization using zirconocene/MMAO catalysts

Polymer has played significant role in our life, especially linear low density polyethylene (LLDPE). Due to its useful properties such as low density, good mechanical properties, and easy to fabricate and recycling, thus it has been used to produce many products [1-3]. The demand of LLDPE is quite high comparing with other polymers. For the production of LLDPE, the polymer can be synthesized by the copolymerization of the ethylene and short chain 1-olefins, namely 1-hexene, 1-octene and 1-decene. Although LLDPE commonly produces by using Ziegler-Natta catalysts, metallocene catalysts exhibit high catalytic activity to give polymer with narrow molecular weight and comonomer composition distribution. Therefore, the development of these catalysts for the synthesis of LLDPE using metallocene catalysts has been considered [97].

However, the properties of LLDPE, such as the average molecular weight and molecular weight distribution of polymer, the crystallinity, the melting temperature as well as the content and distribution of comonomer, are depended on a factor called “comonomer effect”[13,14]. According to previous studies, they showed that the increase of 1-olefin quantities improve the activity which is related to the physical phenomenon by improving the monomer diffusion in the lower crystalline copolymer structure. Besides the comonomer quantity, the length of the 1-olefin also affects the LLDPE properties. Although short chain comonomer is normally used in industrial process, but long chain comonomer can provide LLDPE with different properties. Therefore, the study of long chain comonomer is attractive for future production.

In this part, *rac*-Et(Ind)<sub>2</sub>ZrCl<sub>2</sub> was selected as catalyst and applied for copolymerization of ethylene with various 1-olefin in combination with MMAO cocatalyst to study the effect of comonomer chain length on the characteristics in terms of catalytic activity, polymer properties and morphology (.

### 4.3.1 Homo- and co-polymerization activities

This study is aimed to investigate the polymerization of ethylene with short and long chain 1-olefins, namely 1-hexene, 1-octene, 1-decene, 1-dodecene, 1-tetradecene and 1-octadecene. The copolymerization of ethylene and 1-olefin with zirconocene catalyst activated with MMAO is shown in **Figure 4.17**. The catalytic activities obtained with different 1-olefins are shown in **Table 4.6**

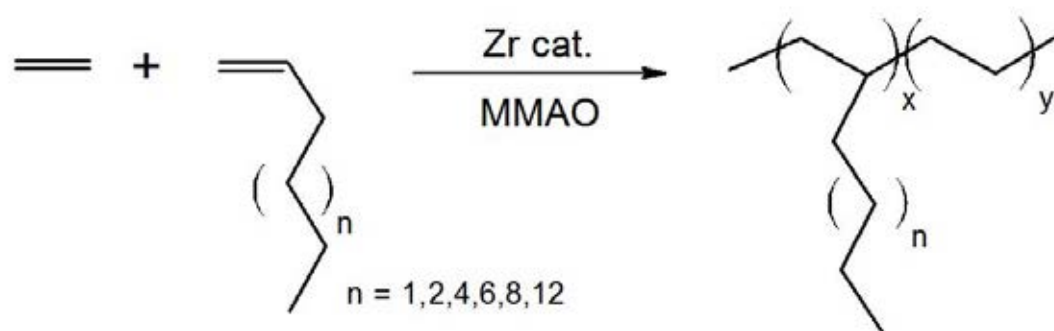


**Figure 4.17** Copolymerization of ethylene and 1-olefin with zirconocene/MMAO catalysts

**Table 4.6 Copolymerization of ethylene with longer chained 1-olefins by using *rac*-Et[Ind]<sub>2</sub>ZrCl<sub>2</sub>/MAO, as catalytic system**

Run number	Olefin type	Activity <sup>a)</sup> ( $\times 10^{-4}$ kgPol/molZr · h)	C <sub>n</sub> (mol%) <sup>b)</sup>	T <sub>m</sub> (°C) <sup>c)</sup>	$\chi_c$ (%) <sup>d)</sup>	d <sup>e)</sup> (g/ml)
1	-	1.8	-	135.00	65.00	0.95
2	1-C <sub>6</sub>	2.9	7	121.64	7.36	0.88
3	1-C <sub>8</sub>	3.8	16	113.62	2.44	0.88
4	1-C <sub>10</sub>	3.5	18	116.25	2.33	0.88
5	1-C <sub>12</sub>	3.6	13	117.61	6.21	0.89
6	1-C <sub>14</sub>	3.7	20	112.98	1.33	0.87
7	1-C <sub>18</sub>	4.5	15	117.58	4.34	0.88

<sup>a)</sup>Activities were measured at polymerization temperature of 343 K, [ethylene]= 0.018 mol, [Al]<sub>MMAO</sub> / [Zr]<sub>cat</sub> = 1135, in toluene with total volume = 30 ml and [Zr]<sub>cat</sub> =  $5 \times 10^{-5}$  M.

<sup>b)</sup>Content of 1-olefin in the copolymer from <sup>13</sup>C NMR.

<sup>c)</sup>Melting temperature from DSC.

<sup>d)</sup>Crystallinity degree:  $\chi_c = 100 \cdot (\Delta H / \Delta H^\circ)$ , where  $\Delta H^\circ = 290$  J/g for linear polyethylene.

<sup>e)</sup>Copolymer density calculated from the semi-empirical equation:  $d = (2195 + \Delta H) / 2500$  [105].

From **Table 4.6**, when comparing the activities between the homopolymerization and co-polymerization, it was found that the addition of the comonomer in the system gives higher activity. An improvement of polymerization rate in ethylene and 1-olefins copolymerization is called “comonomer effect”. This phenomenon can be found not only in Ziegler-Natta catalysts [13,58,98] but also in metallocene catalysts in zirconocene and titanocene system [99]. This interesting phenomenon can be described in chemical and physical functions [54-56].

According to the chemical function, an addition of comonomer increases the number of active center ( $C^*$ ). Taniike et al. [57] revealed that comonomer can activate potential active site which is not easily to activate by ethylene monomer. Although some site is not active for ethylene homopolymerization, it can active for copolymerization of ethylene. Thus, an increase in polymerization rate was observed. For physical function, the introduction of comonomer decreases the crystallinity of the obtained polymer, resulting in a less-crystalline copolymer. Therefore, monomers are easier to diffuse and react with active site, and thus lead to the better catalytic activity. Moreover, it is also found that comonomer can accelerates the fragmentation of catalyst during polymerization and causes the new active sites in heterogeneous system.

In addition, Karol *et al.* [58] have proposed that 1-olefins can function as ligands. By coordination to the active center, the 1-olefin can alter the charge density on the cationic zirconocenium ion. Metal centers with higher mobility, lower steric interference, and higher electrophilicity are believed to form stronger ion pairs. Monomers that cause a greater separation between the cationic metal centers and the MAO aggregates can enhance the activity of the catalyst, consequently increase the rate polymerization.

On the other hand, the effect of the comonomer chain-length can be described in two cases. Considering the short chain length comonomer (run 2-4), it indicated that the increase of the comonomer length resulted in lower activity due to the increase of steric hindrance effect. The longer comonomer which is sterically hindered the insertion of ethylene, leading to slower propagation reaction process. Therefore, it was then lead to lower activity for polymerization [4,58,100].

On the contrary, for the long chain length 1-olefins (run 5-7), we observed an increased of polymerization activity when the length of 1-olefin was increased. The effect may be attributed to the opening of the gap aperture between  $C_p(\text{centroid})-M-C_p(\text{centroid})$  in metallocene complex, which forced the coordination site to open more (**Figure 4.18**). This effect caused ethylene monomer to easier polymerize at the catalytic sites, and thus the activity increased [11,99]. A similar behavior was observed by Kaminsky *et al.* [100] for ethylene/ long chain 1-olefins copolymerization with  $[\text{Ph}_2\text{C}(2,7\text{-di-tert-BuFlu})(\text{Cp})]\text{ZrCl}_2/\text{MAO}$  catalyst system, under different experimental conditions ( $T=60\text{ }^\circ\text{C}$  and the presence of hydrogen) but no reason was given for the trend.

The obtained result is also consistent with the study of Braunschweig and Breitling [27] which reported that the opening angle of  $\beta C_p(\text{centroid})-M-C_p(\text{centroid})$  can be found in the polymerization of ethylene and long chain olefins, and moreover, the longer chain 1-olefin can open the angle of  $C_p(\text{centroid})-M-C_p(\text{centroid})$  wider in metallocene catalysts.

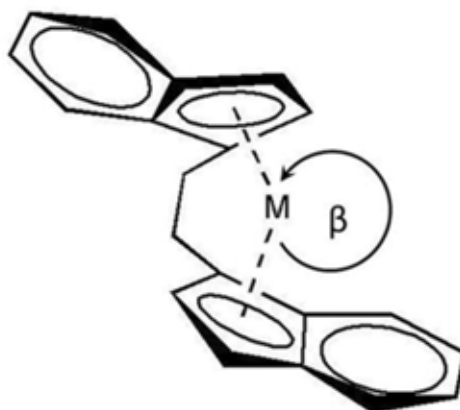


**Figure 4.18 Redrawn conceptual idea by Braunschweig and Breitling [27]**

Considering the influence of comonomer chain-length on rate-time profile, it was found that, the rate-time profile for ethylene and 1-olefin copolymerization is similar as presented in **Figure 4.19**.

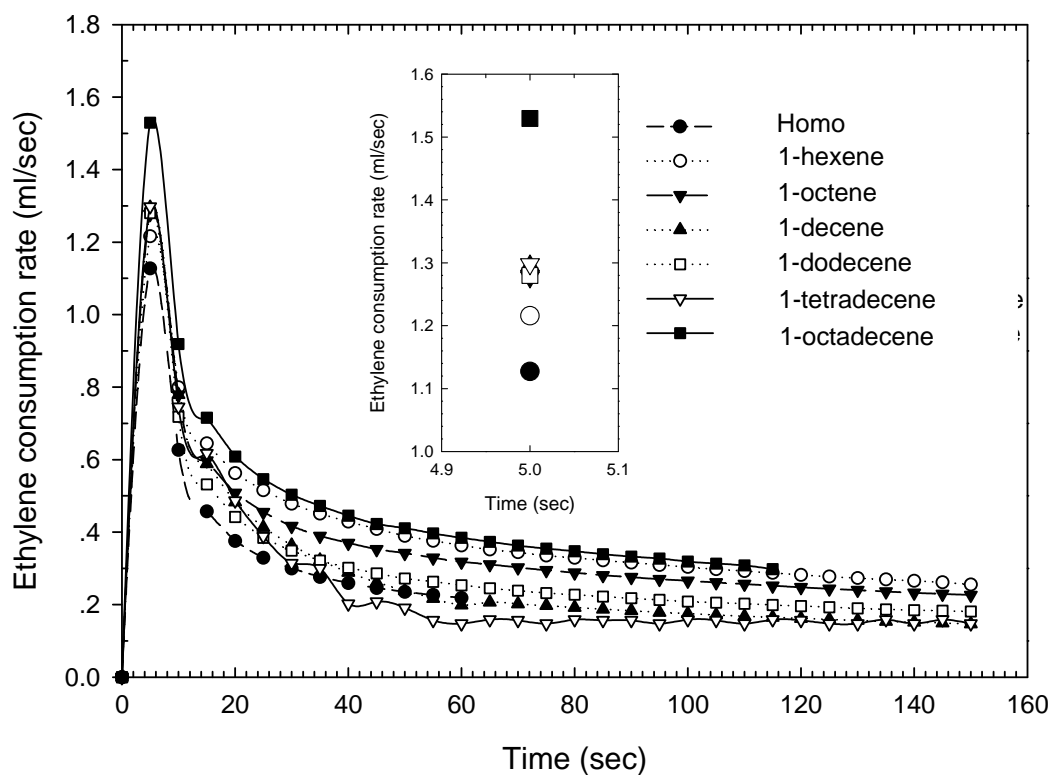


**Figure 4.19 Rate-time profile of ethylene polymerization with various comonomer**

Both ethylene homo- and copolymerization, rate-time profile increased rapidly at the beginning and reached the maximum point in 5 minutes followed by a slower propagation rate. The decline in rate-time profile is related to the lowering activity of some active centers with time. In the presence of comonomer, polymerization was activated much faster and initially polymerized at a much higher rate. The maximum point of rate-time profile for copolymerization was higher than ethylene homopolymerization. This is due to the fact that 1-olefin comonomer polymerize with ethylene rapidly, leading to the accelerating of active site. 1-octadecene comonomer showed the highest maximum profile.



### 4.3.2 Characterization of resulting polymer

Homo- and copolymer with different 1-olefins (copolymers containing 6 to 18 carbon atoms), synthesized with metallocene catalyst, have been analyzed using four characterization techniques:

- **SEM measurements**

**Figure 4.2** presents the scanning electron micrograph (SEM) of the obtained polymers from homo-polymerization and co-polymerization. Considering the effect of morphology with the length of 1-olefin, the results indicated that the crystalline structure of the obtained polymer seems to be lower with the increase in the comonomer length. The low crystallinity was probably due to more steric hindrance when higher comonomer was introduced. The longer-chained comonomer added, the more amount of amorphous observed. Therefore, the amount and type (chain length) of comonomer affected the morphology of polymer samples.

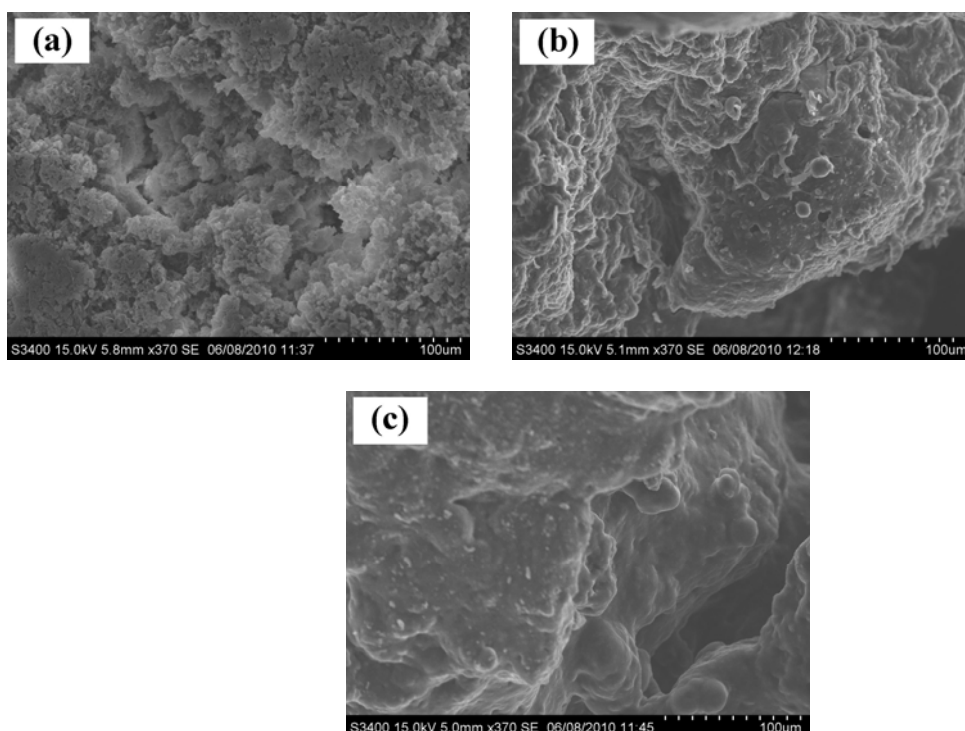


**Figure 4.2** SEM micrograph of LLDPE produced with metallocene catalyst; (a) homopolymer (b) ethylene/1-hexene copolymer (c) ethylene/1-octadecene copolymer

- **X-ray Diffraction (XRD) Analysis**

The XRD diffractograms of the different samples which acquired at room temperature are shown in **Figure 4.21**. As expect, it can be seen all samples display peaks at three positions. The broad amorphous peak centered around 19.5-20 degree, indicating the side branches of 1-olefin participating in the crystalline structure. While the two peaks appeared at  $2\theta = 21.8$  and  $24.3$  degrees are the (110) and (200) reflections characteristic of the orthorhombic cell of polyethylene [101-103], respectively. Moreover, the longer chain of the additional comonomers seemed to disturb the polymer recrystallization which probably attribute to most of the steric hindrance presented, leading to reducing in crystalline peak intensity, but clearly increasing the amorphous peak [59,101].

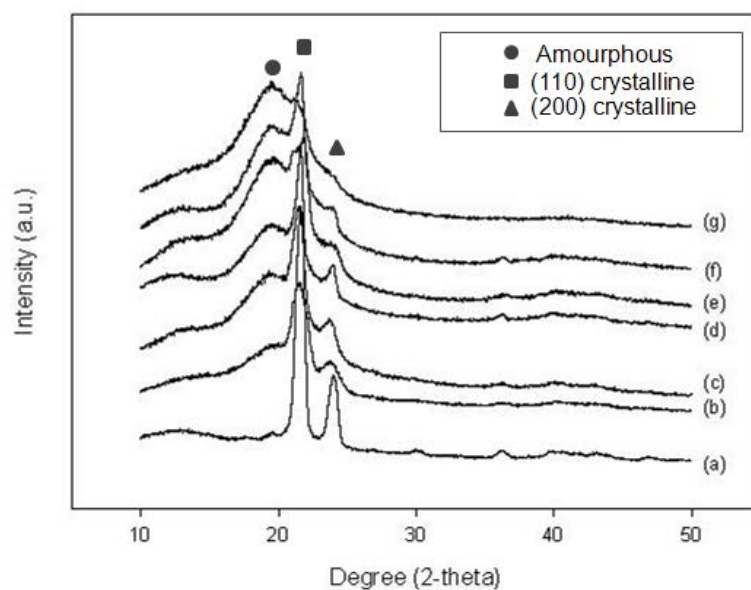


**Figure 4.21 X-ray diffractograms of different samples. From bottom to top; (a) homopolymer (b) ethylene/1-C<sub>6</sub> (c) ethylene/1-C<sub>8</sub> (d) ethylene/1-C<sub>10</sub> (e) ethylene/1-C<sub>12</sub> (f) ethylene/1-C<sub>14</sub> and (g) ethylene/1-C<sub>18</sub> copolymers**

- **NMR Analysis**

In order to investigate the influence of the length on the comonomer distribution, the obtained samples were also characterized by <sup>13</sup>C NMR measurement.

The chemical-shift assignments of ethylene/ 1-C<sub>12</sub> to ethylene/ 1-C<sub>18</sub> copolymer and some resonance of the main chain and side chain are shown in **Table 4.7** and **Figure 4.22**. The quantitative analysis of triad distribution for all copolymers is reported in **Table 4.8**. From table, it was found that ethylene incorporation in all systems gave copolymers with similar triad distribution, and only the random copolymers can be produced in all systems. However, the olefin chain length has no effect on the comonomer distribution [104].

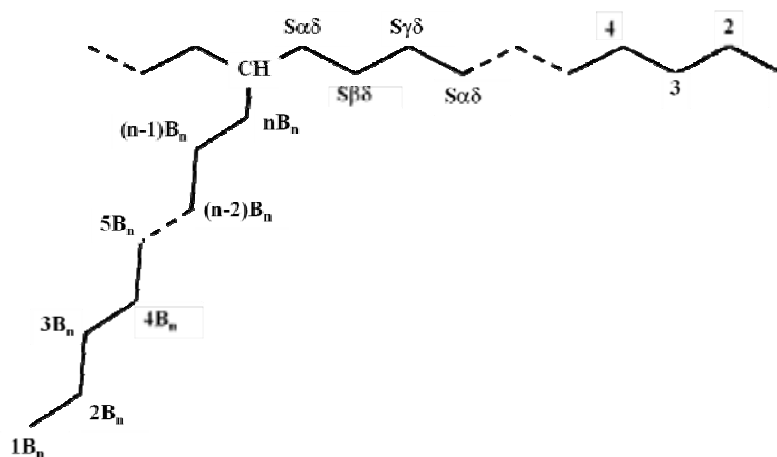


**Figure 4.22 Resonance of the main chain methylenes and the side chain of the ethylene/1-olefin copolymer**

**Table 4.7 Chemical-shift assignment of ethylene/1-dodecene, ethylene/1-tetradecene and ethylene/1-octadecene copolymers [104]**

Carbon type <sup>a)</sup>	Chemical shift <sup>b)</sup> (ppm)		
	ethylene/1-dodecene (1-C <sub>12</sub> )	ethylene/1-tetradecene (1-C <sub>14</sub> )	ethylene/1-octadecene (1-C <sub>18</sub> )
1B <sub>n</sub>	14.10	14.10	14.10
2 B <sub>n</sub>	22.80	22.80	22.80
3 B <sub>n</sub>	32.13	32.13	32.13
4 B <sub>n</sub>	29.50	29.50	29.50
5 B <sub>n</sub>	29.85	29.85	29.85
6 B <sub>n</sub>	29.90 <sup>c)</sup>	29.90 <sup>c)</sup>	29.90 <sup>c)</sup>
7 B <sub>n</sub>	29.90 <sup>c)</sup>	29.90 <sup>c)</sup>	29.90 <sup>c)</sup>
8 B <sub>n</sub>	30.36	29.90 <sup>c)</sup>	29.90 <sup>c)</sup>
9 B <sub>n</sub>	27.18	29.90 <sup>c)</sup>	29.90 <sup>c)</sup>
10 B <sub>n</sub>	34.45	30.37	29.90 <sup>c)</sup>
11 B <sub>n</sub>	-	27.18	29.90 <sup>c)</sup>
12 B <sub>n</sub>	-	34.46	29.90 <sup>c)</sup>
13 B <sub>n</sub>	-	-	29.90 <sup>c)</sup>
14 B <sub>n</sub>	-	-	30.37
15 B <sub>n</sub>	-	-	27.18
16 B <sub>n</sub>	-	-	34.46
CH	38.11	38.11	38.11
Sαδ	34.49	34.49	34.49
Sβδ	27.20	27.20	27.20
Sγδ	30.38	30.38	30.38
Sδδ	29.90	29.90	29.90

<sup>a)</sup> See Scheme 4.8.

<sup>b)</sup> According to Randall [105].

<sup>c)</sup> Overlapped to Sδδ peak at 29.90 ppm.

**Table 4.8 Triad distribution and properties of the resulting ethylene/1-olefin copolymers**

Entry	Olefin type	Triad distribution <sup>a)</sup>						C <sub>n</sub> (mol%) <sup>b)</sup>
		[EEE]	[XEE]	[EXE]	[XEX]	[EXX]	[XXX]	
2	1-C <sub>6</sub>	0.823	0.151	0.055	0.018	0.015	0.000	7
3	1-C <sub>8</sub>	0.412	0.379	0.164	0.045	0.000	0.000	16
4	1-C <sub>10</sub>	0.471	0.310	0.176	0.043	0.000	0.000	18
5	1-C <sub>12</sub>	0.499	0.331	0.135	0.035	0.000	0.000	13
6	1-C <sub>14</sub>	0.794	0.202	0.119	0.114	0.085	0.000	20
7	1-C <sub>18</sub>	0.591	0.214	0.152	0.043	0.000	0.000	15

<sup>a)</sup>Obtained from <sup>13</sup>C NMR, where E refers to ethylene monomer and X refers to 1-olefin comonomer.

<sup>b)</sup>Content of 1-olefin in the copolymer from <sup>13</sup>C NMR.

#### • Differential scanning calorimetric Analysis

When dealing with the thermal properties of the polymer, the DSC measurement is usually consider the second melting of the sample. All the experimental results, including melting temperature ( $T_m$ ), % crystallinity ( $\chi_c$ ), and density are also reported in the **Table 4.6**. The PE sample (run 1) is a high density polymer with a linear microstructure, a high melting temperature ( $T_m \sim 135^\circ\text{C}$ ), a degree of crystallinity of 65% and a high density (0.95 g/ml) (is not shown in table).

As can be seen in **Table 4.6**, the polymer with higher incorporated comonomers in its chain had less crystallinity and lower melting temperature. This is in correspondence with the percent insertion from <sup>13</sup>C NMR results. In addition, when considered the crystallinity results from DSC measurement, the results indicated that the length of comonomer did not affect the crystallization behavior which different from XRD results. These differences were because XRD was analyzed the sample at room temperature. Therefore, the amorphous peak of the branched 1-olefin may still

participate in the polymer structure. However, the DSC measurement was performed sample at high temperature. The determination relies on the measurement of the enthalpy of melting and on the assumption of a unique enthalpy of melting for the crystal. Thus, the enthalpy of melting of long side chain had to be taken into account the determination of crystallinity. Therefore, the crystallinity value may be different between the various determinations. [58,101,106-109]. However, from these results, it can be concluded that the increase in the chain length of comonomer is reflected on a decrease of the melting temperature. The density of all samples is in the range of 0.87-0.95 g/cm<sup>3</sup> indicating the structure of typical LLDPE.

# CHAPTER V

## CONCLUSIONS & RECOMMENDATIONS

### 5.1 CONCLUSIONS

The ethylene polymerization activated with metallocene catalyst and constrained geometry catalyst (CGC) in homogenous system was studied and divided into three parts: **Part 4.1** studied how the catalyst structure affected on the copolymerization ability, **Part 4.2** investigated the effect of comonomer on ethylene terpolymerization and the last **Part 4.3**, investigated the influence of comonomer chain length on ethylene copolymerization. The conclusion of each part was described in the following,

For the first part, two constrained geometry catalysts ( $\text{Me}_2\text{Si}(\eta^3\text{-C}_{13}\text{H}_8)(\eta^1\text{-N}^t\text{Bu})\text{TiMe}_2$  (**1**) and  $\text{Me}_2\text{Si}(\eta^3\text{-C}_{29}\text{H}_{36})(\eta^1\text{-N}^t\text{Bu})\text{TiMe}_2$  (**2**) with different substituents on fluorenyl ligand were synthesized and used as catalyst precursors for ethylene and 1-hexene copolymerization. It was found that the catalyst structure significantly affected on the copolymerization ability. The introduction of octamethyltetrahydrodibenzo substituent on the fluorenyl ligand significantly enhanced the copolymerization activity. The octamethyltetrahydrodibenzo substituent, which acts as an electron-donating group on fluorenyl ligand reduces the positive charge on metallocenium cation leading to the formation of the coordinatively-unsaturated active cationic species. In addition, this complex produced high molecular weight polymer with MWD approximately 2, indicating the characteristic of single-site metallocene catalysts. The octamethyltetrahydrodibenzofluorenyl-ligated complex **2** not only improved the catalytic activity and molecular weight, but also enhanced the comonomer incorporation. From the monomer reactivity ratio results,  $r_E = 3.0 \pm 0.15$ ,  $r_H = 0.19 \pm 0.06$  for **1**;  $r_E = 2.9 \pm 0.15$ ,  $r_H = 0.27 \pm 0.02$  for **2**, it indicates the superior ability of the present catalysts (**1** and **2**) for 1-hexene incorporation among the single site catalysts.

. Additionally, the octamethyltetrahydrodibenzofluorenyl-ligated complex **2** activated by MMAO was found to be an excellent catalyst for copolymerization of ethylene and 1-alkene.

In the second part, terpolymerization of ethylene and 1-hexene with dicyclopentadiene activated with  $\text{Me}_2\text{Si}(\eta^3\text{-C}_{29}\text{H}_{36})(\eta^1\text{-N}^t\text{Bu})\text{TiMe}_2$  catalyst was studied. It was found that the octamethyltetrahydrodibenzofluorenyl-ligated complex shows excellent ability for ethylene/1-hexene copolymerization and ethylene/dicyclopentadiene copolymerization as well as ethylene and 1-hexene with dicyclopentadiene terpolymerization. The explanation to describe the effect was divided into two cases. At constant ethylene and 1-hexene in feed, the activity for terpolymerization was decreased with an increase in dicyclopentadiene and lower compared to ethylene and 1-hexene copolymerization. The decrease in catalytic activity is due to the fact that one double bond of dicyclopentadiene may chelate with active center, and thus lead to the lower catalytic activity. Additionally, at ethylene and dicyclopentadiene concentration constant, the terpolymerization activity was increased with an increase in 1-hexene concentration and showed higher catalytic activity compared to ethylene and dicyclopentadiene copolymerization. The increase in 1-hexene would obstruct dicyclopentadiene coordination to active site. When increasing 1-hexene concentration, the 1-hexene incorporation was increased, while dicyclopentadiene insertion was also increased with an increase in dicyclopentadiene in feed. Based on  $^{13}\text{C}$  NMR analysis, the 1-hexene incorporation was significantly depended on dicyclopentadiene concentration. However, 1-hexene concentration seems did not affect on dicyclopentadiene incorporation. No melting temperature was observed, suggesting that the resultant polymers are amorphous material. In conclusion, terpolymerization of ethylene and 1-hexene with dicyclopentadiene catalyzed with the present catalyst was found to be as a promising alternative approach of the synthesis of polyolefin containing functional group. This offers new promising possibility to develop polymer industry.



For the third part, the copolymerization of ethylene and 1-olefin via metallocene/MMAO catalysts by varying the comonomer chain length was investigated. It was found that in case of short chain length, from 1-C6 to 1-C10, the increase in comonomer chain length resulted in the decrease in catalytic activity. This is due to more steric hindrance around active site. On the contrary, when long comonomer chain length was used, 1-C12 to 1-C18, the enhancement of the activity was observed. The longer comonomer chain length can force the opening of supplementary angle, making the olefin coordination site open wider, and thus leading to an enhancement in catalytic activity. However, the increase of comonomer chain length had no significant effect on polymer characteristics in terms of melting temperature and comonomer distributions. The crystallinity tended to decrease with increased chain length, based on XRD analysis.

## 5.2 RECOMMENDATIONS

In the preliminary study on the effect of substituent on the catalytic ability of Ti complexes, the results showed that the introduction of substituent on fluorenyl ligand affected on the activity and properties of polymer. The comonomer incorporation, comonomer distribution and monomer reactivity ratios were also found to depend on the ligand substitution. In general, instead of the ligand structure, the used cocatalyst seems to influence on the catalytic performance. More detailed studies on the difference in cocatalyst, i.e. MAO, dMMAO, MMAO-BHT should be found out to achieve a better understanding of their ability for ethylene copolymerization and to find the correlation between the cocatalyst and the characteristics in terms of comonomer incorporation and distribution.

Although ethylene and 1-hexene with dicyclopentadiene terpolymer are considered as a promising alternative approach of synthesis of polyolefin containing (polar) functionality, the introduction of functional groups through the chemical reaction such as epoxidation should be employed in order to check whether the resultant polymer can be modified through the chemical reaction or not. The remaining double bond in the ethylene terpolymer would be converted into the functional group, producing polyolefin

containing functionality. Therefore, the use of IR and NMR techniques would be a power tool to check and confirm the chemical reaction of the resultant polymer. In addition, the more detailed study on the different dienes which contain two olefins with different reactivities such as 1,4-hexadiene and 3,3'-divinylbiphenyl should be further investigated in order to find the possibility to produce new polymers.

For the case of the comonomer chain length effect, more detailed study on the polymer properties including molecular weight should be further determined. This is possible that the comonomer chain length affected on the molecular weight of the resultant polymer. In order to support those results,  $^1\text{H}$  NMR technique should be measured. The signal peak of vinyl chain-end, the vinylidene chain-end and the internal double bond, which results from the  $\beta$ -H elimination would answer how the relation between comonomer chain length and the molecular weight of copolymer is.

## REFERENCES

- [1] Van Grieken, R., Carrero, A., Suarez, I., Paredes, B. Effect of 1-hexene comonomer on polyethylene particle growth and kinetic profiles. Macromol. Symp. 259 (2007): 243–252.
- [2] Piel, C., Starck, P., Seppälä, J.V., Kaminsky, W. Thermal and mechanical analysis of metallocene-catalyzed ethene- $\alpha$ -olefin copolymers: The influence of the length and number of the crystallizing side chains. J. Polym Sci, Part A: Polym. Chem. 44 (2006): 1600–1612.
- [3] Smit, M., Zheng, X., Brüll, R., Loos, J., Chadwick, J.C., Koning, C.E. Effect of 1-hexene comonomer on polyethylene particle growth and copolymer chemical composition distribution. J. Polym Sci, Part A: Polym. Chem. 44 (2006): 2883–2890.
- [4] Awudza, J.A.M., Tait, P.J.T. The “comonomer effect” in ethylene/ $\alpha$ -Olefin copolymerization using homogeneous and silica-supported Cp<sub>2</sub>ZrCl<sub>2</sub>/MAO catalyst systems: some insights from the kinetics of polymerization, active center studies, and polymerization temperature. J. Polym Sci, Part A: Polym. Chem. 46 (2008): 267–277.
- [5] Ewen, J.A. Symmetry rules and reaction mechanisms of Ziegler-Natta catalysts. J. Mol. Catal. A: Chem. 128 (1998): 103–109.
- [6] Park, H.W., Chung, J.S., Lim, S.S., Song, I.K., Chemical composition distributions and microstructures of ethylene–hexene copolymers produced by a *rac*-Et(Ind)<sub>2</sub>ZrCl<sub>2</sub>/TiCl<sub>4</sub>/MAO/SMB catalyst. J. Mol. Catal. A: Chem. 264 (2007): 202–207.
- [7] Kaminsky, W. The discovery of metallocene catalysts and their present state of the art. J. Polym Sci, Part A: Polym. Chem. 42 (2004): 3911–3921.

- [8] Paredes, B., Soares, J.B.P., Van Grieken, R., Carrero, A., Suarez, I. Characterization of ethylene-1-hexene copolymers made with supported metallocene catalysts: Influence of support type. Macromol. Symp. 257 (2007): 103–111.
- [9] Cano, J. Kunz, K.. Effect of 1-hexene comonomer on polyethylene particle growth and kinetic profiles. J. Organomet. Chem. 692 (2007): 4411-4423.
- [10] Razavi, A. Metallocene catalysts technology and environment. Comptes Rendus de l'Academie des Sciences - Series IIC: Chemistry 3 (2000): 615–625.
- [11] Mcknight, A. L., Waymouth, R. M. Group 4 Ansa-Cyclopentadienyl-Amido Catalysts for Olefin Polymerization. Chem. Rev. 98 (1998): 2587-2598.
- [12] Gibson, V.C. and Spitzmesser S.K. Advances in non-metallocene olefin polymerization catalysis. Chem. Rev. 103 (2003): 283-316.
- [13] Chien, J.C.W., Nozaki, T. Ethylene–hexene copolymerization by heterogeneous and homogeneous Ziegler–Natta catalysts and the “comonomer” effect. J. Polym. Sci., Part A: Polym. Chem. 31 (1993): 227-237.
- [14] Simanke, A.G., Galland, G.B., Freitas, L., Da Jornada, J.A.H., Quijada, R., Mauler, R.S. Influence of the comonomer content on the thermal and dynamic mechanical properties of metallocene ethylene/1-octene copolymers. Polymer 40 (1999): 5489-5496.
- [15] Sernetz, F.G., Muñhaupt, R. Metallocene-Catalyzed Ethene/styrene Co- and Terpolymerization with Olefinic Termonomers. J. Polym. Sci., Part A: Polym. Chem. 35 (1997): 2549-2560.

- [16] Marconi, R., Boggioni, L., Ravasio, A., Colo, F.D., Tritto I., Stehling, U.M. Terpolymerization of Linear and Alicyclic R-Olefins with Norbornene and Ethylene by ansa-Metallocene Catalysts. Macromolecules 44 (2011): 795–804.
- [17] Galland, G.B., Nunes, F. <sup>13</sup>C Carbon nuclear magnetic resonance characterization of ethylene–propylene–1-octadecene terpolymers and comparison with ethylene–propylene–1-hexene and 1-decene terpolymers. Polymer 47 (2006): 2634–2642.
- [18] Mortazavi, M., Arabi, H., Ahmadjo, S., Nekoomanesh, M., Zohuri, G. H. Comparative Study of Copolymerization and Terpolymerization of Ethylene/Propylene/Diene Monomers Using Metallocene Catalyst. J. Appl. Polym. Sci. 122 (2011):1838-1846.
- [19] Kaminsky, W., Laban, A. Metallocene catalysis. Appl. Catal. A: Gen. 222 (2001): 47-61.
- [20] Huang, J., Rempel, G.L. Ziegler-Natta catalysts for olefin polymerization: Mechanistic insights from metallocene system. Prog. Polym. Sci. 20 (1995): 459-526.
- [21] Kissin, Y.V. Active centers in Ziegler–Natta catalysts: Formation kinetics and structure. J. Catal. 292 (2012): 188–200.
- [22] Hamielec, A.E., Soares, J.B.P. Polymerization reaction engineering: Metallocene catalysis. Prog. Polym. Sci. 21 (1996): 651-706.
- [23] Kaminsky, W., Arndt, M. Metallocenes for Polymer Catalysis. Advances in Polymer Science 127 (1996):143-188.
- [24] Sinn, H. and Kaminsky, W. Ziegler-Natta Catalysis. Advances in Organometallic Chemistry 18 (1980): 99-149.

- [25] Helmut, G., Koppl, A. Effect of the nature of metallocene complexes of Group IV Metals on their Performance in Catalytic Ethylene and Propylene Polymerization. Chem. Rev. 100 (2000): 1205-1222.
- [26] Review: Itte, S.D., Johnson, L.K., Brookhart, M., Late Metal Catalysts for Ethylene Homo- and Copolymerization. Chem. Rev. 100 (2000): 1169-1203.
- [27] Braunschweig, H., Breitling, F.M. Constrained geometry complexes-Synthesis and applications. Coord. Chem. Rev. 250 (2006): 2691-2720.
- [28] Okuda, J., Musikabhumma, K., Sinnema, P. The Kinetic Stability of Cationic Benzyl Titanium Complexes that Contain a Linked Amido-Cyclopentadienyl Ligand: The Influence of the Amido-Substituent on the Ethylene Polymerization Activity of "Constrained Geometry Catalysts". Israel J. Chem. 42 (2002): 383-392.
- [29] Cai, Z., Ikeda, T., Akita, M., Shiono, T. Substituent Effects of tert-Butyl Groups on Fluorenyl Ligand in Syndiospecific Living Polymerization of Propylene with ansa-Fluorenylamidodimethyltitanium Complex. Macromolecules 38 (2005): 8135-8139.
- [30] McKnight, A.L., Masood, Md.A., Waymouth, R.M. Selectivity in Propylene Polymerization with Group 4 Cp-Amido Catalysts. Organometallics 16 (1997): 2879-2885.
- [31] Hagihara, H., Shiono, T., Ikeda, T. Living Polymerization of Propene and 1-Hexene with the [*t*-BuNSiMe<sub>2</sub>Flu]TiMe<sub>2</sub>/B(C<sub>6</sub>F<sub>5</sub>)<sub>3</sub> Catalyst. Macromolecules 31 (1998): 3184-3188.
- [32] Shiono, T., Sugimoto, M., Hasan, T., Cai, Z., Ikeda, T. Random Copolymerization of Norbornene with Higher 1-Alkene with ansa-Fluorenylamidodimethyltitanium Catalyst. Macromolecules 41 (2008): 8292-8294.

- [33] Irwin, L.J., Reibenspies, J.H., Miller, S.A. A Sterically Expanded “Constrained Geometry Catalyst” for Highly Active Olefin Polymerization and Copolymerization: An Unyielding Comonomer Effect. J. Am. Chem. Soc. 126 (2004): 16716-16717.
- [34] Li, H. and Niu, Y. Ethylene/ $\alpha$ -olefin copolymerization by nonbridged (cyclopentadienyl)(aryloxy)titanium(IV) dichloride/ $\text{Al}(\text{t-Bu})_3/\text{Ph}_3\text{CB}(\text{C}_6\text{F}_5)_4$  catalyst systems. J. Appl. Polym. Sci. 121 (2011): 3085-3092.
- [35] Devore D.D., Timmers F.J., Hasha D.L., Rosen R.K., Marks T.J., Deck P.A., Stern C.L. Constrained-Geometry Titanium(II) Diene Complexes. Structural Diversity and Olefin Polymerization Activity. Organometallics 14 (1995): 3132-3134.
- [36] Canich J.A.M., (Exxon). PCT Int. Appl. 1996, WO96/00244.
- [37] Kleinschmidt, R., Griebenow, Y., Fink, G. Stereospecific propylene polymerization using half-sandwich metallocene/MAO systems: a mechanistic insight. J. Mol. Catal. A Chem. 157 (2000): 83-90.
- [38] Li, J., Li, H., Zhang, Y., Mu, Y. Ethylene/1-octadecene copolymerization using  $[\eta^5:\eta^1\text{-C}_5\text{Me}_4\text{-4-R}_1\text{-6-R-C}_6\text{H}_2\text{O}]\text{TiCl}_2$  catalysts. J. Appl. Polym. Sci. 120 (2011): 1514-1519.
- [39] Lü, C., Zhang, Y., Mu, Y. Propylene polymerization catalyzed by constrained geometry (cyclopentadienyl)phenoxytitanium catalysts. J. Mol. Catal. A: Chem. 258 (2006): 146-151.
- [40] Janiak, C., Togni, A., Halterman, R.L. (Eds.), *Metallocenes*, vol. 2, Wiley-VCH, Weinheim, 1998, p. 547.
- [41] Review: Pasykiewicz S. The lectures of the macromolecular colloquium on alumoxanes in Hamburg. Polyhedron 9 (1990): 429-453.

- [42] Chien, J.C.W., Wang, B.P. Metallocene–methylaluminoxane catalysts for olefin polymerization. I. Trimethylaluminum as coactivator. J. Polym. Sci., Part A: Polym. Chem. 26 (1988): 3089-3102.
- [43] Harlan, C.J., Mason, M.R., Barron, A.R. Tert-Butylaluminum Hydroxides and Oxides: Structural Relationship between Alkylalumoxanes and Alumina Gels. Organometallics 13 (1994): 2957-2969.
- [44] Peng, K., Xiao, S. Studies on methylaluminoxane and ethylene polymerization. J. Mol. Catal. 90 (1994): 201-211.
- [45] Chien, J.C.W., Sugimoto, R. Kinetics and stereochemical control of propylene polymerization initiated by ethylene bis(4,5,6,7-tetrahydro-1-indenyl) zirconium dichloride/methyl aluminoxane catalyst. J. Polym. Sci., Part A: Polym. Chem. 29 (1991): 459-470.
- [46] Madri, S. Heterogenization on silica of metallocene catalysts for olefin polymerization: Technische Universiteit Eindhoven, (2005) ISBN 90-386-2697-5.
- [47] Chen, E.Y.-X., Marks, T.J. Cocatalysts for Metal-Catalyzed Olefin Polymerization: Activators, Activation Processes, and Structure-Activity Relationships. Chem. Rev. 100 (2000): 1391-1434.
- [48] Pédeutour, J.-N., Radhakrishnan, K., Cramail, H., Deffieux, A. Reactivity of Metallocene Catalysts for Olefin Polymerization: Influence of Activator Nature and Structure. Macromol. Rapid. Commun. 22 (2001): 1095-1123.
- [49] Cossee, P.J. Ziegler-Natta catalysis I. Mechanism of polymerization of  $\alpha$ -olefins with Ziegler-Natta catalysts. J. Catal. 3 (1964): 80-89.
- [50] Arlman, E. J., Cossee, P. Ziegler-Natta catalysis III. Stereospecific polymerization of propene with the catalyst system  $\text{TiCl}_3/\text{AlEt}_3$ . J. Catal. 3 (1964): 99-104.



- [51] Ciardelli, F., Altomare, A., Michelotti, M., From homogeneous to supported metallocene catalysts. Catal. Today. 41 (1998): 149-157.
- [52] Univation Technologies—EXXPOL Metallocene Catalysts ,(2002), [http://www.univation.com/offerings/emt\\_01.asp](http://www.univation.com/offerings/emt_01.asp)
- [53] Gabriel, C., Lilge, D. Comparison of different methods for the investigation of the short-chain branching distribution of LLDPE Polymer 42 (2001): 297-303.
- [54] Chien, J.C.W. and Nozaki. T. Ethylene–hexene copolymerization by heterogeneous and homogeneous Ziegler–Natta catalysts and the “comonomer” effect. J. Polym. Sci., Part A: Polym. Chem.31 (1993): 227-237.
- [55] Uozumi, T. and Soga, K. Copolymerization of olefins with Kaminsky-Sinn-type catalysts. Makromol. Chem. 193 (1992): 823-831.
- [56] Gan, S.N., Chen, S.I., Ohnishi, R. Soga, K. Homo- and copolymerization of ethylene and propylene using a heterogeneous chromium catalyst system. Polymer 28 (1987): 1391-1395.
- [57] Taniike, T., Nguyen, B.T., Takahashi, S., Vu, T.Q., Ikeya, M., Terano, M. Kinetic Elucidation of Comonomer-Induced Chemical and Physical Activation in Heterogeneous Ziegler-Natta Propylene Polymerization. J. Polym. Sci., Part A: Polym. Chem. 49 (2011): 4005–4012.
- [58] Karol, F.J., Kao, S.-C., Cann, K.J. Comonomer effects with high-activity titanium- and vanadium-based catalysts for ethylene. J. Polym. Sci., Part A: Polym. Chem. 31 (1993) 2541:2553.
- [59] Hong, H., Zhang, Z., Chung, T. C. M., LEE, R.W. Synthesis of new 1-decene-based LLDPE resins and comparison with the corresponding 1-octene- and 1-hexene-based LLDPE resins. J. Polym. Sci., Part A: Polym. Chem. 45 (2007): 639-649.

- [60] Yoon, J.S., Lee, D.H., Park, E.S., Lee, I.M., Park, D.K., Jung, S.O. Copolymerization of Ethylene/ $\alpha$ -Olefins over (2-MeInd)<sub>2</sub>ZrCl<sub>2</sub>/MAO and (2-BzInd)<sub>2</sub>ZrCl<sub>2</sub>/MAO Systems. J. Appl. Polym. Sci. 75 (2000): 928-937.
- [61] Yu, Z., Marques, M., Rausch, M. D., Chein, J. C. W. Olefin terpolymerizations. III. Symmetry, sterics, and monomer structure in *ansa*-zirconocenium catalysis of EPDM synthesis. J. Polym. Sci., Part A: Polym. Chem. 33 (1995): 2795-2801.
- [62] Lasarov, H., Pakkanen, T.T. Copolymerization of ethylene with 5-vinyl-2-norbornene in the presence of the Ph<sub>2</sub>C(Flu)(Cp)ZrCl<sub>2</sub>/MAO catalyst. Macromol. Chem. Phys. 201 (2000): 1780-1786.
- [63] Li, X.F., Hou, Z.M. Scandium-Catalyzed Copolymerization of Ethylene with Dicyclopentadiene and Terpolymerization of Ethylene, Dicyclopentadiene, and Styrene. Macromolecules. 38 (2005): 6767-6769.
- [64] Apisuk, W., Suzuki, N. Kim, H. J., Kim, D. H., Kitiyanan, B., Nomura, K. Efficient terpolymerization of ethylene and styrene with  $\alpha$ -olefins by aryloxo- modified half-titanocene-based catalysts and cocatalyst systems. J. Polym. Sci., Part A: Polym. Chem. 51 (2013): 2565-2574.
- [65] Apisuk, W., Kitiyanan, B., Kim, H.J., Kim, D.H., Nomura, K. Introduction of Reactive Functionality by the Incorporation of Divinylbiphenyl in Ethylene Copolymerization with Styrene or 1-Hexene Using Aryloxo-Modified Half-Titanocenes and MAO Catalysts. J. Polym. Sci., Part A: Polym. Chem. 51 (2013): 2581-2587.
- [66] Univation Technologies—EXXPOL Metallocene Catalysts, (2002), [http://www.univation.com/offerings/emt\\_01.asp](http://www.univation.com/offerings/emt_01.asp)
- [67] Phillip Townsend Associates, (2001), [http://www.ptai.com/pages/news/2001\\_02\\_05.html](http://www.ptai.com/pages/news/2001_02_05.html)

- [68] Nishii, K., Hagihara, H., Ikeda, T., Akita, M., Shiono, T. Stereospecific polymerization of propylene with group 4 *ansa*-fluorenylamidodimethyl complexes. J. Organomet. Chem. 691 (2006): 193-201.
- [69] Okuda, J., Schattenmann, F.J., Wokadlo, S., Massa, W. Synthesis and Characterization of Zirconium Complexes Containing a Linked Amido-Fluorenyl Ligand. Organometallics 14 (1995): 789-795.
- [70] Shiono, T., Harada, R., Cai, Z., Nakayama, Y. A Highly Active Catalyst Composed of *ansa*-Fluorenylamidodimethyltitanium Derivative for Propene Polymerization. Top. Catal. 52 (2009): 675-680.
- [71] Nishi, K., Hayano, S., Tsunogae, Y., Cai, Z., Nakayama, Y., Shiono, T. Highly Active Copolymerization of Ethylene and Dicyclopentadiene with  $[(\eta^1\text{-}t\text{-BuN})\text{SiMe}_2(\eta^1\text{-C}_{29}\text{H}_{36})]\text{TiMe}_2(\text{THF})$  Complex. Chem. Lett. 37 (2008): 590-591.
- [72] Li, J., Li, H., Zhang, Y., Mu, Y. Ethylene/1-octadecene copolymerization using  $[\eta^5:\eta^1\text{-C}_5\text{Me}_4\text{-4-R}_1\text{-6-R-C}_6\text{H}_2\text{O}]\text{TiCl}_2$  catalysts J. Appl. Polym. Sci. 120 (2011): 1514-1519.
- [73] Lee, I.-M., Gauthier, W.J., Ball, J.M., Bhagavathi, I., Collins, S. Electronic effects of Ziegler-Natta polymerization of propylene and ethylene using soluble metallocene catalysts. Organometallics 11 (1992): 2115-2122.
- [74] Price, C.J., Zeits, P.D., Reibenspies, J.H., Miller, S.A. Octamethyloctahydrodibenzofluorenyl: Electronic Comparisons between a Sterically Expanded Ligand and Its Cyclopentadienyl Analogues. Organometallics 27(2008): 3722-3727.
- [75] Li, H., Niu, Y. Ethylene/ $\alpha$ -olefin copolymerization by nonbridged (cyclopentadienyl)(aryloxy)titanium(IV)

- dichloride/ $\text{Al}^i\text{Bu}_3/\text{Ph}_3\text{CB}(\text{C}_6\text{F}_5)_4$  catalyst systems. J. Appl. Polym. Sci. 121(2011): 3085-3092.
- [76] Nishii, K., Matsumae, T., Dare, E.O., Shiono, T., Ikeda, T. Effect of Solvents on Living Polymerization of Propylene with  $[t\text{-BuNSiMe}_2\text{Flu}]\text{TiMe}_2\text{-MMAO}$  Catalyst System. Macromol. Chem. Phys. 205 (2004): 363–369.
- [77] Soga, K., Uozumi, T., Park, J.R. Effect of catalyst isospecificity on olefin copolymerization. Makromol. Chem. 191 (1990): 2853-2864.
- [78] Irwin, L.J., Miller, S.A. Unprecedented Syndioselectivity and Syndiotactic Polyolefin Melting Temperature: Polypropylene and Poly(4-methyl-1-pentene) from a Highly Active, Sterically Expanded  $\eta^1$ -Fluorenyl-  $\eta^1$ -Amido Zirconium Complex. J. Am. Chem. Soc. 127 (2005): 9972-9973.
- [79] Nishi, K., Hayano, S., Tsunogae, Y., Cai, Z., Nakayama, Y., Shiono, T. Highly Active Copolymerization of Ethylene and Dicyclopentadiene with  $[(\eta^1\text{-}t\text{-BuN})\text{SiMe}_2(\eta^1\text{-C}_{29}\text{H}_{36})]\text{TiMe}_2(\text{THF})$  Complex. Chem. Lett. 37 (2008): 590-591.
- [80] Fineman, M., Ross, S.D. Linear Method for Determining Monomer Reactivity Ratios in Copolymerization. J. Polym. Sci. 5 (1950): 259-262.
- [81] Kelen, T., Tüdös, F., J. Macromol. Sci. Chem. 1975, A9, 1.
- [82] Nomura, K., Oya, K., Imanishi, Y. Ethylene/ $\alpha$ -olefin copolymerization by various nonbridged (cyclopentadienyl)(aryloxy)titanium(IV) complexes — MAO catalyst system. J. Mol. Catal. A: Chem. 174 (2001): 127-140.
- [83] Nomura, K., Oya, K., Komatsu, T., Imanishi, Y. Effect of the Cyclopentadienyl Fragment on Monomer Reactivities and Monomer Sequence Distributions in Ethylene/ $\alpha$ -Olefin Copolymerization by a

- Nonbridged (Cyclopentadienyl)(aryloxy)titanium(IV) Complex–MAO Catalyst System. Macromolecules 33 (2000): 3187-3189.
- [84] Nomura, K., Fujita, K., Fujiki, M. Olefin polymerization by (cyclopentadienyl)(ketimide)titanium(IV) complexes of the type, Cp'TiCl<sub>2</sub>(N=C'Bu<sub>2</sub>)-methylaluminoxane (MAO) catalyst systems. J. Mol. Catal. A.: Chem. 220 (2004): 133-144.
- [85] Quijada, R., Dupont, J., Miranda, M.S.L., Scipioni, R.B., Galland, G.B. Copolymerization of ethylene with 1-hexene and 1-octene: correlation between type of catalyst and comonomer incorporated. Macromol. Chem. Phys., 196 (1995): 3991-4000.
- [86] Uozumi, T., Soga, K. Copolymerization of olefins with Kaminsky-Sinn-type catalysts. Makromol. Chem. 193 (1992): 823-831.
- [87] Reybuck, S.E., Waymouth, R.M. Investigation of Bridge and 2-Phenyl Substituent Effects on Ethylene/ $\alpha$ -Olefin Copolymerization Behavior with 1,2'-Bridged Bis(indenyl)zirconium Dichlorides. Macromolecules. 37 (2004): 2342-2347.
- [88] Yang, G., Hong, M., Li, Y., Yu, S. Synthesis of Novel Bis( $\beta$ -enamino-ketonato)titanium Catalyst with High Activity and Excellent Ability to Copolymerize Olefins. Macromol. Chem. Phys. 213 (2012): 2311-2318.
- [89] Cai, Z., Harada, R., Nakayama, Y., Shiono, T. Highly Active Living Random Copolymerization of Norbornene and 1-Alkene with *ansa*-Fluorenylamidodimethyltitanium Derivative: Substituent Effects on Fluorenyl Ligand. Macromolecules 43(2010): 4527-4531.
- [90] Chung, T.C., Lu, H. L, Li, C. L. Synthesis and Functionalization of Unsaturated Polyethylene: Poly(ethylene-co-1,4-hexadiene). Macromolecules 27 (1994): 7533-7537.

- [91] Marathe, S., Sivaram, S. Regioselective Copolymerization of 5-Vinyl-2-norbornene with Ethylene Using Zirconocene-Methylaluminoxane Catalysts: A Facile Route to Functional Polyolefins. Macromolecules 27 (1994): 1083-1086.
- [92] Itagaki, K., Nomura, K. Efficient Synthesis of Functionalized Polyolefin by Incorporation of 4-Vinylcyclohexene in Ethylene Copolymerization Using Half-Titanocene Catalysts. Macromolecules 42 (2009): 5097-5103.
- [93] Busico, V.; Corradini, P.; Ferraro, A.; Proto, A. Polymerization of propene in the presence of MgCl<sub>2</sub>-supported Ziegler-Natta catalysts, 3. Catalyst deactivation, Makromol. Chem. 187(1986): 1125–1130.
- [94] Li, X.F., Hou, Z.M. Scandium-Catalyzed Copolymerization of Ethylene with Dicyclopentadiene and Terpolymerization of Ethylene, Dicyclopentadiene, and Styrene. Macromolecules. 38 (2005): 6767-6769.
- [95] Pan, L., Hong, M., Li, Y.S. Living Copolymerization of Ethylene with Dicyclopentadiene Using Titanium Catalyst: Formation of Well-Defined Polyethylene-*block*-poly(ethylene-*co*-dicyclopentadiene)s and Their Transformation into Novel Polyolefin-*block*-(functional polyolefin)s. Macromolecules. 42 (2009): 4391-4393.
- [96] Hong, M., Pana, L., Li, B.-X., Li, Y.-S. Synthesis of novel poly(ethylene-*ter*-1-hexene-*ter*-dicyclopentadiene)s using bis(β-enaminoketonato)titanium catalysts and their applications in preparing polyolefin-*graft*-poly(ε-polycaprolactone). Polymer. 51 (2010): 3636-3643.
- [97] Halterman, R.L. Synthesis and applications of chiral cyclopentadienylmetal complexes. Chem. Rev. 92 (1992): 965–994.

- [98] Bialek, M., Czaja, K. The effect of the comonomer on the copolymerization of ethylene with long chain  $\alpha$ -olefins using Ziegler-Natta catalysts supported on  $\text{MgCl}_2(\text{THF})_2$ . Polymer 41 (2000): 7899-7904.
- [99] Koivumäki, J., Fink, G., Seppälä, J.V. Copolymerization of ethene/1-dodecene and ethene/1-octadecene with the stereorigid zirconium catalyst systems  $\text{iPr}[\text{FluCp}]_2\text{ZrCl}_2/\text{MAO}$  and  $\text{Me}_2\text{Si}[\text{Ind}]_2\text{ZrCl}_2/\text{MAO}$ : Influence of the comonomer chain length. Macromolecules. 27 (1994): 6254-6258.
- [100] Kaminsky, W., Piel, C., Scharlach, K. Polymerization of ethene and longer chained olefins by metallocene catalysis. Macromol. Symp. 226 (2005): 25-34.
- [101] Pérez, E., Benavente, R., Quijada, R., Narváez, A., Barrera Galland, G. Structure characterization of copolymers of ethylene and 1-octadecene. J. Polym. Sci., Part B: Polym. Phys. 38 (2000): 1440-1448.
- [102] Li, K.-T., Dai, C.-L., Kuo, C.-W. Ethylene polymerization over a nano-sized silica supported  $\text{Cp}_2\text{ZrCl}_2/\text{MAO}$  catalyst. Catal. Commun. 8 (2007): 1209-1213.
- [103] Krimm, S., Tobolsky, A.V. Quantitative x-ray studies of order in amorphous and crystalline polymers. Quantitative x-ray determination of crystallinity in polyethylene. J. polym. Sci. 7 (1951): 57-76.
- [104] Camurati, I., Cavicchi, B., Dall'Occo, T., Piemontesi, F. Synthesis and characterization of ethylene/1-olefin copolymers obtained by "single centre" catalysis. Macromol. Chem. Phys. 202 (2001): 701-709.
- [105] Randall, J.C. Carbon-13 NMR of ethylene-1-olefin copolymers: extension to the short-chain branch distribution in a low-density polyethylene. J. Polym. Sci., Part A-2: Polym. Phys. 11 (1973): 275-287.

- [106] Liu, S., Yu, G., Huang B. Polymerization of ethylene by zirconocene  $B(C_6F_5)_3$  catalysts with aluminum compounds. J. Appl. Polym. Sci. 66 (1997): 1715- 1720.
- [107] Kim, C., Kim, H. Copolymerization of propylene with various higher  $\alpha$ -olefins using silica supported *rac*- $Me_2Si(Ind)_2ZrCl_2$ . J. Polym. Sci., Part A: Polym. Chem. 39 (2001): 3294-3303.
- [108] Quijada, R., Galland, G.B., Mauler, R.S. The influence of the comonomer in the copolymerization of ethylene with  $\alpha$ -olefins using  $C_2H_4[Ind]_2ZrCl_2$ /methylaluminoxane as catalyst system. Macromol. Chem. Phys. 197 (1996): 3091-3098.
- [109] Clas, S.D., Mcfaddin, D.C., Russell, K.E., Scammell-Bullock, M.V., Peat, I.R. Melting points of homogeneous random copolymers of ethylene and 1-alkenes. J. Polym. Sci., Part A: Polym. Chem. 41 (2000): 7899-7904.



## **APPENDICES**

**APPENDIX A**  
**(NUCLEAR MAGNETIC RESONANCE)**

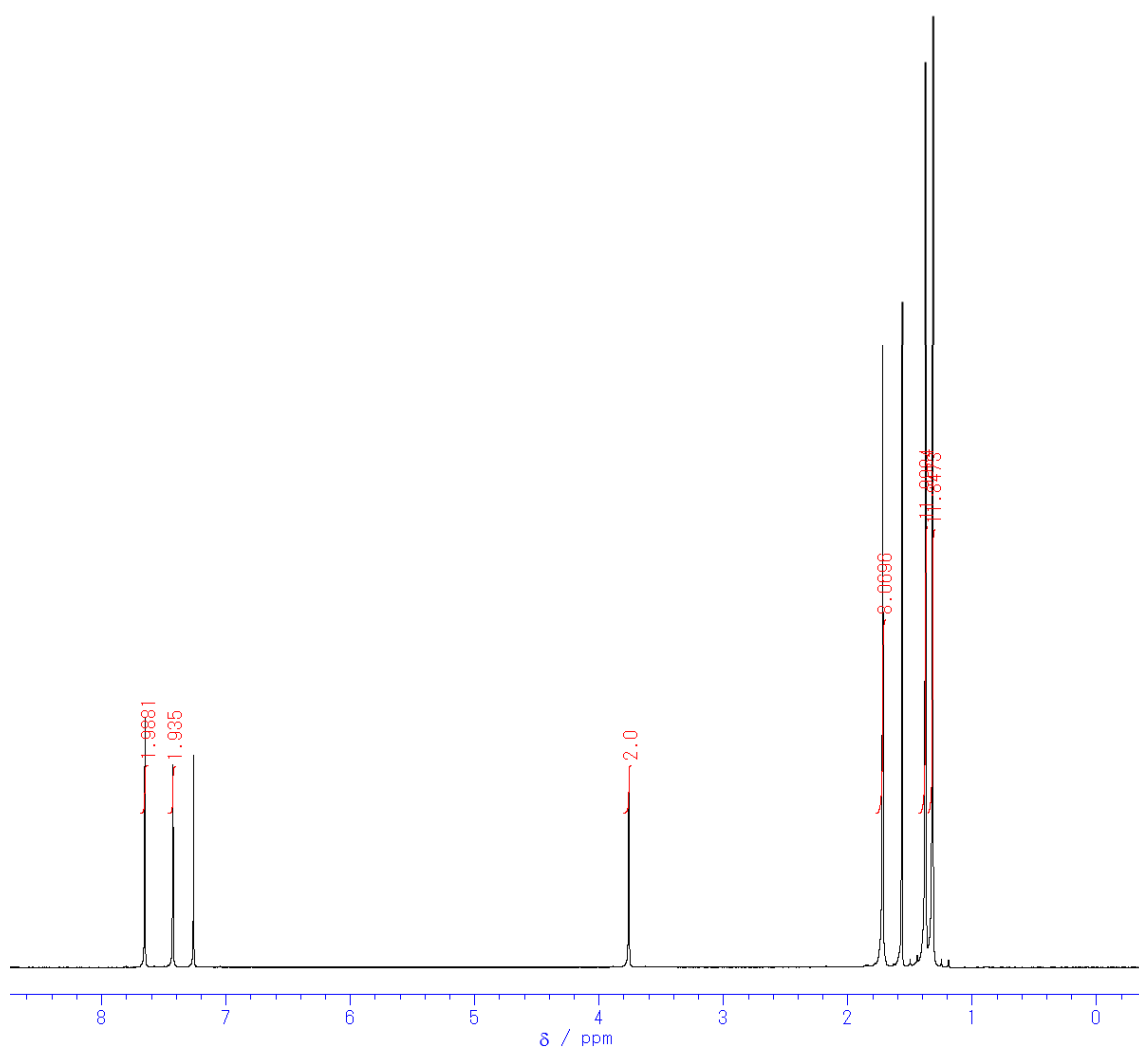


**Figure A-1**  $^1\text{H}$  NMR spectrum of octamethyloctahydrodibenzofluorene

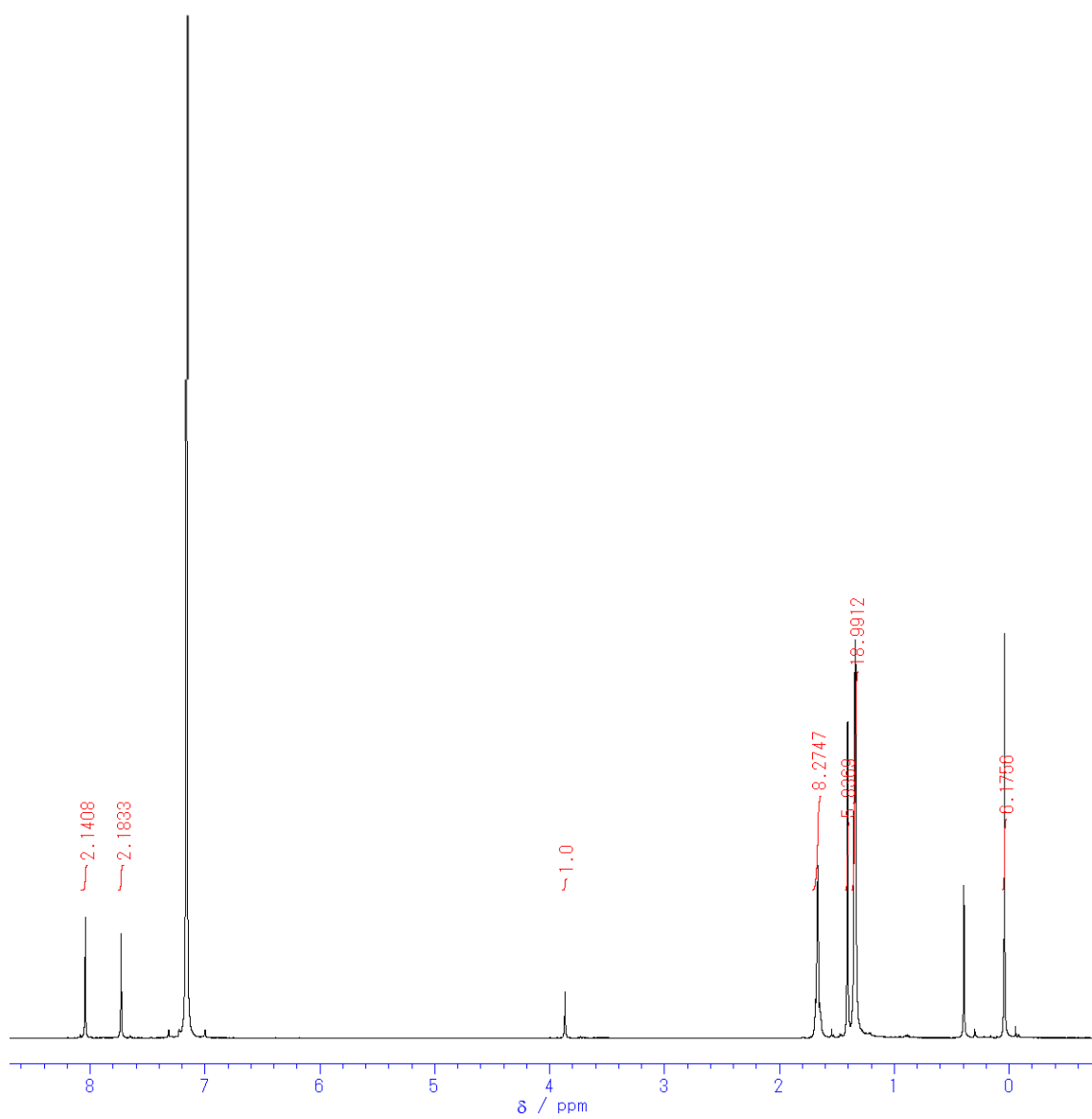


Figure A-2  $^1\text{H}$  NMR spectrum of  $\text{ClSiMe}_2(\text{C}_{29}\text{H}_{37})$

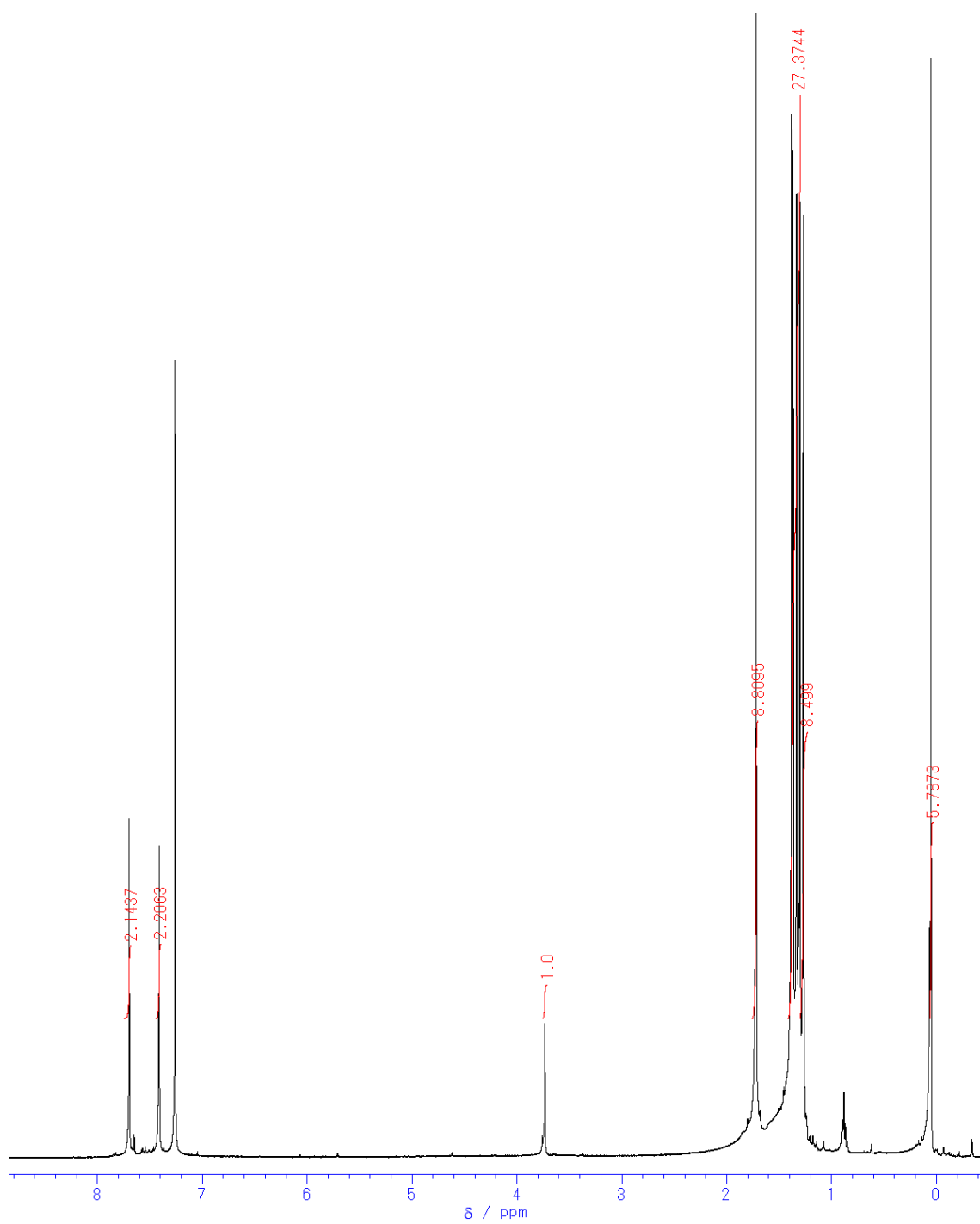


Figure A-3  $^1\text{H}$  NMR spectrum of  $\text{Me}_2\text{CNHMe}_2\text{Si}(\text{C}_{29}\text{H}_{37})$  ligand

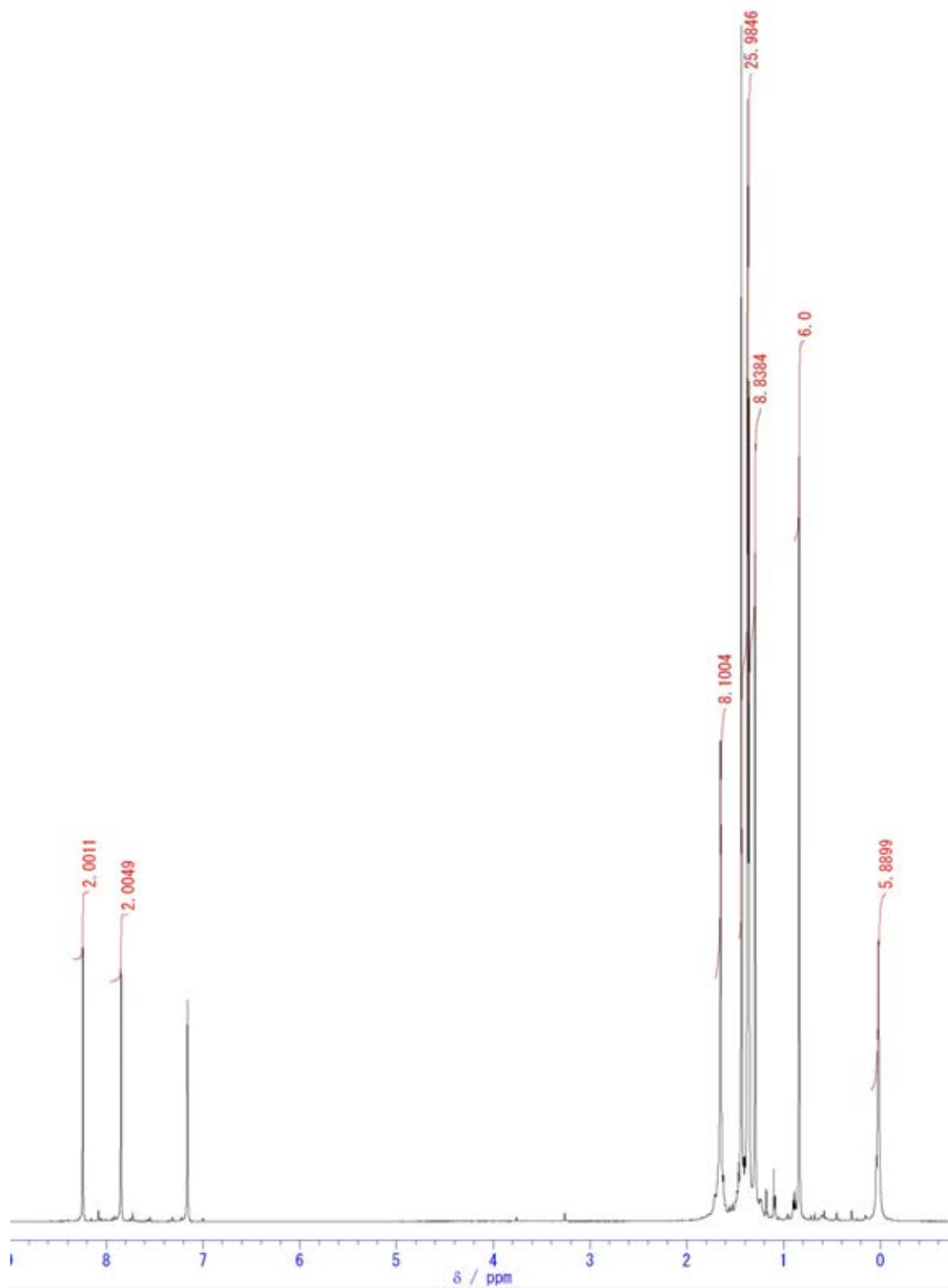
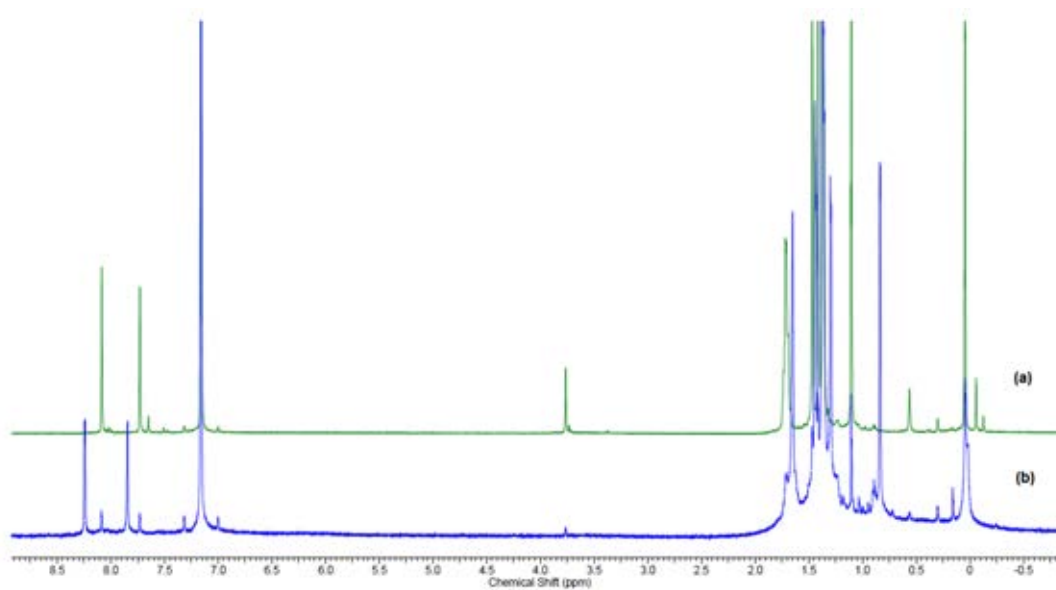
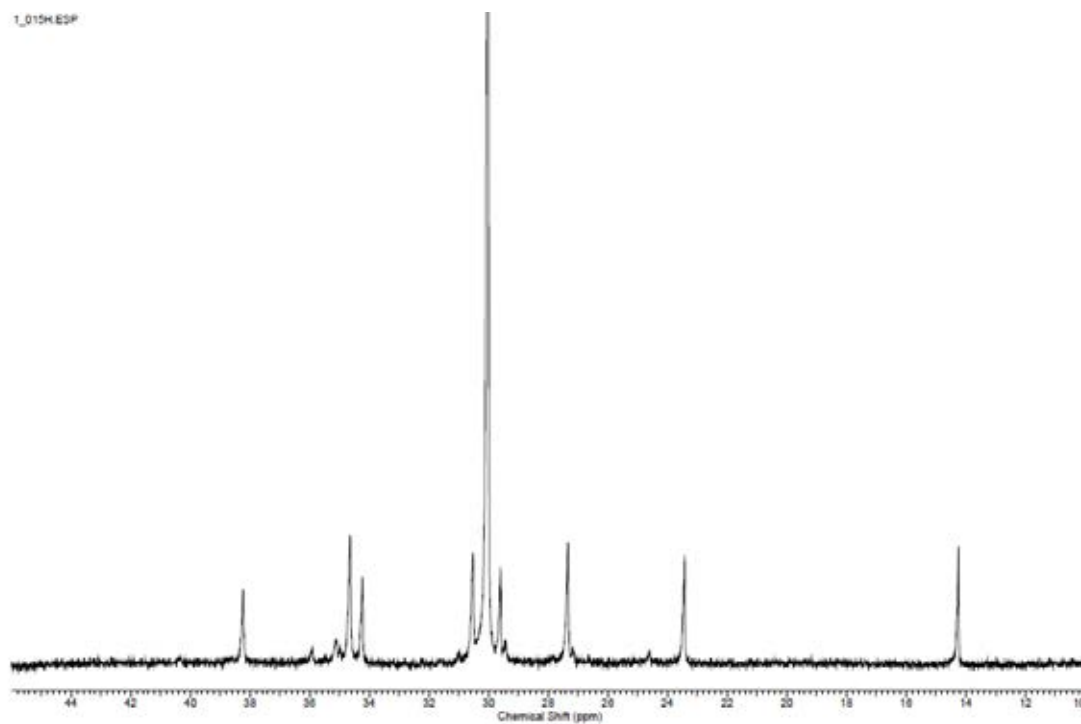


Figure A-4  $^1\text{H}$  NMR spectrum of  $\text{Me}_2\text{Si}(\eta^3\text{-C}_{29}\text{H}_{36})(\eta^1\text{-N}^t\text{Bu})\text{TiMe}_2$  complex



**Figure A-5**  $^1\text{H}$  NMR spectra of (a)  $\text{Me}_2\text{CNHMe}_2\text{Si}(\text{C}_{29}\text{H}_{37})$  ligand and (b)  $\text{Me}_2\text{Si}(\eta^3\text{-C}_{29}\text{H}_{36})(\eta^1\text{-N'Bu})\text{TiMe}_2$  complex



**Figure A-6**  $^{13}\text{C}$  NMR spectrum of ethylene/1-hexene copolymer (0.15H) entry 1

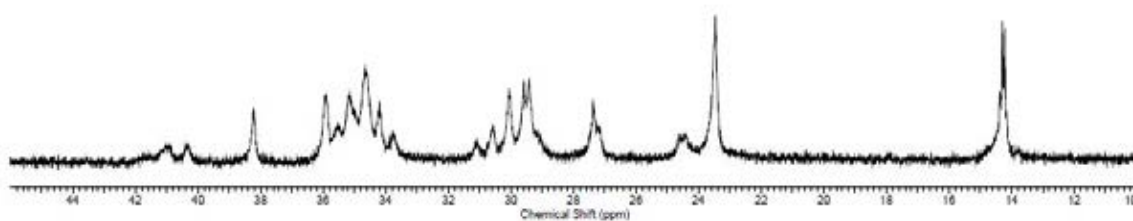


**Figure A-7**  $^{13}\text{C}$  NMR spectrum of ethylene/1-hexene copolymer (0.45H) entry 2

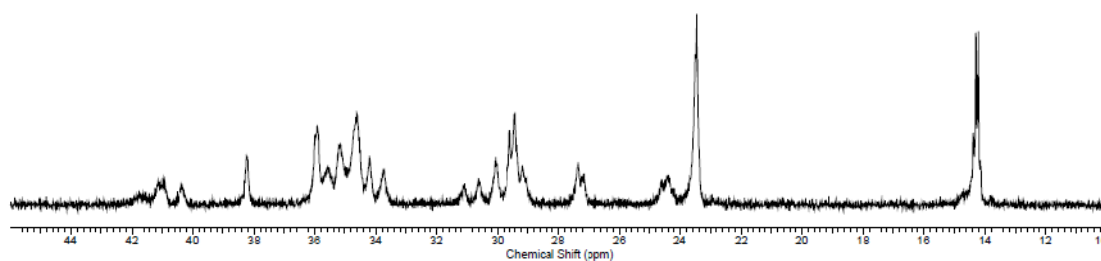


**Figure A-8**  $^{13}\text{C}$  NMR spectrum of ethylene/1-hexene copolymer (0.75H) entry 3



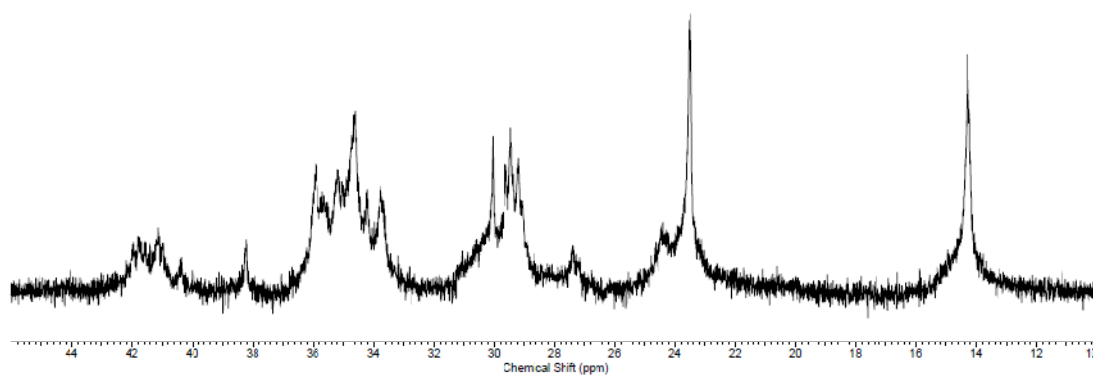


**Figure A-9**  $^{13}\text{C}$  NMR spectrum of ethylene/1-hexene copolymer (1.5H) entry 4

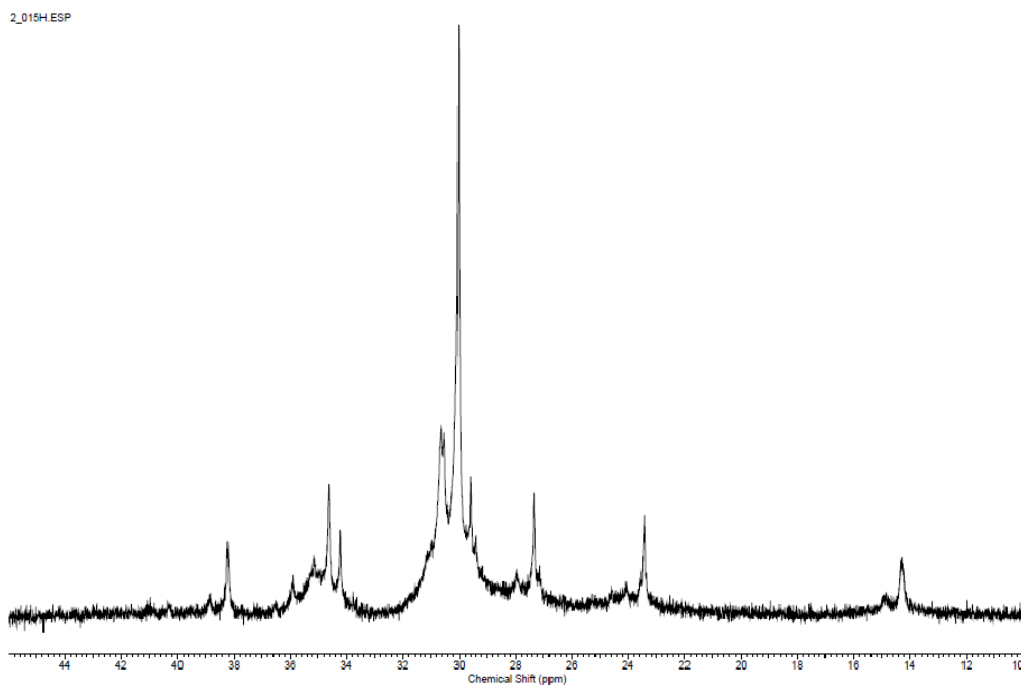


**Figure A-10**  $^{13}\text{C}$  NMR spectrum of ethylene/1-hexene copolymer (0.15H) entry 5

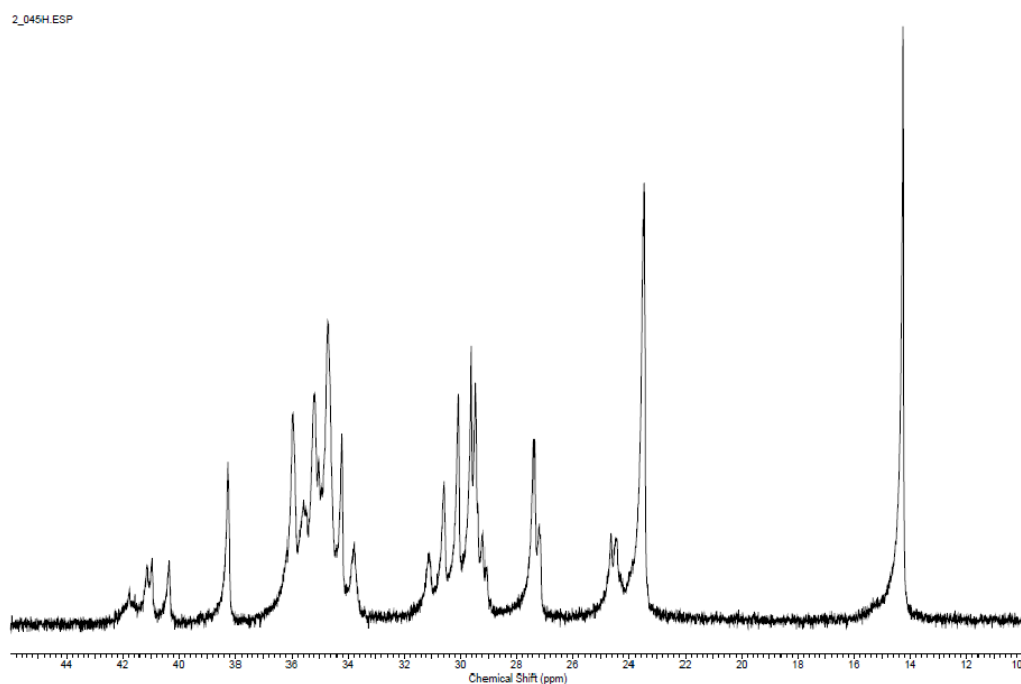


**Figure A-11** <sup>13</sup>C NMR spectrum of ethylene/1-hexene copolymer (0.45H) entry 6

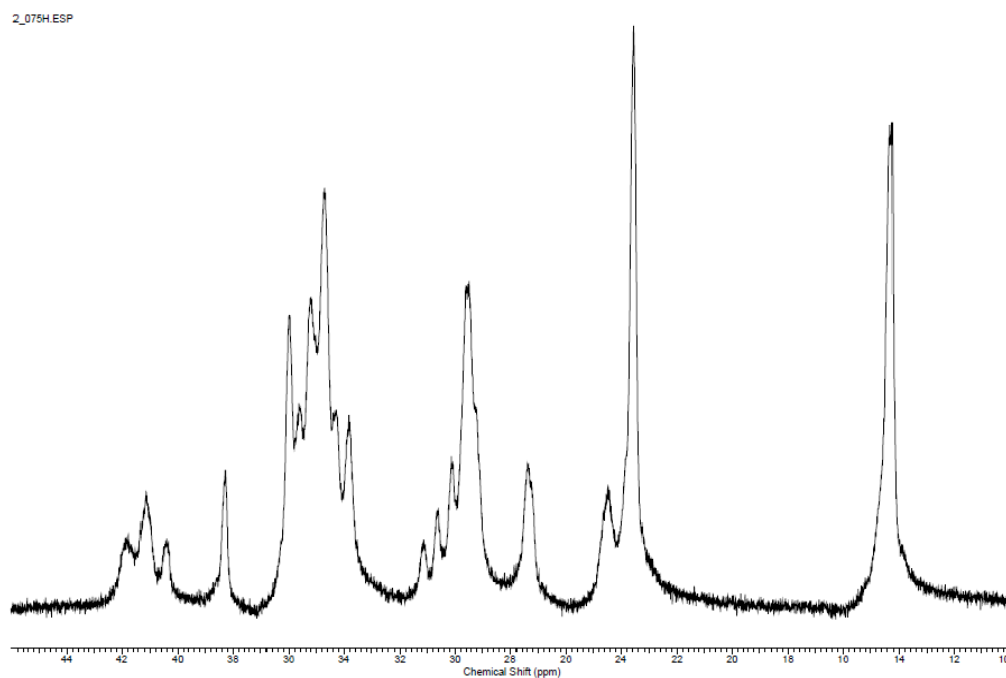


**Figure A-12** <sup>13</sup>C NMR spectrum of ethylene/1-hexene copolymer (0.75H) entry 7

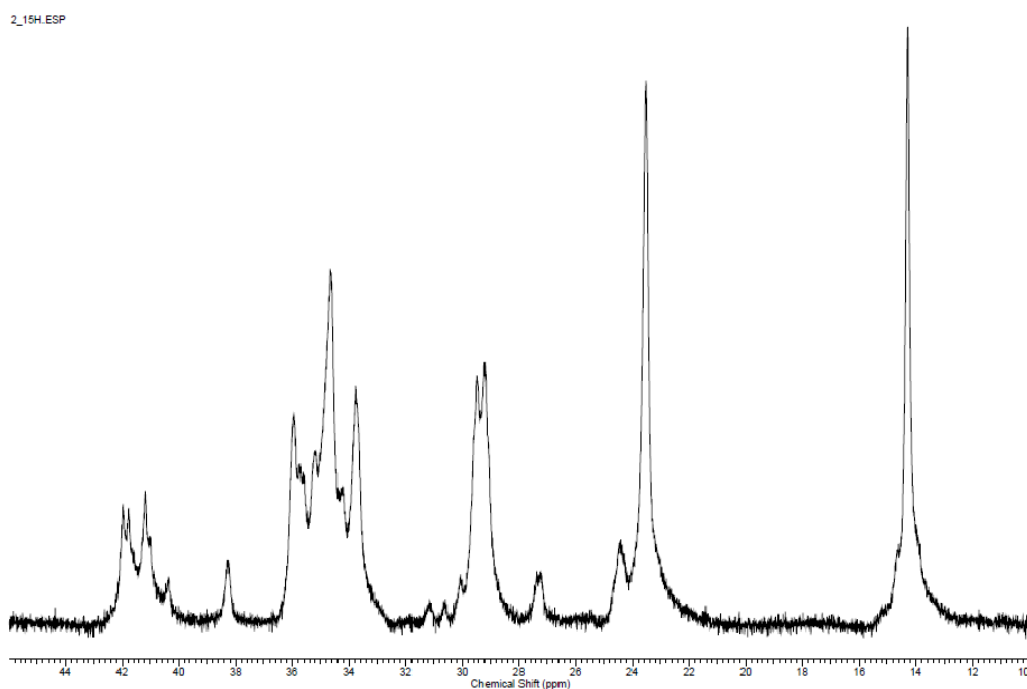


Figure A-13  $^{13}\text{C}$  NMR spectrum of ethylene/1-hexene copolymer (1.5H) entry 8

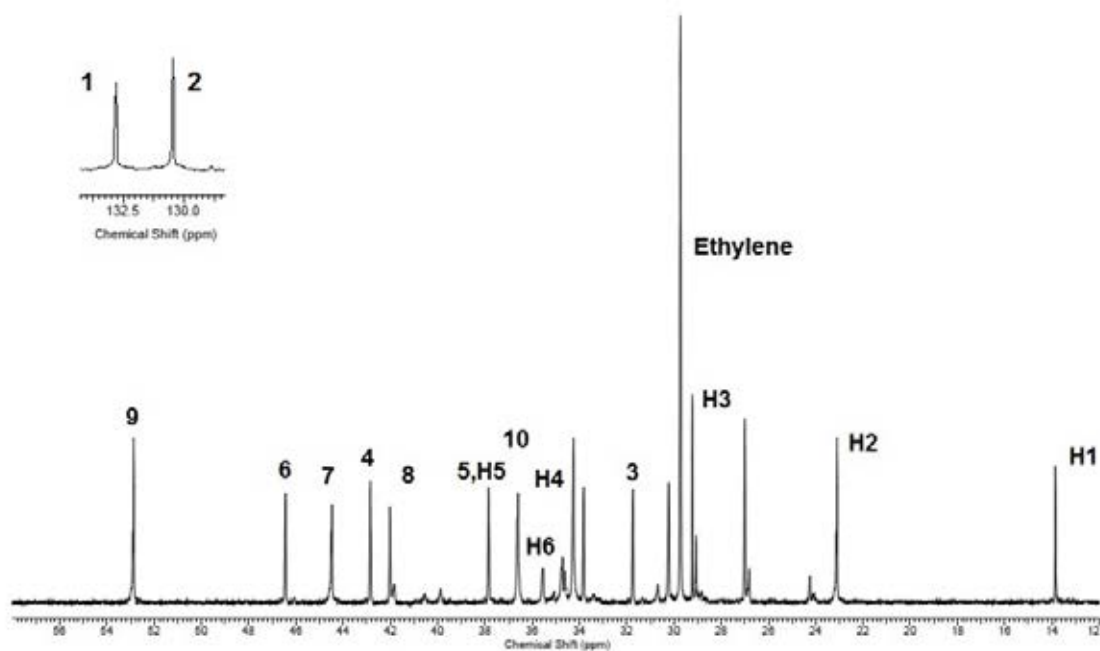


Figure A-14  $^{13}\text{C}$  NMR spectrum of ethylene/1-hexene/DCP terpolymer entry 4

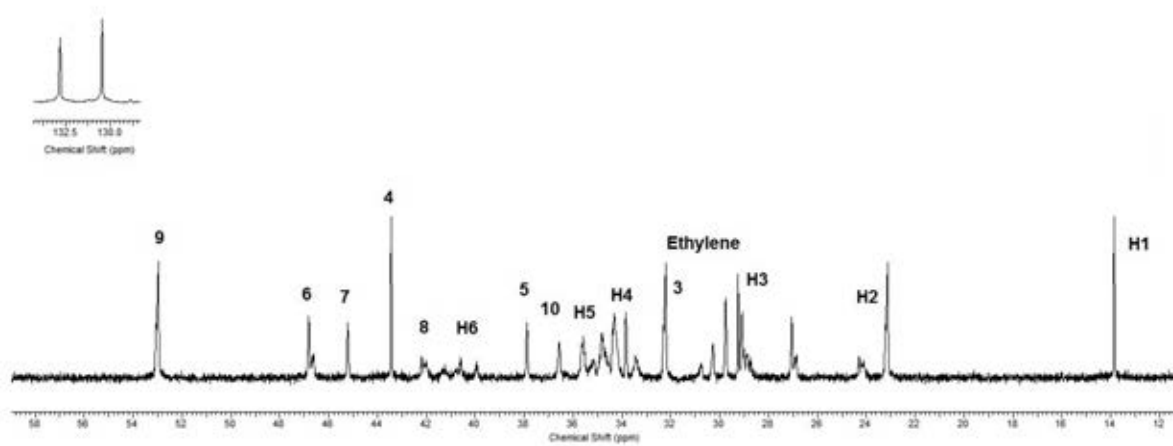


Figure A-15  $^{13}\text{C}$  NMR spectrum of ethylene/1-hexene/DCP terpolymer entry 5

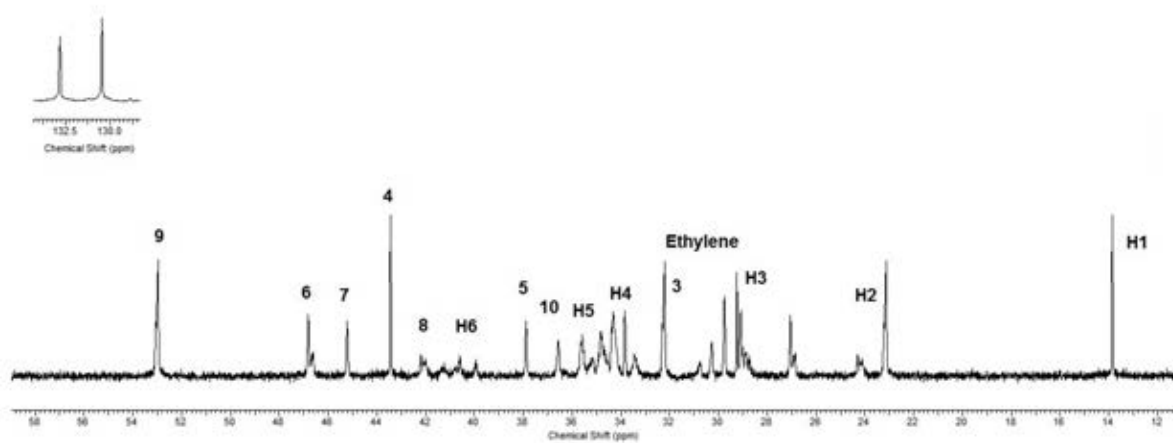
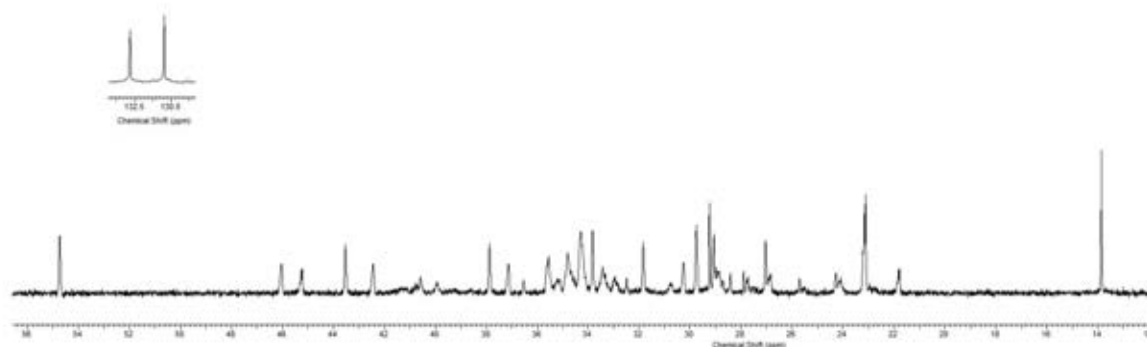
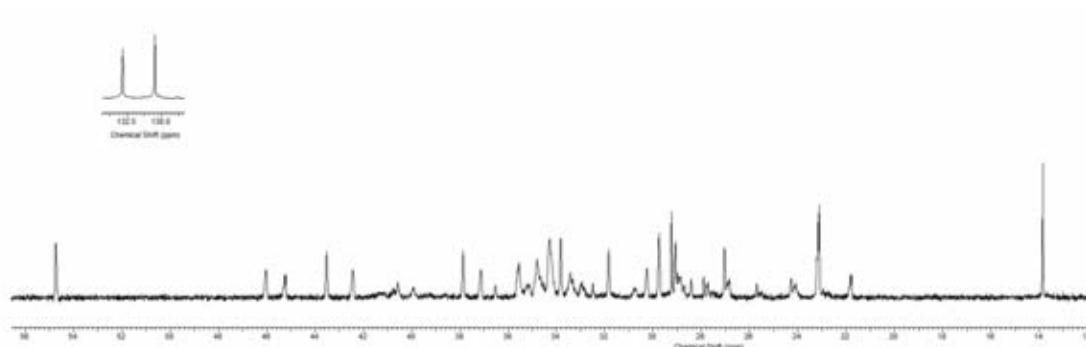


Figure A-16  $^{13}\text{C}$  NMR spectrum of ethylene/1-hexene/DCP terpolymer entry 6



**Figure A-17**  $^{13}\text{C}$  NMR spectrum of ethylene/1-hexene/DCP terpolymer entry 7



**Figure A-18**  $^{13}\text{C}$  NMR spectrum of ethylene/1-hexene/DCP terpolymer entry 8

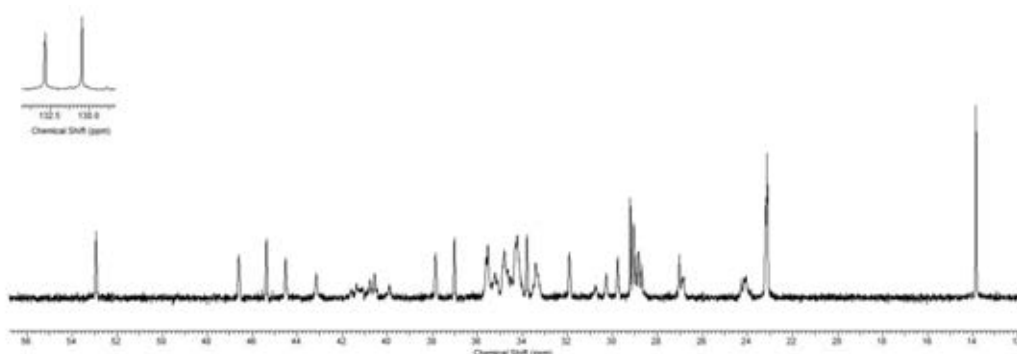


**Figure A-19**  $^{13}\text{C}$  NMR spectrum of ethylene/1-hexene/DCP terpolymer entry 9

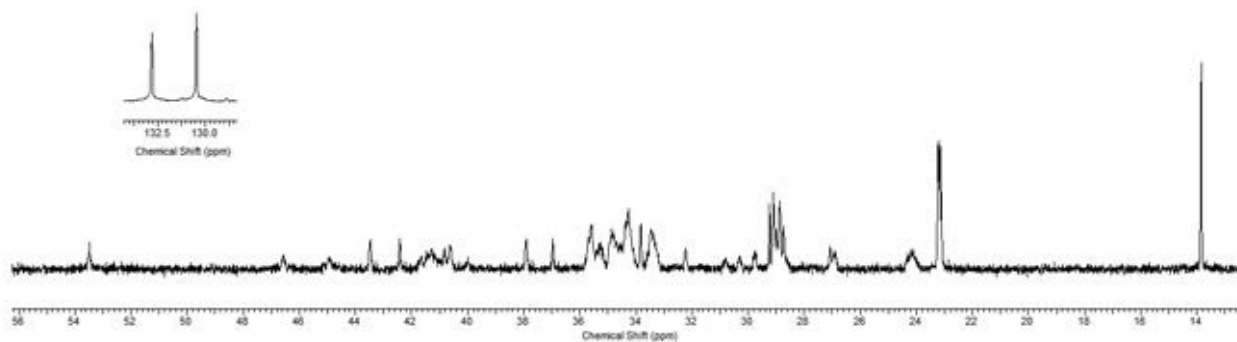


**Figure A-20**  $^{13}\text{C}$  NMR spectrum of ethylene/1-hexene/DCP terpolymer entry 10

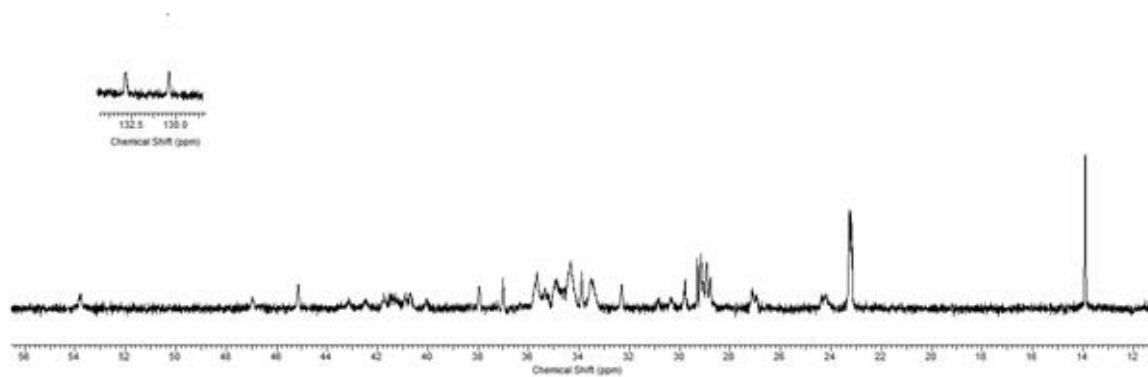


**Figure A-21**  $^{13}\text{C}$  NMR spectrum of ethylene/1-hexene/DCP terpolymer entry 11

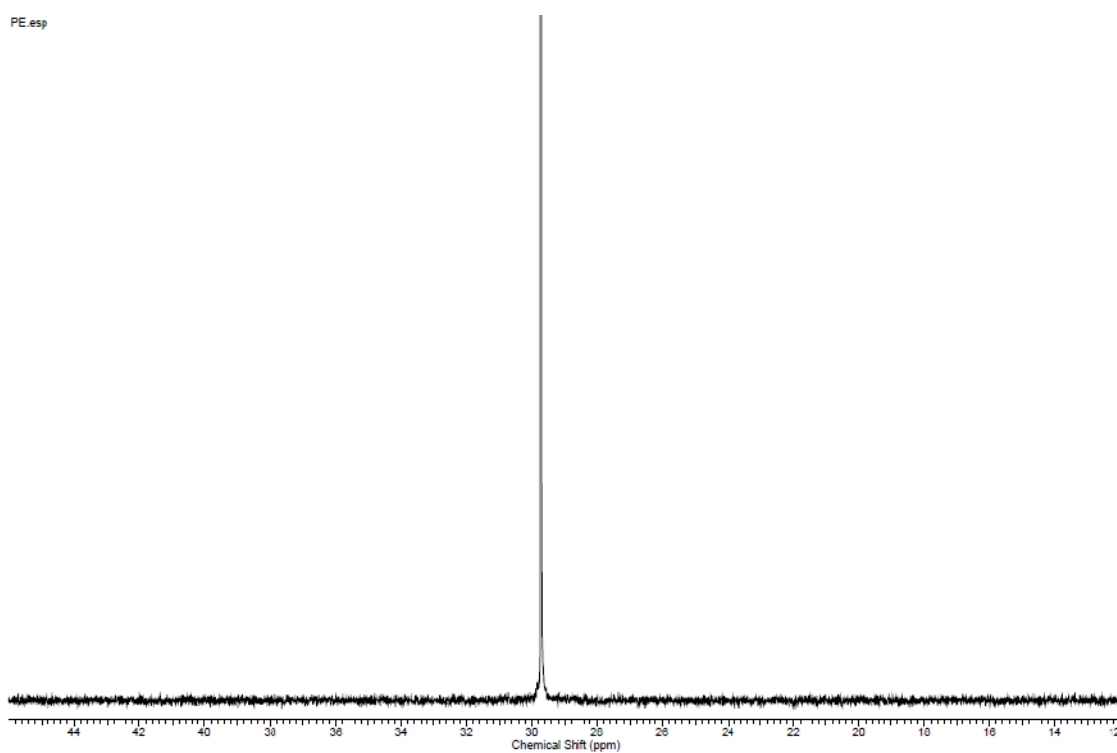


Figure A-22 <sup>13</sup>C NMR spectrum of polyethylene (part 3)

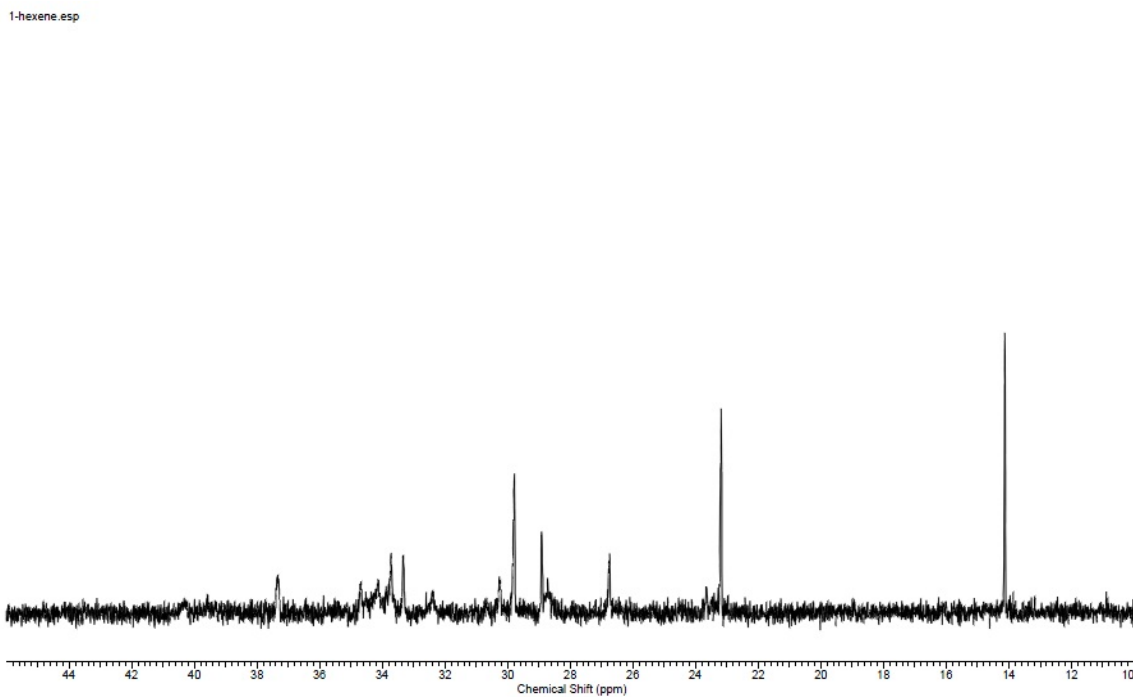
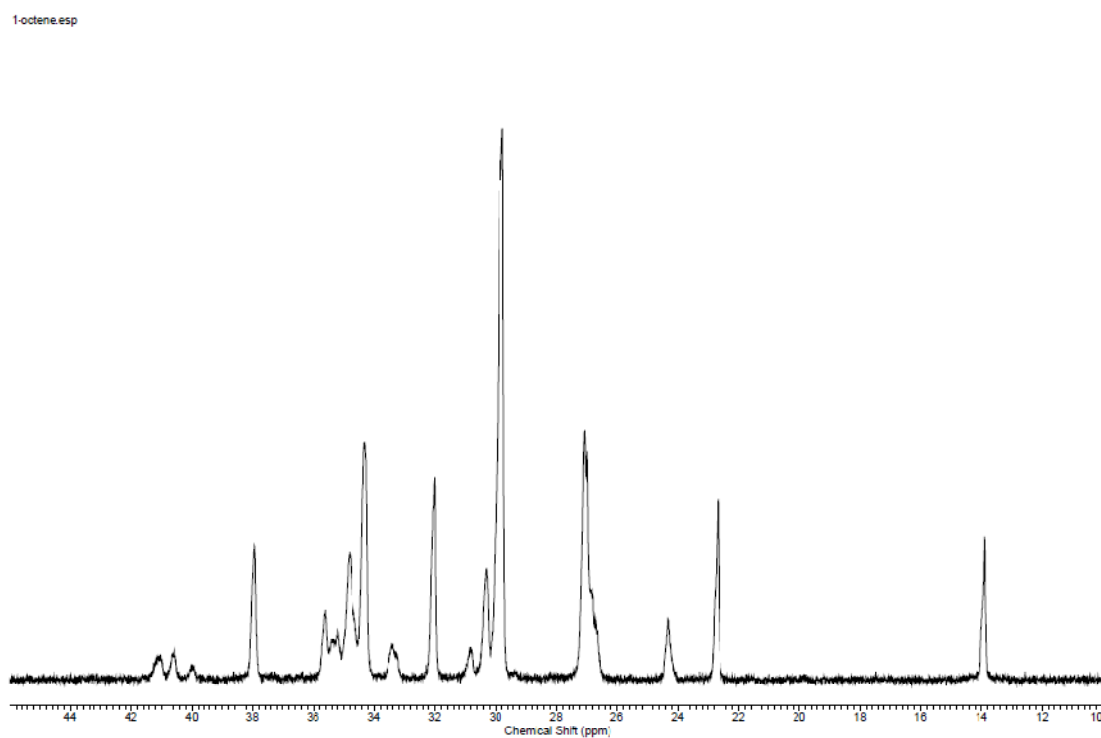
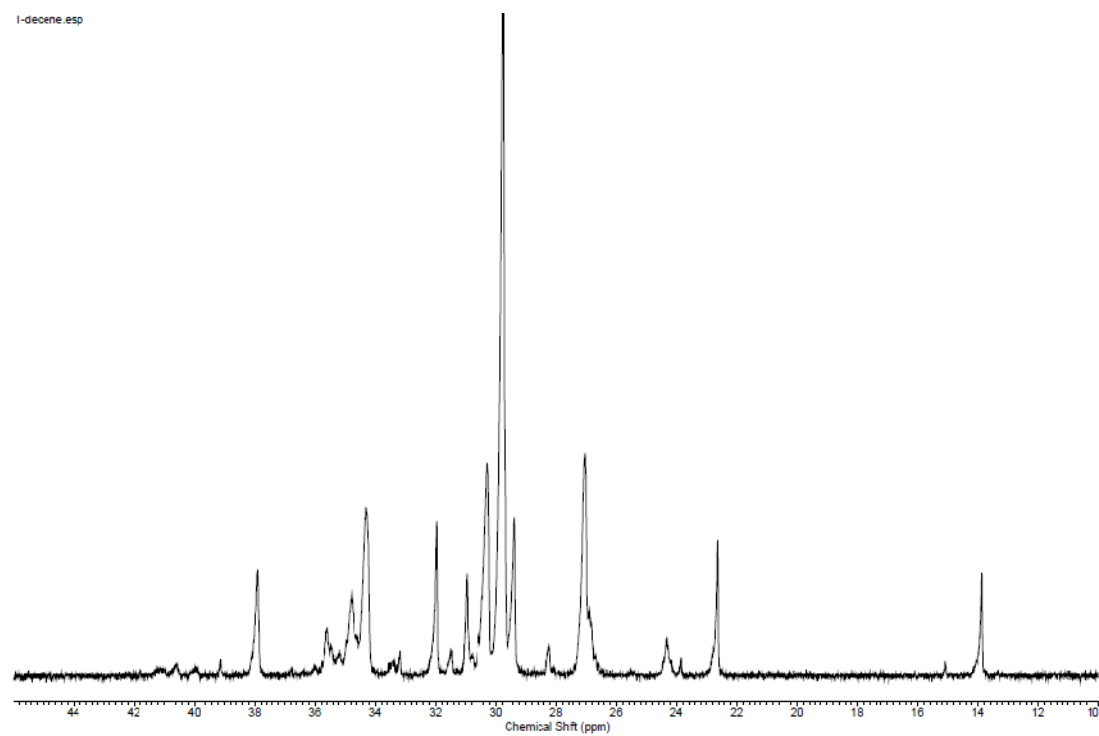


Figure A-23 <sup>13</sup>C NMR spectrum of ethylene/1-hexene copolymer



**Figure A-24**  $^{13}\text{C}$  NMR spectrum of ethylene/1-octene copolymer



**Figure A-25**  $^{13}\text{C}$  NMR spectrum of ethylene/1-decene copolymer



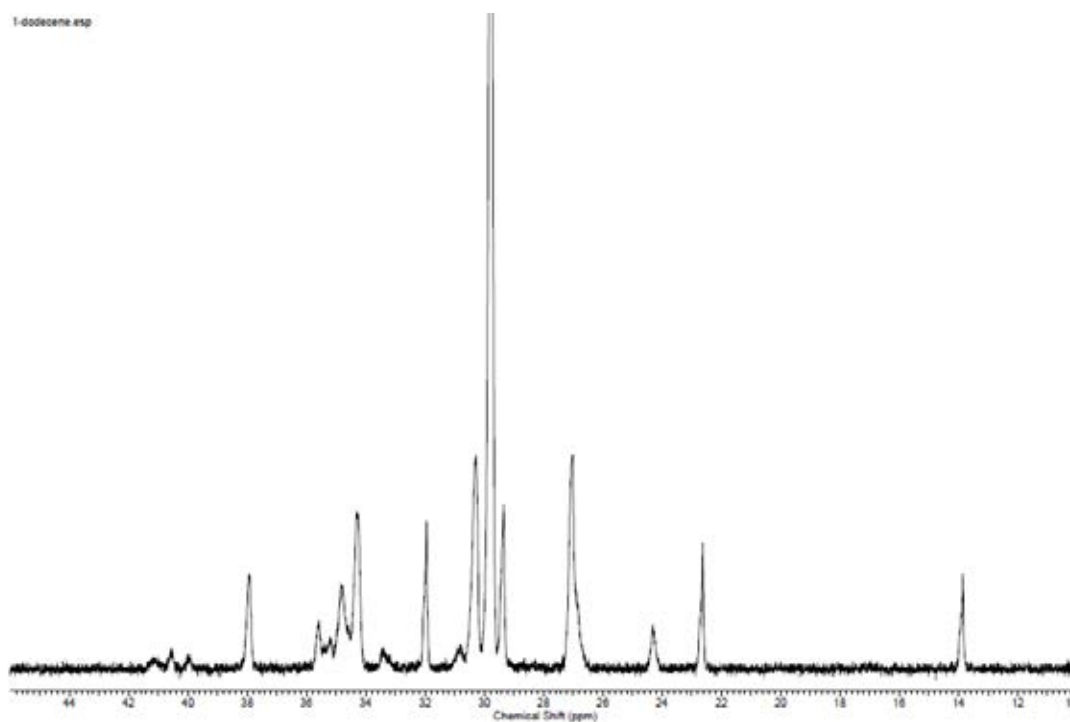


Figure A-26 <sup>13</sup>C NMR spectrum of ethylene/1-dodecene copolymer

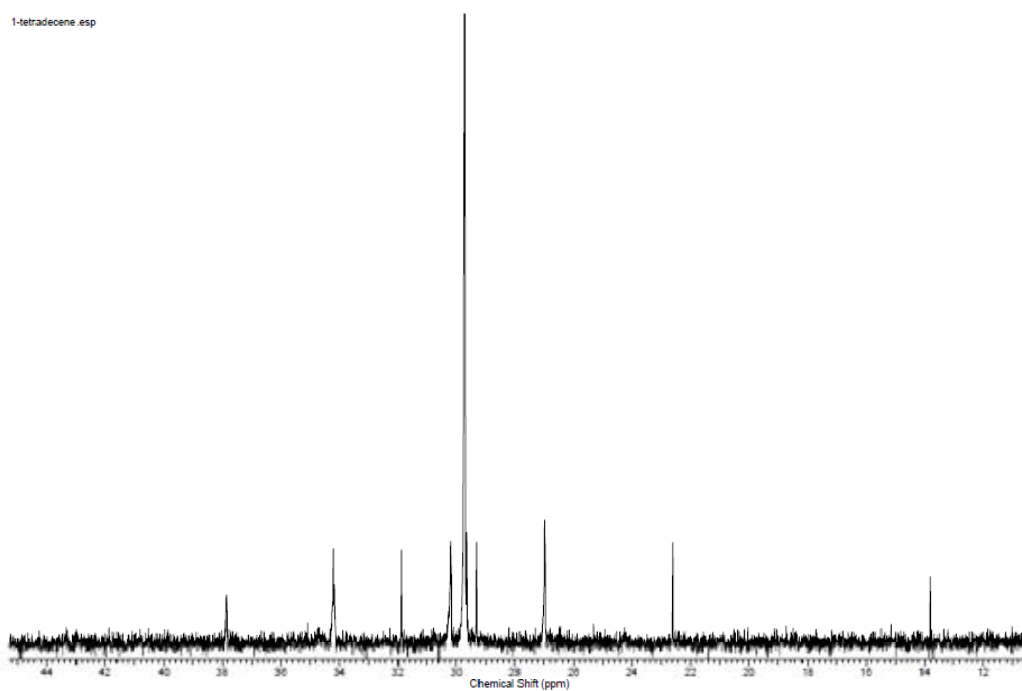
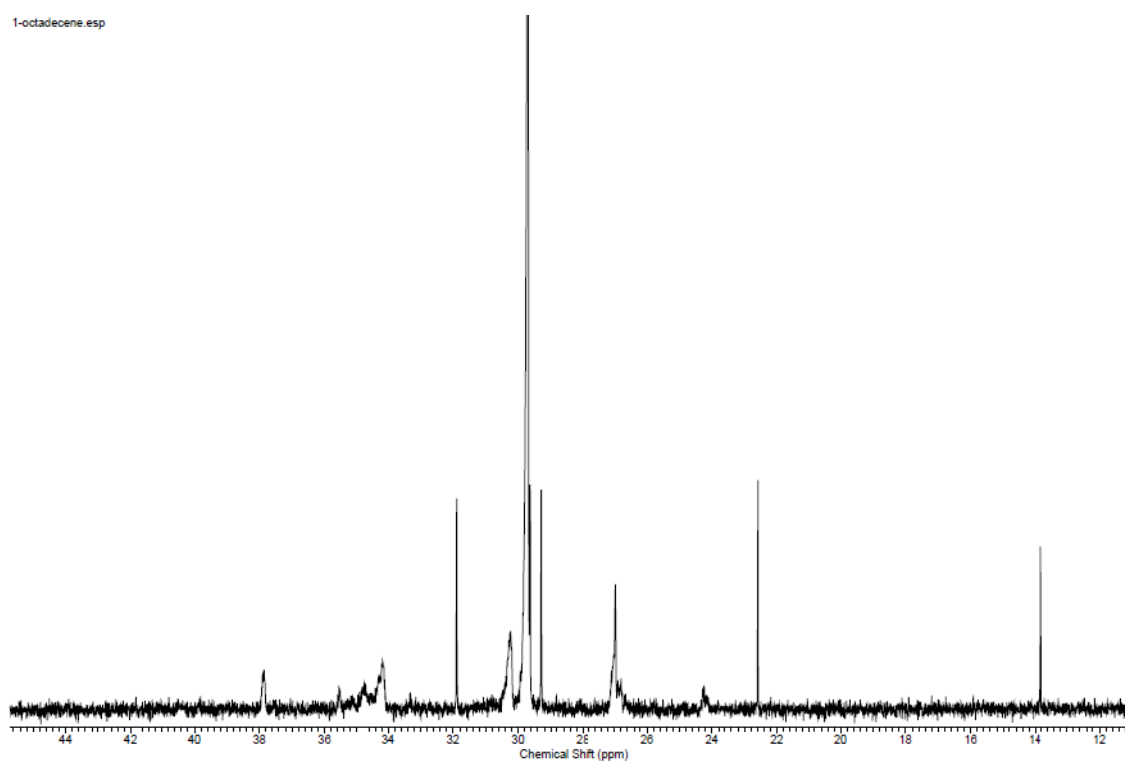
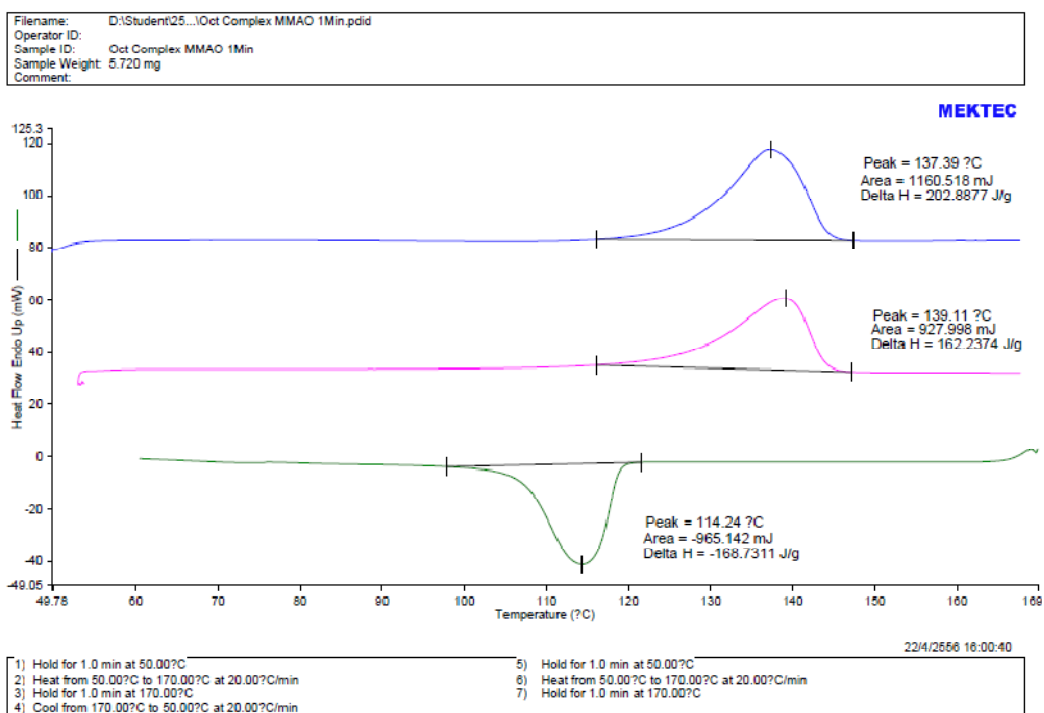


Figure A-27 <sup>13</sup>C NMR spectrum of ethylene/1-tetradecene copolymer



**Figure A-29**  $^{13}\text{C}$  NMR spectrum of ethylene/1-octadecene copolymer

**APPENDIX B**  
**(DIFFERENTIAL SCANNING CALORIMETER)**



**Figure B-1 DSC curve of ethylene homopolymer entry 1**

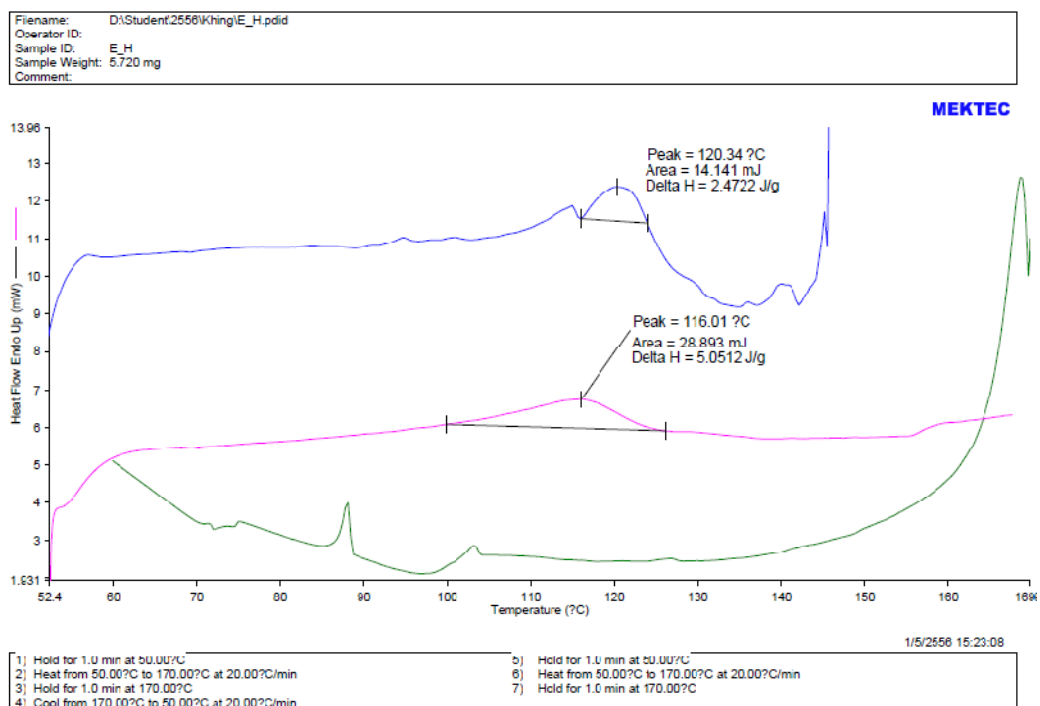


**Figure B-2 DSC curve of ethylene/1-hexene copolymer entry 2**

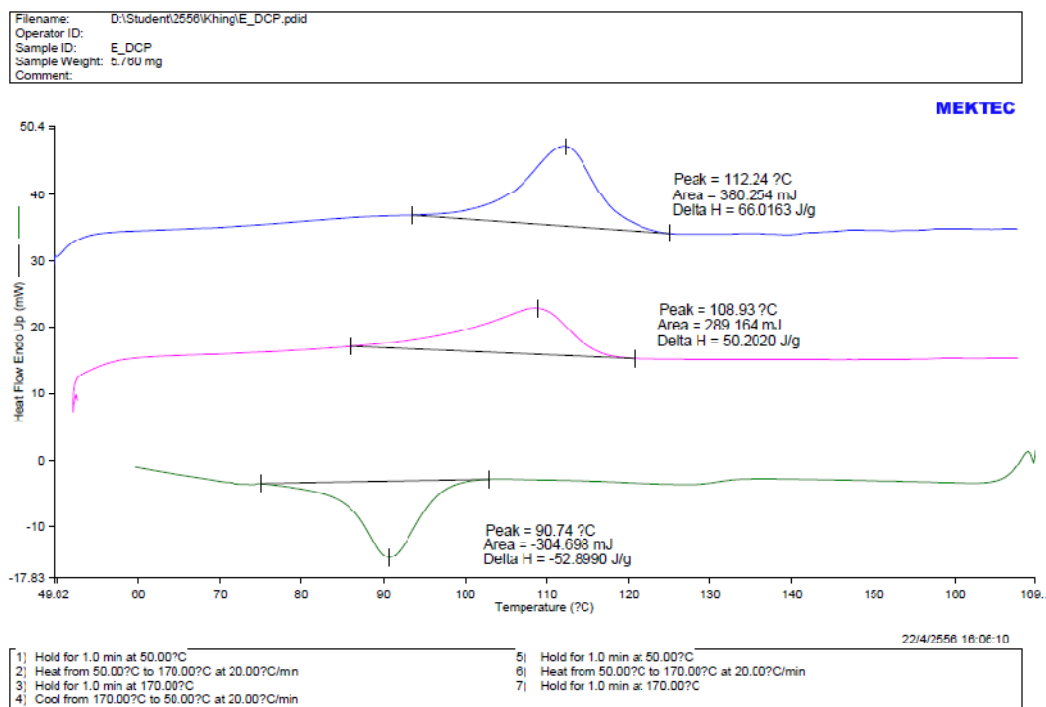


**Figure B-3 DSC curve of ethylene/dicyclopentadiene copolymer entry 3**

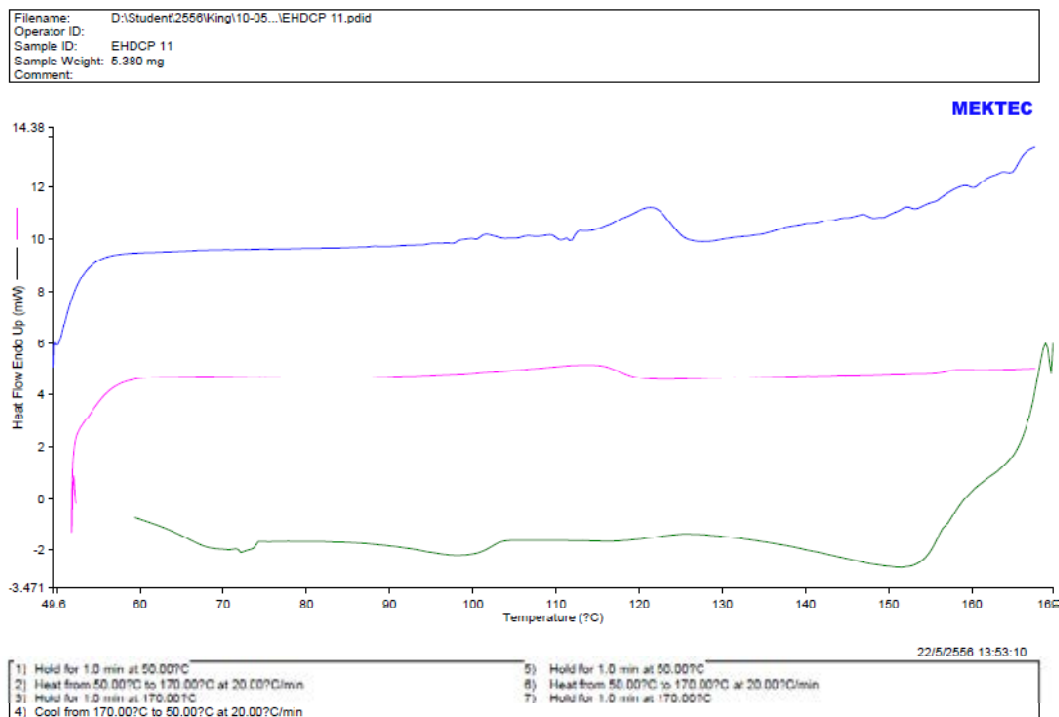


**Figure B-4 DSC curve of ethylene/1-hexene/DCP terpolymer entry 4**

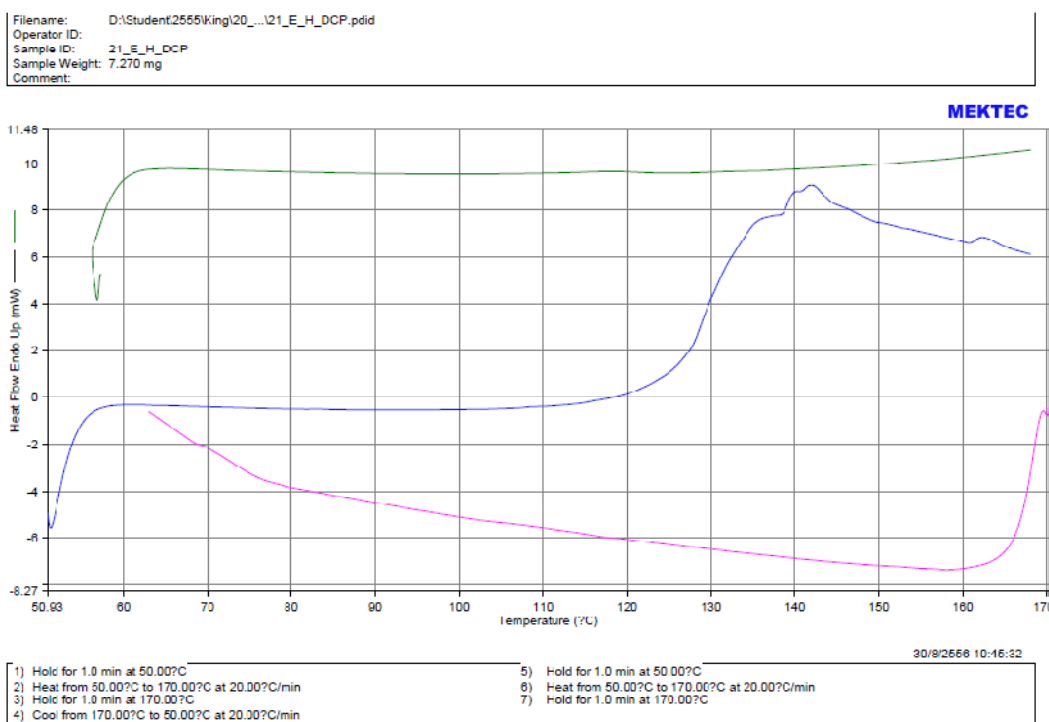


**Figure B-5 DSC curve of ethylene/1-hexene/DCP terpolymer entry 5**

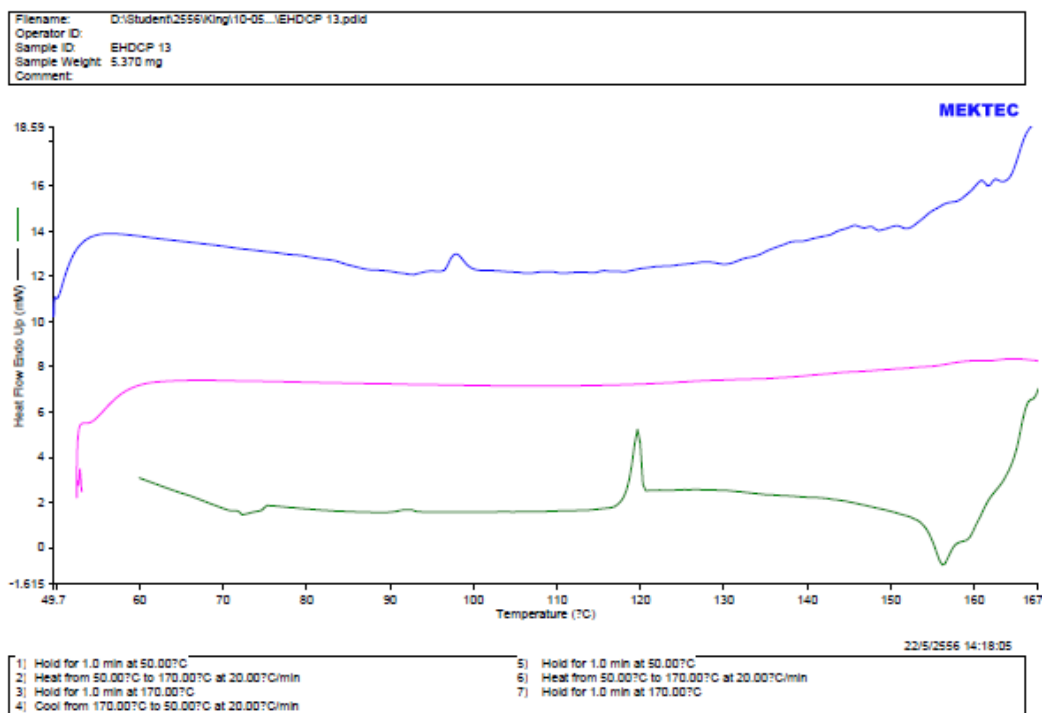


**Figure B-6 DSC curve of ethylene/1-hexene/DCP terpolymer entry 6**

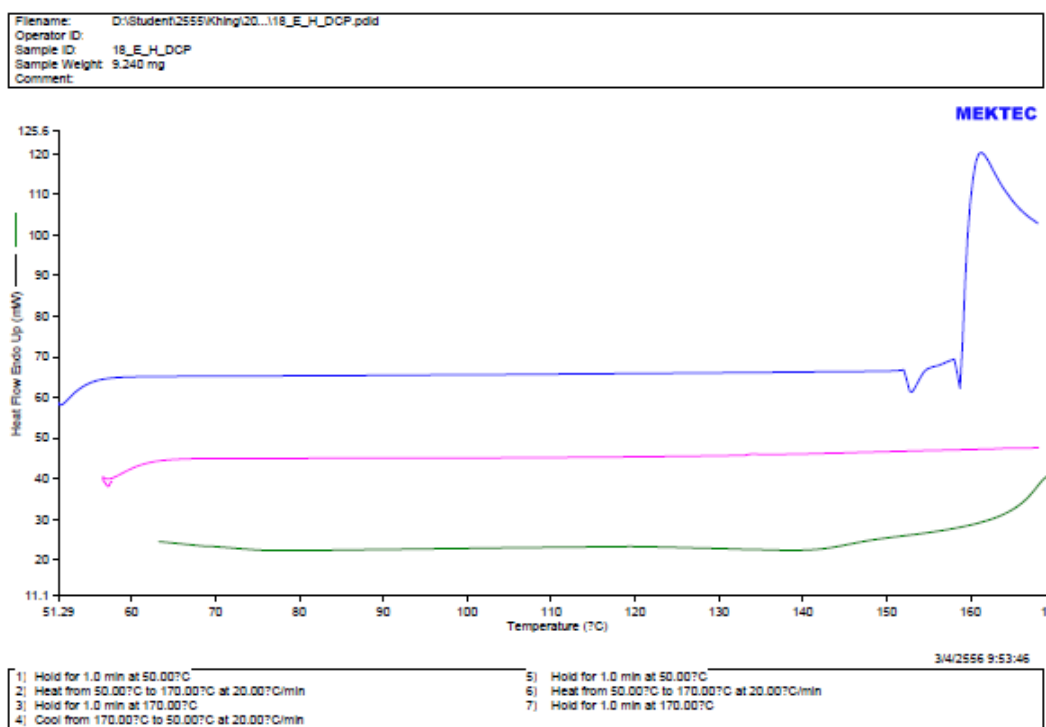


Figure B-7 DSC curve of ethylene/1-hexene/DCP terpolymer entry 7

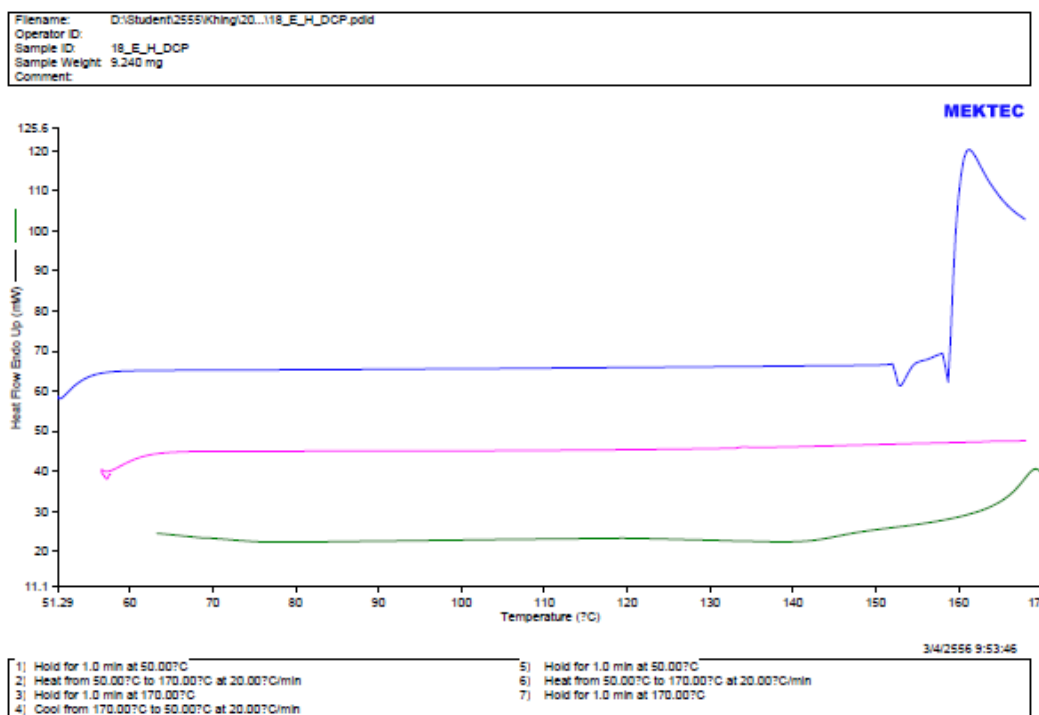
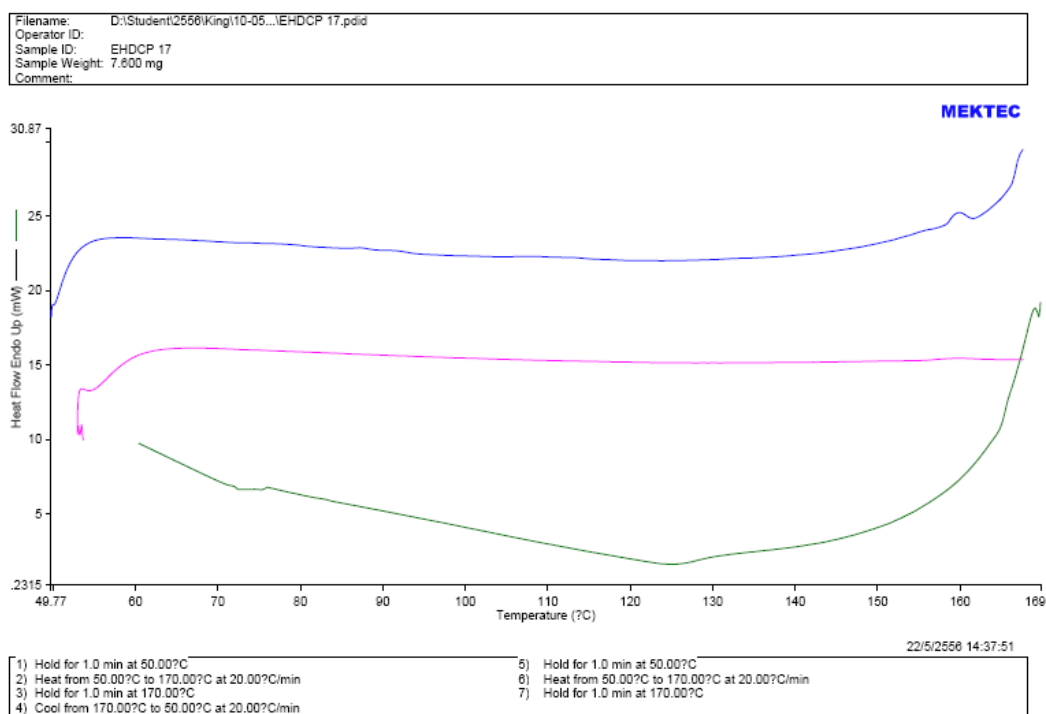
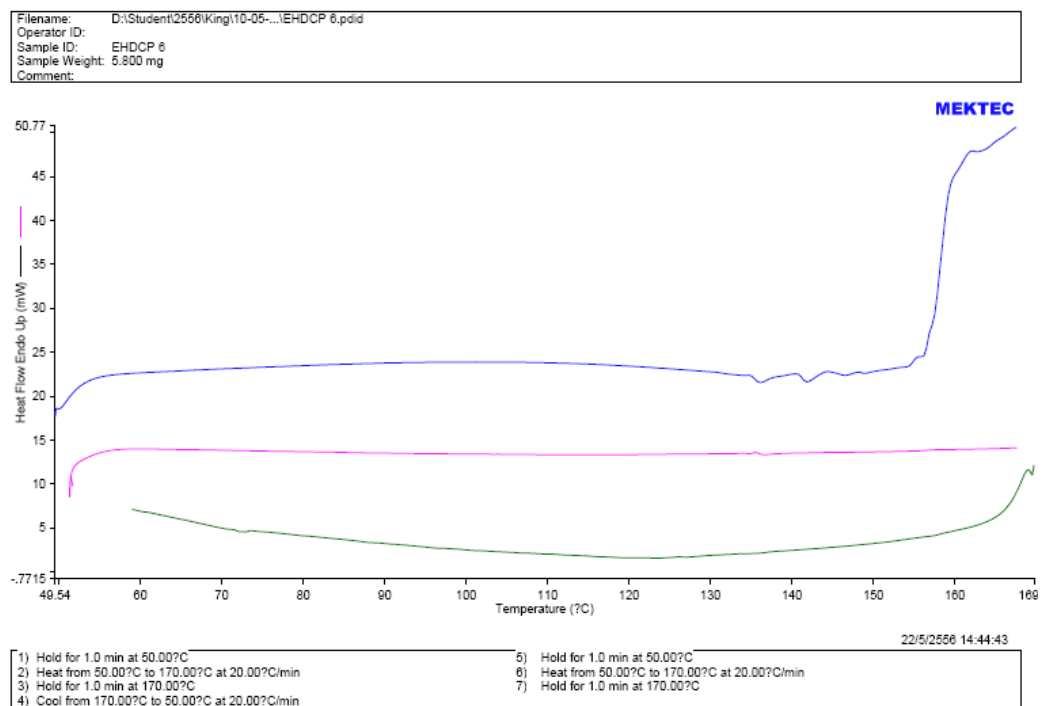


Figure B-8 DSC curve of ethylene/1-hexene/DCP terpolymer entry 8



**Figure B-9 DSC curve of ethylene/1-hexene/DCP terpolymer entry 9**



**Figure B-10 DSC curve of ethylene/1-hexene/DCP terpolymer entry 10**



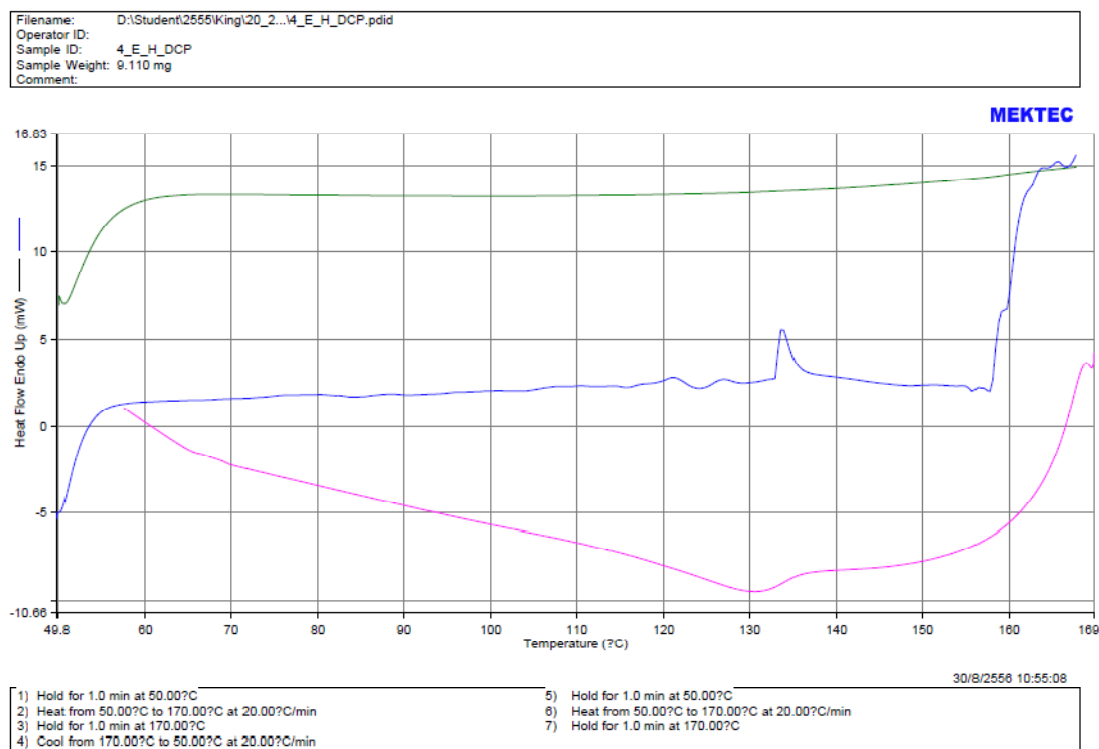


**Figure B-11 DSC curve of ethylene/1-hexene/DCP terpolymer entry 11**

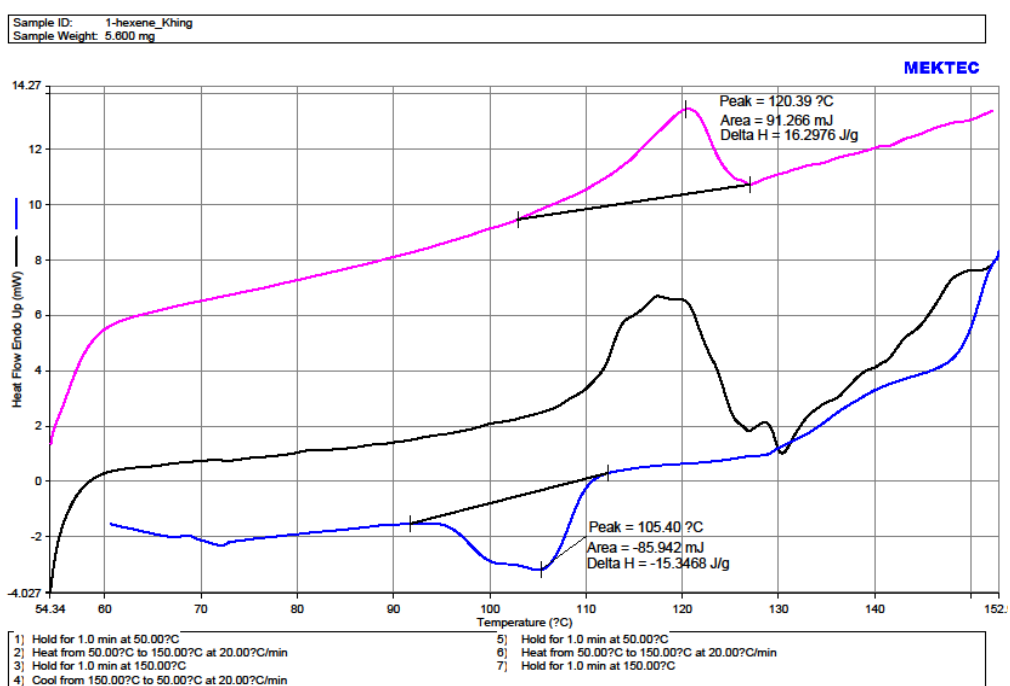


**Figure B-12 DSC curve of ethylene/1-hexene copolymer (part 3)**

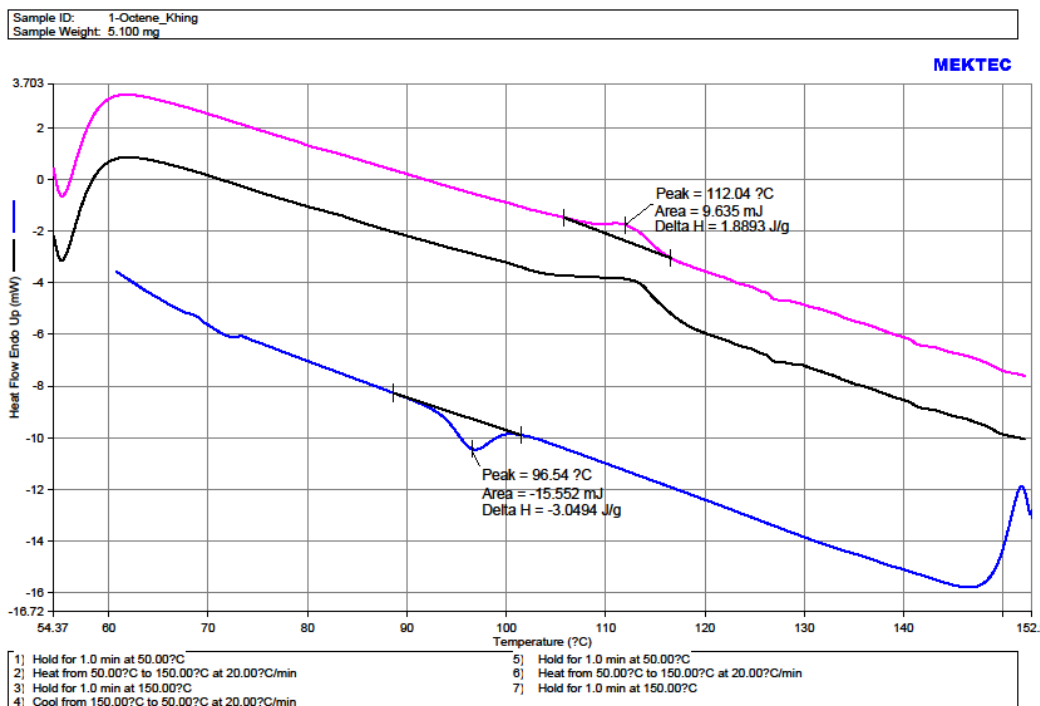


Figure B-13 DSC curve of ethylene/1-octene copolymer

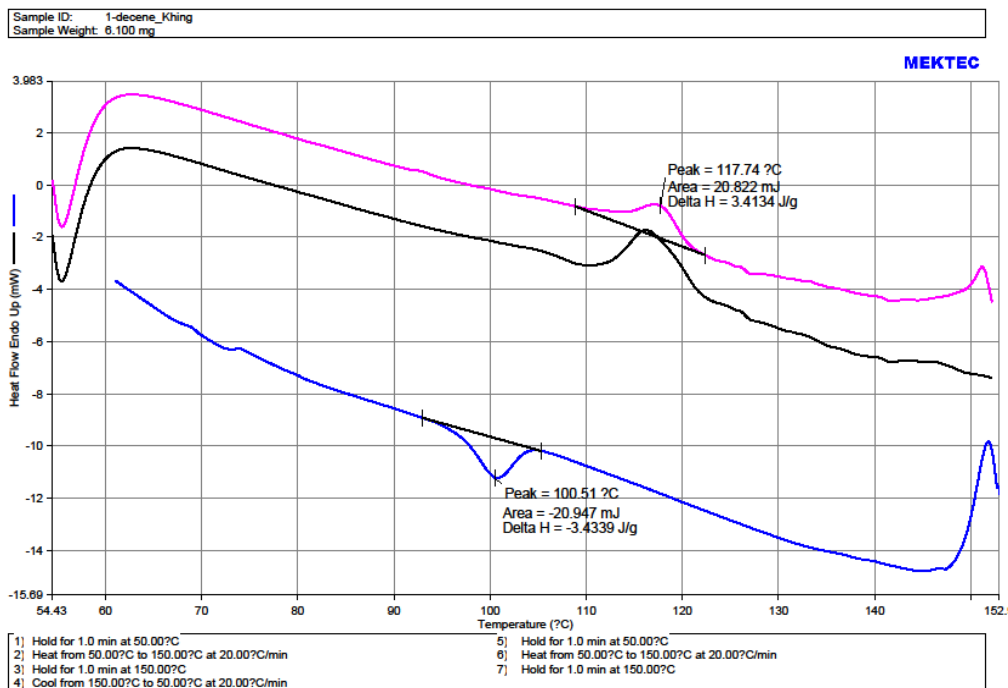


Figure B-14 DSC curve of ethylene/1-decene copolymer

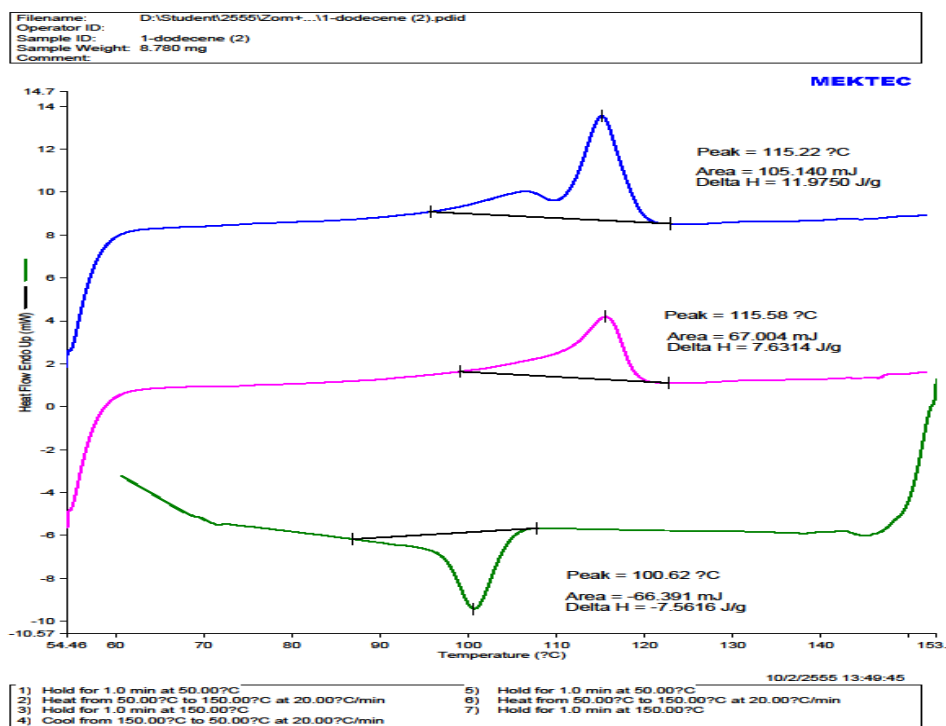


Figure B-15 DSC curve of ethylene/1-dodecene copolymer

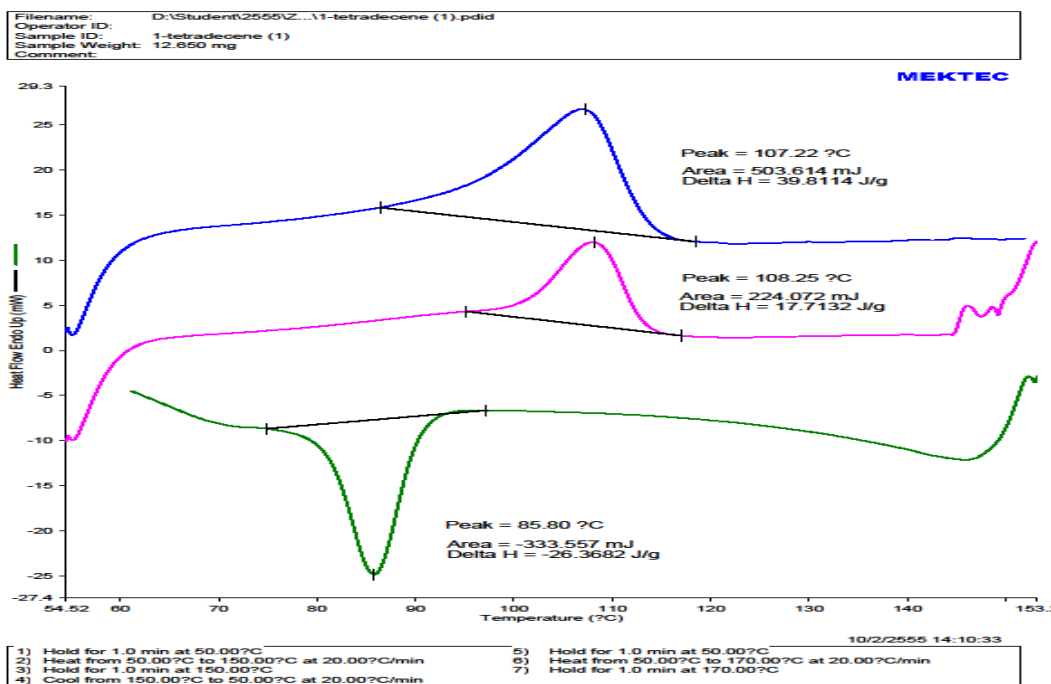


Figure B-16 DSC curve of ethylene/1-tetradecene copolymer

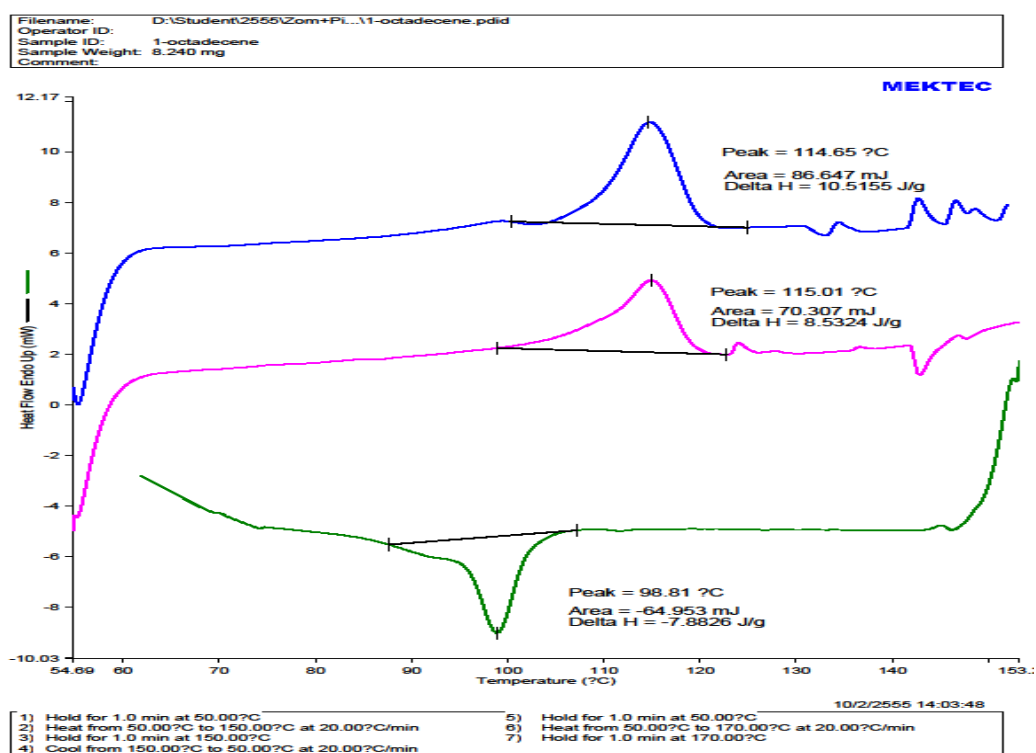


Figure B-17 DSC curve of ethylene/1-octadecene copolymer

## **APPENDIX C**

**(CALCULATION OF POLYMER MICROSTRUCTURE)**

### C-1 Calculation of monomer triad distributions

The triad distributions of the comonomers were determined from the spectra according to the Soga K. et al. [77]. The detail of calculation for ethylene/ $\alpha$ -olefin copolymer was interpreted as follow.

#### For ethylene and 1-hexene copolymer

The integral area of  $^{13}\text{C}$ -NMR spectrum in the specify range are listed.

$$T_A = 39.5 - 42 \quad \text{ppm}$$

$$T_B = 38.1 \quad \text{ppm}$$

$$T_C = 33 - 36 \quad \text{ppm}$$

$$T_D = 28.5 - 31 \quad \text{ppm}$$

$$T_E = 26.5 - 27.5 \quad \text{ppm}$$

$$T_F = 24 - 25 \quad \text{ppm}$$

$$T_G = 23.4 \quad \text{ppm}$$

$$T_H = 14.1 \quad \text{ppm}$$

Triad distribution was calculated as the followed formula.

$$k[\text{HHH}] = 2T_A + T_B - T_G$$

$$k[\text{EHH}] = 2(T_G - T_B - T_A)$$

$$k[\text{EHE}] = T_B$$

$$k[\text{EEE}] = 0.5(T_A + T_D + T_F - 2T_G)$$

$$k[\text{HEH}] = T_F$$

$$k[\text{HEE}] = 2(T_G - T_A - T_F)$$

### For ethylene and 1-octene copolymer

The triad distributions of the ethylene and 1-octene copolymer were determined from the spectra according to Randall [105]. The detail of calculation for ethylene/1-octene copolymer and ethylene/1-decene copolymer were interpreted as follow.

$$T_A = 39.5 - 42 \text{ ppm}$$

$$T_B = 38.1 \text{ ppm}$$

$$T_C = 36.4 \text{ ppm}$$

$$T_D = 33 - 36 \text{ ppm}$$

$$T_E = 32.2 \text{ ppm}$$

$$T_F = 28.5 - 31 \text{ ppm}$$

$$T_G = 25.5 - 27.5 \text{ ppm}$$

$$T_H = 24 - 25 \text{ ppm}$$

$$T_I = 22 - 23 \text{ ppm}$$

$$T_J = 14 - 15 \text{ ppm}$$

Triad distribution was calculated as the followed formula.

$$k[OOO] = T_A - 0.5T_C$$

$$k[EEO] = T_C$$

$$k[EOE] = T_B$$

$$k[EEE] = 0.5T_F - 0.25T_E - 0.25T_G$$

$$k[OEO] = T_H$$

$$k[OEE] = T_G - T_E$$

**For ethylene and 1-decene copolymer**

The integral area of  $^{13}\text{C}$ -NMR spectrum in the specify range are listed.

$$T_A = 39.5 - 42 \text{ ppm}$$

$$T_B = 38.1 \text{ ppm}$$

$$T_C = 36.4 \text{ ppm}$$

$$T_D = 33 - 36 \text{ ppm}$$

$$T_E = 32.2 \text{ ppm}$$

$$T_F = 28.5 - 31 \text{ ppm}$$

$$T_G = 25.5 - 27.5 \text{ ppm}$$

$$T_H = 24 - 25 \text{ ppm}$$

$$T_I = 22 - 23 \text{ ppm}$$

$$T_J = 14 - 15 \text{ ppm}$$

Triad distribution was calculated as the followed formula.

$$k[\text{DDD}] = T_A - 0.5T_C$$

$$k[\text{EDD}] = T_C$$

$$k[\text{EDE}] = T_B$$

$$k[\text{EEE}] = 0.5T_F - 0.5T_E - 0.5T_G - T_I$$

$$k[\text{DED}] = T_H$$

$$k[\text{DEE}] = T_G - T_I$$



### C-2 Calculation of monomer reactivity ratios

Monomer reactivity ratios ( $r_E$ ,  $r_C$ ) were determined from the triads according to the following equations:

$$r_E = 2[EE]/([EC]X)$$

$$r_C = 2[CC]X/[EC]$$

where  $r_E$  = ethylene reactivity ratio,  $r_C$  = comonomer ( $\alpha$ -olefin) reactivity ratio

$$[EE] = [EEE] + 0.5[CEE]$$

$$[EC] = [CEC] + 0.5[CEE] + [ECE] + 0.5[ECC]$$

$$[CC] = [CCC] + 0.5[ECC]$$

$X = [E]/[C]$  in the feed = the ratio of concentration of ethylene (mol/l) to concentration of comonomer (mol/l) in the feed.

$$\%E = [EEE] + [EEC] + [CEC]$$

$$\%C = [CCC] + [CCE] + [ECE]$$

To confirm the monomer reactivity ratios determined from the monomer feed ratio and the dyad contents, the monomer ratios were also determined by Fineman-Ross (F-R) [80] and Kelen-Tüdös (K-T) methods [81]

#### The Fineman-Ross equation:

$$\frac{F(f-1)}{f} = \left( \frac{F^2}{f} \right) r_E - r_C$$

where,  $f$  is the molar ratio of the monomers in the copolymer and  $F$  is the mole ratio of monomer in feed.

From the plot between  $F(f-1)/F$  vs  $(F^2/f)$ , it can be obtained  $r_E$  and  $r_C$  from the slope and the origin.

**The Kelen-Tüdös (K-T) method:**

$$\eta = \left( r_E + \frac{r_C}{\alpha} \right) \xi - \left( \frac{r_C}{\alpha} \right)$$

where,  $\eta = G / (\alpha + F')$ ,  $\xi = F' / (\alpha + F')$ ,  $G = F(f - 1)$ ,  $F' = F^2 / f$ ,  $\alpha = (F' \max \cdot F, \min)^{0.5}$

$r_E$  and  $r_C$  can be obtained from the origin and slope from the plot between  $\eta$  vs.  $\xi$ .

The standard deviation calculated as  $[(1/(N - 1)) \sum (r_{E,C(\text{exp})} - r_{E,C(\text{opt})})^2]^{1/2}$

**C-3 Calculation of crystallinity for ethylene/ $\alpha$ -olefin copolymer**

The crystallinities of copolymers were determined by differential scanning Calorimeter (DSC). % crystallinity of copolymers is calculated from equation [106].

$$\chi (\%) = \frac{\Delta H_m}{\Delta H_{m_0}} \times 100$$

where,  $\chi (\%) = \% \text{crystallinity}$

$\Delta H_m$  = the heat of fusion of sample (J/g)

$\Delta H_{m_0}$  = the heat of fusion of perfectly crystalline polyethylene (286 J/g)

[104]

**APPENDIX D**  
**(LIST OF PUBLICATIONS)**

### D-1 Publications

- Wannaborworn, M., Praserttham, P., Jongsomjit, B. Observation of Different Catalytic Activity of Various 1-Olefins during Ethylene/1-Olefin Copolymerization with Homogeneous. *Molecules*. 16 (2011): 373-383.
- Wannaborworn, M., Praserttham, P., Jongsomjit, B., Cai, Z., Yano, H., Shiono, T. Copolymerization of ethylene and 1-hexene with *ansa*-dimethylsilylene(fluorenyl)(*t*-butylamido)dimethyltitanium complexes activated by modified methylaluminumoxane. *Macromol. Chem. Phys.* **Article in press**
- Wannaborworn, M., Praserttham, P., Jongsomjit, B., Cai, Z., Yano, H., Shiono, T. Terpolymerization of ethylene and 1-hexene with dicyclopentadiene with  $\text{Me}_2\text{Si}(\eta^3\text{-C}_{29}\text{H}_{36})(\eta^1\text{-N}^t\text{Bu})\text{TiMe}_2$  complex. **Will be submitted to Journal of Applied Polymer Science**

### D-2 Conference contributions

- Poster: M. Wannaborworn, B. Jongsomjit, T. Shiono, Effect of substituent on titanocene/MMAO catalyst for ethylene/1-hexene copolymerization, International Conference on Materials International Conference on Materials Engineering and Technology 2012, Kuala Lumpur, Malaysia 28-29 August, 2012
- Poster: Mingkwan Wannaborworn, Bunjerd Jongsomjit and Takeshi Shiono, Effect of octamethyltetranidorodibenzo substituent on fluorenyl ligand of  $\text{Me}_2\text{Si}(\eta^3\text{-C}_{13}\text{H}_8)(\eta^1\text{-N}^t\text{Bu})\text{TiMe}_2/\text{MMAO}$ , RGJ-Ph.D. Congress XIV, Pattaya, Thailand 5-7 April, 2012

## VITA

Mingkwan Wannaborworn was born on January 25, 1985 in Nakhon Sri Thammarat, Thailand. In March 2007, she completed the Bachelor's Degree of Science with 1<sup>st</sup> class honor from the Department of Industrial Chemistry, Faculty of Science, King Mongkutt' s Institue of Technology Ladkrabang. Thereafter, she began studies at department of Chemical Engineering and joined catalysis and catalytic reaction engineering research group under the supervision of Assoc.Prof. Dr. Bunjerd Jongsomjit. She completed her Master's Degree in 2009 and continued studying in the Doctor's Degree in the same laboratory under the Royal Golden Jubilee program of Thailand Research Fund (TRF).